



# Annual Report

Leibniz-Institut für Kristallzüchtung  
im Forschungsverbund Berlin e.V.

# 2022



Leibniz-Institut für Kristallzüchtung (IKZ)  
Director: Prof. Dr. Thomas Schröder  
Max-Born-Straße 2  
12489 Berlin  
Germany

Phone +49 (0)30 6392 3001  
Fax +49 (0)30 6392 3003  
Email [cryst@ikz-berlin.de](mailto:cryst@ikz-berlin.de)  
Online [www.ikz-berlin.de](http://www.ikz-berlin.de)

Annual Report 2022

Editor: Dr. Maike Schröder

Layout & typesetting: [www.typoly.de](http://www.typoly.de)

Print: [www.katalogdruck-berlin.de](http://www.katalogdruck-berlin.de)

Cover photo: IKZ 1992 (top), IKZ 2022 (bottom; photo: Sebastian Rost)

All rights reserved.  
Reproduction requires the permission  
of the director of the institute.

© Leibniz-Institut für Kristallzüchtung  
im Forschungsverbund Berlin e.V.

Berlin, September 2023

# Annual Report

**Leibniz-Institut für Kristallzüchtung**  
im Forschungsverbund Berlin e.V.

# 2022

## Preface



Von links nach rechts:  
IKZ Direktor Prof. Thomas Schroeder begrüßt den früheren IKZ Direktor Prof. Roberto Fornari und den früheren Interim-IKZ Direktor Prof. Günther Tränkle anlässlich des 30 jährigen IKZ Geburtstages.

From left to right:  
IKZ director Prof. Thomas Schroeder welcomes former IKZ director Prof. Roberto Fornari and former acting IKZ director Prof. Günther Tränkle during the celebrations of IKZ's 30th anniversary.

## Liebe Leser:innen,

Der Forschungsverbund Berlin (FVB) e.V. und unser Institut IKZ feierten im Jahre 2022 den 30sten Geburtstag. Der FVB e.V. wurde ursprünglich als Übergangsstruktur gegründet, um im Jahre 1992 nach der deutschen Wiedervereinigung den Verwaltungsbedarf der neu gegründeten Leibniz-Institute Ostberlins zu bedienen. Heute, auch angesichts des Fachkräftemangels, gilt der FVB e.V. als Erfolgsmodell für gemeinsam ausgebaute administrative Dienste hoher Qualität & Expertise auch für andere Forschungsorganisationen. Unser Institut IKZ ist heute ohne Zweifel das größte Forschungsinstitut in Europa, das sich auf die Forschung und Entwicklung kristalliner Materialien im gesamten Spektrum von Grundlagen, Anwendungen bis hin zur Industrie positioniert. Unsere Arbeit ist intensiv nachgefragt, was am besten durch den Fakt belegt ist, dass das Institut von einer Personalstärke im Jahre 1992 von zirka 50 Personen auf zirka 140 Personen im Jahre 2022 angewachsen ist. Kurzum, es gab viele gute Gründe für eine Feier anlässlich unseres 30sten Jubiläums. Wir organisierten eine tolle Sommerparty am schönen Müggelsee im Garten des Leibniz-Instituts für Gewässerökologie und Binnenfischerei (IGB) für die administrativen und technischen FVB Kräfte. Am IKZ führten wir einen wissenschaftlichen Workshop für die IKZ Mitarbeiter:innen durch und freuten uns über diverse Gastsprecher:innen, die das Institut seit langem intensiv begleiten. Frau Dr. Jutta Koch-Unterseher zeichnet für das Land Berlin seit vielen Jahren für das Institut verantwortlich und hat das Haus stets intensiv unterstützt. Prof. Stefan Hecht stellte die IKZ Zusammenarbeiten mit unserem wichtigen Partner Humboldt Universität hier in Adlershof dar. Prof. Kookrin Char von der Universität Seoul beleuchtete das Gebiet der Oxidelektronik; Prof. Char erhielt 2021 einen begehrten Humboldt Preis mit dem IKZ als gastgebendem Institut. Mit großer Freude durften wir auch unseren früheren IKZ Direktor Prof. Roberto Fornari

und unseren früheren InterimDirektor Prof. Günther Tränkle als Redner begrüßen; der IKZ Gründungsdirektor Prof. Winfried Schröder verstarb leider vor einigen Jahren. Das IKZ dankt insbesondere dem Land Berlin für seine kontinuierliche Unterstützung über die zurückliegenden 30 Jahre. Selbstverständlich dankt das IKZ neben den Direktoren all seinen im Ruhestand befindlichen und allen aktiven IKZ Mitarbeiter:innen für ihr Engagement und ihre erzielten Leistungen für das Haus über diese spannenden 30 Jahre.

Im Jahre 2022 erlaubte uns das Ende der Covid Pandemie zu einem im wesentlich normalen Arbeitsmodus mit vielen Präsenzveranstaltungen zurückzukehren. „Lessons learnt“ war jedoch eine wichtige Richtlinie bei der erfolgten Neuorganisation. Positive Elemente wie z.B. flexible mobile Arbeitsregeln für alle unsere Angestellten, Digitalisierung administrativer Prozesse, die Nutzung von IKZ Laptops als solide & sichere IT Hardware Basis und hybride Präsentationsformen für Seminare und Besprechungen wurden erhalten und ausgebaut. Unglücklicherweise veränderte sich die Welt erneut in dramatischer Weise durch den grausamen russischen Angriff auf die Ukraine am 24. Februar 2022. Es ist eine zentrale Essenz der Wissenschaft, in einem offenen und gegenseitigen Prozess des Austausches international weltweite Herausforderungen anzugehen und Lösungen zu entwickeln; Klimakrise und Biodiversitätskrise können nur gemeinsam gelöst werden. Heute müssen wir indes zur Kenntnis nehmen, dass geopolitische Verwerfungen diesen wissenschaftlichen Austausch verändern. Das IKZ muss auch unter diesen veränderten politischen Randbedingungen Partnerschaften neu definieren. Mittels der Leitung des Leibniz-Strategieforums „Technologische Souveränität“ ist das IKZ in diesen Diskussionsprozess in Wissenschaft & Gesellschaft eingebettet, so dass wir hier die richtigen

## Preface

Schlüsse ziehen können. Eine direkte und ernste Folge für den Betrieb des IKZ war durch die enorme Inflation im Jahre 2022 gegeben, wesentlich getrieben durch die Kosten für Energie. Die Materialsynthese auf einer breiten experimentellen Basis ist das Herz des IKZ; folglich, trotz einer Reduktion unseres Energieverbrauchs durch Umorganisationen um 15 – 20 %, erhöhten sich unsere Energiekosten um 120 % im Jahre 2022. Die schlechte Nachricht: Wir verloren viel Geld, dass wir für Wissenschaft einplanten. Die gute Nachricht: Es gelang uns, dass IKZ voll betriebsfähig zu halten, so dass a) die Qualität unserer Arbeit und b) die Zuverlässigkeit unseres Institutes (in Bezug auf gemachte Projektzusagen gegenüber F & E Partnern) aufrecht erhalten werden konnte. Dies wurde nur ermöglicht durch die erfolgreiche Einwerbung weiterer Drittmittel, ein Erfolg, der nur durch viele helfende Hände ermöglicht wurde. Wir danken somit all unseren IKZ Kolleg:innen für die Unterstützung des Hauses, i.B. in schwierigen Jahren wie dem Jahr 2022.

Wir wünschen Ihnen viel Vergnügen beim Lesen des IKZ Jahresberichtes 2022 mit vielen spannenden wissenschaftlichen Ergebnissen & Highlights !

Thomas Schroeder

## Dear Readers,

the Forschungsverbund Berlin (FVB) e.V. and our institute IKZ celebrated in 2022 their 30th anniversaries. The FVB e.V. was originally intended as a temporary arrangement to cover the administration needs of the newly established East Berlin Leibniz-Institutes after German reunification. Today, it acts as a successful role model with respect to shared administration services on a high level of expertise also for other research organizations; this is a particular value in times of skilled labor shortage. Our institute IKZ is without doubt today the biggest research center in Europe, focusing on crystalline materials in the fields of basic, applied & pre-industrial research and development. Our work is in high demand, best demonstrated by the growth of the institute from around 50 persons in 1992 to about a staff of 140 in 2022. So, there were many reasons to celebrate our 30th anniversary. We organized a nice Summer garden party at lake Müggelsee with the support of the Leibniz-Institute of Freshwater Ecology and Inland Fisheries (IGB) for the administrative and technical FVB support staff. At IKZ we held a scientific workshop and were happy to welcome as guest speakers Dr. Jutta Koch-Unterseher as responsible representative of the Land Berlin, Prof. Stefan Hecht from our important partner Humbolt-University here in Adlershof as well as Prof. Kookrin Char from the University of Seoul, Humboldt award prize winner in 2021 at IKZ. It was our great

pleasure to welcome our former IKZ director Prof. Roberto Fornari and our former acting IKZ director Prof. Günther Tränkle to the event as speakers; IKZ foundation director Prof. Winfried Schröder unfortunately passed away several years ago. The IKZ is grateful to the Land Berlin for its continuous support for the institute over 30 years. As a matter of course, the IKZ wishes to thank all its former directors as well as retired & current employees for their dedication to the jobs and achievements for the institute over the years.

The year 2022 allowed us with the end of the Covid pandemic to return back to a normal work organization with many meetings, taking place in presence again. 'Lessons learnt' was however an important guideline in this reorganization of our work flow in 2022. Positive elements like e.g. flexible mobile work arrangements for all employees, digitalization of administrative processes, the use of IKZ lab-tops as a solid & secure hardware basis for IT services and hybrid forms of online lectures & seminars were maintained and further developed. Unfortunately, the world changed tremendously again in 2022 with the cruel Russian attack on Ukraine on 24th February. It is the very essence of science to exchange ideas and perspectives on an international level in an open and reciprocal communication process to address and solve common worldwide challenges; climate and biodiversity crisis can only be addressed together. Today, we face however the fact that geopolitical tensions limit this exchange process in science. IKZ will need to redefine partnerships under these new political boundary conditions. IKZ takes the lead of the Leibniz strategy forum "Technology Sovereignty" and is thus deeply embedded in these discussions in science & society to take the right steps. A direct and severe threat to the functioning of the institute was given by the rising inflation, in particular driven by energy in 2022. Materials synthesis on a broad basis of experimental facilities is at the very heart of IKZ; in consequence, despite reducing our energy consumption by roughly 15-20 % through smart reorganization, our energy costs increased in 2022 by 120 %. The bad news: We lost a lot of money we planned to spend for science. The good news: We succeeded to keep the institute fully operational without compromising a) the quality of our work and b) the reliability of our institute (with respect to commitments given to R & D partners). This became only possible by the successful acquisition of additional third-party funds, an important achievement made possible by many helping & dedicated hands at IKZ. We thank all our colleagues at IKZ who support the institute, especially in a difficult year like 2022 !

Enjoy the IKZ Annual Report 2022 with many exciting scientific results & highlights !

Thomas Schroeder

# **Content**

<b>2</b>	Preface
<b>6</b>	The Institute
<b>26</b>	Volume Crystals
<b>34</b>	Nanostructures & Layers
<b>42</b>	Materials Science
<b>50</b>	Application Science
<b>56</b>	Appendix

## The Institute



*Photo: Sebastian Rost Fotografie*

### **Leibniz-Institut für Kristallzüchtung im Forschungsverbund Berlin e.V.**

Founded 1992  
Part of Forschungsverbund Berlin e.V.  
Member of the Leibniz Association



## The Institute

### Das Leibniz-Institut für Kristallzüchtung (IKZ)

ist ein internationales Kompetenzzentrum für Wissenschaft & Technologie sowie Service & Transfer im Bereich kristalliner Materialien. Das Spektrum der Forschung und Entwicklung reicht dabei von Themen der Grundlagen- und angewandten Forschung bis hin zu vorindustriellen Forschungsaufgaben.

Kristalline Materialien sind technologische Schlüsselkomponenten zur Realisierung von elektronischen und photonischen Lösungen für gesellschaftliche Herausforderungen. Hierzu gehören künstliche Intelligenz (Kommunikation, Sensorik etc.), Energie (erneuerbare Energien, Energiewandlung etc.) und Gesundheit (medizinische Diagnostik, moderne chirurgische Operationsinstrumente etc.). Das IKZ erarbeitet Innovationen in kristallinen Materialien durch eine kombinierte Expertise im Haus, bestehend aus Anlagenbau, numerischer Simulation und Kristallzüchtung, um so kristalline Materialien höchster Qualität und mit maßgeschneiderten Eigenschaften zu erforschen.

Zusammen mit Partnern aus Instituten mit angegliederten Technologie-Plattformen sowie Industrieunternehmen treibt das Institut auch verstärkt Innovationen durch kristalline Materialien voran. Diese umfassen die zuverlässigen Evaluierungen und Bewertungen innovativer kristalliner Prototypen-Materialien für disruptive Technologieansätze.

#### Arbeitsschwerpunkte des Institutes sind:

- Entwicklung von Züchtungs-, Bearbeitungs- und Charakterisierungsverfahren für Massivkristalle sowie kristalline Gebilde mit Abmessungen im Mikro- und Nanometerbereich sowie von materialübergreifenden Kristallzüchtungstechnologien
- Bereitstellung von Kristallen mit besonderen Spezifikationen für Forschungs- und Entwicklungszwecke
- Modellierung und Erforschung der Kristallwachstums- und Kristallzüchtungsprozesse
- Experimentelle und theoretische Untersuchungen zum Einfluss von Prozessparametern auf Kristallzüchtungsvorgänge und Kristallqualität
- Erforschung von Verfahren zur Kristallbearbeitung und der dabei ablaufenden Vorgänge

### The Leibniz Institute for Crystal Growth

is an international competence center for science & technology as well as service & transfer for crystalline materials. The R&D activities cover basic and applied research up to pre-industrial development.

Crystalline materials are the key to the realization of electronic and photonic solutions to social challenges. This includes artificial intelligence (communication, sensor technology, etc.), energy (renewable energies, energy conversion etc.) and health (medical diagnostics, modern surgical instruments etc.). The IKZ develops innovations in crystalline materials by combining in-house expertise in equipment engineering, numerical simulation and crystal growth to provide highest quality crystalline materials with tailored properties.

In the future, the institute also intensifies its efforts to promote innovation by crystalline materials in cooperation with partners from technology platforms as well as industrial companies. This includes the reliable evaluation and benchmarking of innovative crystalline prototype materials for disruptive technology approaches.

#### The research and service tasks of the institute include:

- Development of technologies for growth, processing and characterization of bulk crystals and of crystalline structures with dimensions in the micro- and nanometer range and of comprehensive growth technologies
- Supply of crystals with non-standard specifications for research and development purposes
- Modelling and investigation of crystal growth processes
- Experimental and theoretical investigations of the influence of process parameters on crystal growth processes and crystal quality
- Development of technologies for the chemo-mechanical processing of crystalline samples and scientific investigation of related processes

## The Institute

- Physikalisch-chemische Charakterisierung kristalliner Festkörper und Entwicklung geeigneter Methoden bis hin zur atomaren Ebene; Aufklärung des Zusammenhangs zwischen Struktur und Eigenschaften kristalliner Materialien
- Entwicklung und Bau von Anlagenkomponenten für die Züchtung, Bearbeitung und Charakterisierung von Kristallen

Die weitere Materialforschung in Richtung Anwendung ermöglicht verstärkt auch Innovationen *durch* kristalline Materialien:

- Kristall-Prototypenforschung zur zuverlässigen Bewertung innovativer, konfektionierter Kristalle für elektronische und photonische Schlüsseltechnologien
- Prototypen-Lieferfähigkeit neuartiger Kristalle bis zur Kleinserie – in der gewünschten Konfektionierung und Spezifikation – zur zuverlässigen Technologie-Forschung und Vorbereitung der Markteinführung
- Entwicklung von Wafering-Prozessen für neue Materialien, Feinbearbeitung optischer Spezialkristalle

### Materialien

- Halbleiter mit großem Bandabstand (Oxide, Aluminiumnitrid) für Hochtemperatur-, Leistungs- und Optoelektronik
- Oxidische und fluoridische Kristalle für Lasertechnik, Optik, Sensorik und Akustoelektronik
- Silizium-Kristalle für Mikro- und Leistungselektronik und Photovoltaik
- Isotopenreine Halbleiter (Silizium und Germanium) für die Quantentechnologie
- Silizium/Germanium Kristalle für Strahlungsdetektoren und Beugungsgitter, kristalline Si/Ge-Schichten für thermoelektrische Anwendungen
- Ferroelektrische und halbleitende Oxidschichten für die Mikro- und Leistungselektronik, Sensoren und Datenspeicher

- Physico-chemical characterisation of crystalline solids and development of suitable methods; investigation of the correlation between crystalline structures and properties
- Development and construction of components for growth, processing and characterization of crystals

The further materials research towards applications will drive innovations *by* crystalline materials:

- Crystal prototypes development for the reliable benchmarking of innovative crystals with tailored properties for key technologies in electronics and photonics
- Prototype supply of innovative crystals up to small-scale batches – with tailored properties and specifications – for reliable technology research, including preparations for market introduction
- Development of wafering processes for new materials, fine processing of special optical crystals.

### Materials

- Wide band gap semiconductors (aluminium nitride, oxides) for high temperature, power- and optoelectronics
- Oxide and fluoride crystals for acousto-electronics, laser-, opto- and sensor technology
- Silicon for power electronics and photovoltaics
- Isotopically pure semiconductors (silicon and germanium) for quantum technology
- Gallium arsenide for wireless communication and in high-frequency technology
- Silicon/germanium-crystals for radiation detectors and diffraction gratings, crystalline Si/Ge layers for thermoelectric devices
- Ferroelectric and semiconducting oxide layers for micro- and power electronics, sensor applications or data storage

## Das IKZ als familienfreundlicher Arbeitgeber

Das IKZ möchte seinen Beschäftigten ein offenes, kooperatives und familienfreundliches Arbeitsumfeld bieten. Das Institut unterstützt daher seine Mitarbeiterinnen und Mitarbeiter bei der Vereinbarkeit von Arbeit und Familie, z.B. durch flexible Regelungen zur täglichen Arbeitszeit oder durch variable Regelungen zu Teil- und Vollzeitbeschäftigung.

Seit 2015 ist das Institut zertifiziert durch das *audit berufundfamilie*. Damit verbunden hat es Ziele einer familienbewussten Personalpolitik definiert und sich diesen verpflichtet. In den folgenden drei Jahren haben wir die in diesem Prozess definierten Maßnahmen umgesetzt. Die Zertifizierung wurde 2018 und 2021 erneut an das Institut vergeben.

Das Audit steht unter der Schirmherrschaft der Bundesfamilienministerin und des Bundeswirtschaftsministers, nähere Informationen finden sich unter [www.beruf-und-familie.de](http://www.beruf-und-familie.de)

## IKZ as family-friendly employer

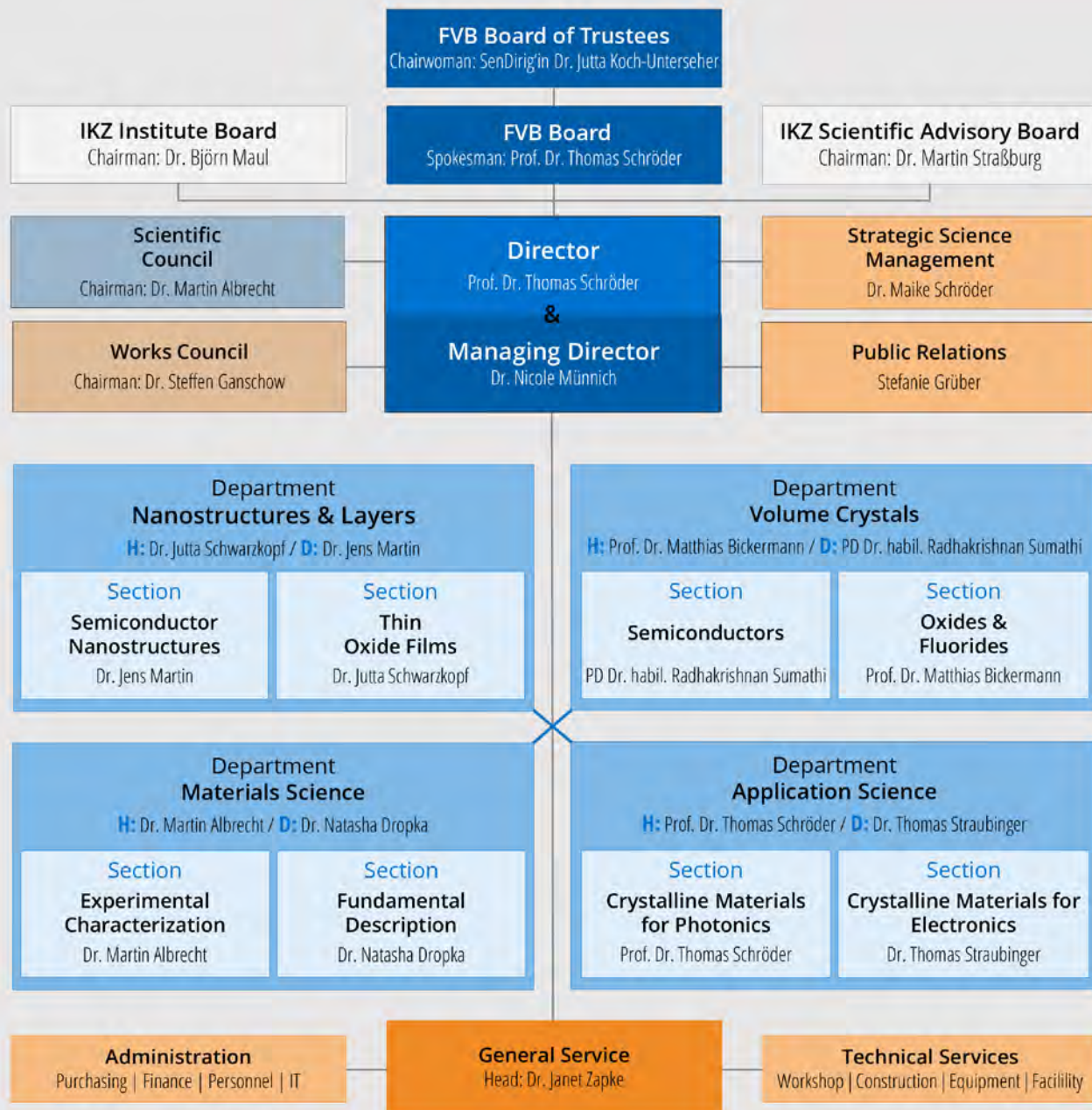
The institute intends to create a co-operative and open working environment for all employees. It places special emphasis on the reconcilability of job and family, offering flexible working time models as well as full or part-time employments. In 2015, the institute has been awarded the *audit berufundfamilie* certificate for its family-friendly human resources policy. During the following three years, we have been implementing the objectives defined in this process. The audit has been renewed in 2018 and 2021.

The certificate is issued under the auspices of the German Federal Minister for Families and the German Federal Economics Minister. More information is available under [www.beruf-und-familie.de](http://www.beruf-und-familie.de)



# The Institute

## Organigramm 2022 Organisation Chart 2022



## Wissenschaftlicher Beirat 2022 Scientific Advisory Board 2022

### Beiratvorsitzender Chair

**Dr. Martin Straßburg**  
ams-Osram International GmbH  
Regensburg, Germany

### Mitglieder Members

**Prof. Dr. Jan Ingo Flege**  
Brandenburgische Technische Universität  
Cottbus- Senftenberg (BTU)  
Cottbus, Germany

**Dr. Martin M. Frank**  
IBM, Thomas J. Watson Research Center  
Yorktown Heights, New York, USA

**Prof. Dr. Lena F. Kourkoutis †**  
School of Applied and Engineering Physics, Cornell  
University, Ithaca, New York, USA

**Dr. Andreas Mühe**  
PVA TePla AG  
Wettenberg, Germany

**Dr. Georg Schwalb**  
Siltronic AG  
Burghausen, Germany

**Prof. Dr. Thomas Südmeyer (vice chair)**  
University of Neuchâtel,  
Physics Institute  
Neuchâtel, Switzerland

**Prof. Dr. Bernd Tillack**  
IHP GmbH - Innovations for High Performance  
Microelectronics / Leibniz-Institut für innovative  
Mikroelektronik  
Frankfurt/Oder, Germany

### Vertreter des Landes Berlin Representative of the State of Berlin

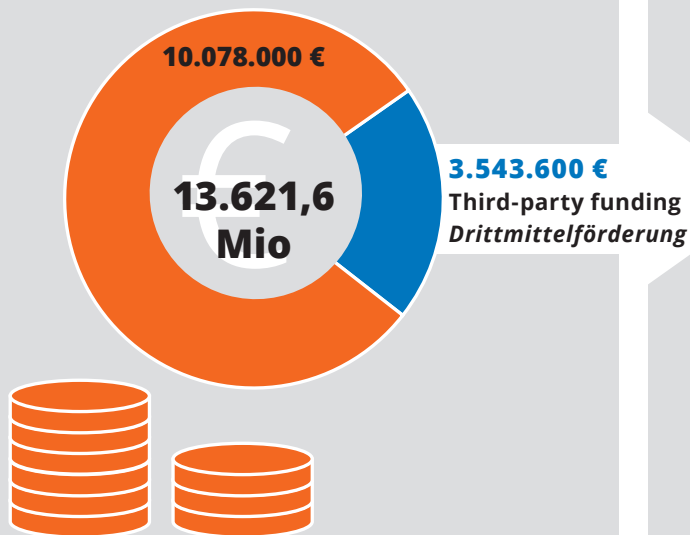
**Dr. Björn Maul**  
Referatsleiter Natur-, Material- und  
Lebenswissenschaften  
Senatsverwaltung für Wissenschaft, Gesundheit,  
Pflege und Gleichstellung  
Berlin, Germany

### Vertreter der Bundesrepublik Deutschland Representative of the Federal Republic of Germany

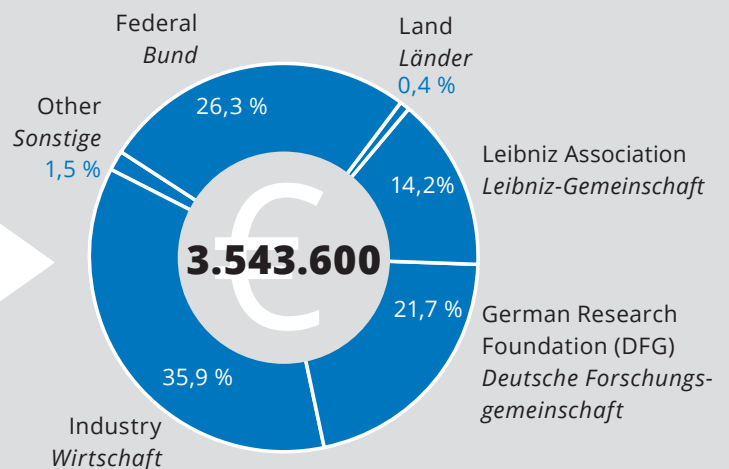
**Christoph Schwickart**  
Bundesministerium für Bildung und Forschung BMBF  
Referat 513 „Vernetzung und Sicherheit digitaler  
Systeme“  
Bonn/Berlin, Germany

# 2022 in Zahlen 2022 in figures

**Budget Gesamt**  
**Total**  
Institutional funding  
*Institutionelle Förderung*

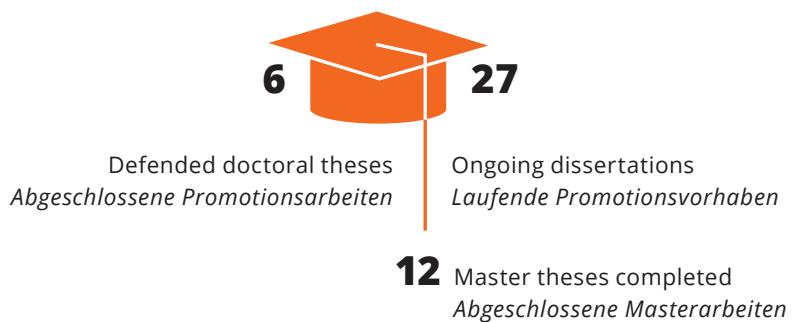


**Drittmittelförderung\***  
**Third-party funding**



\*Einnahmen  
on revenue basis

**Lehre**  
**Education**



**Publikationen**  
**Publications**



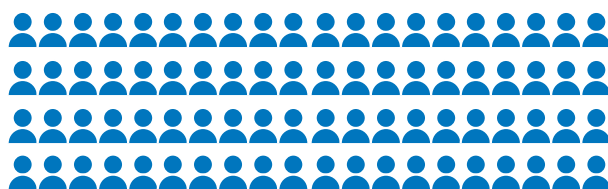
## Internationalisierung Internationalization



Staff members from 21 countries  
*Beschäftigte aus 21 Ländern*

## Personal gesamt Staff total

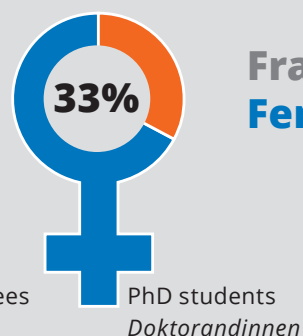
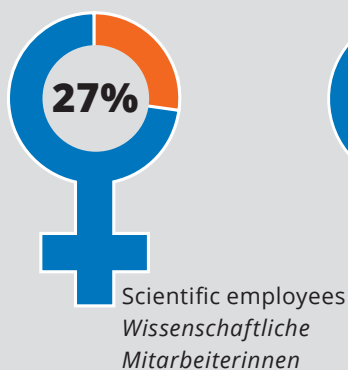
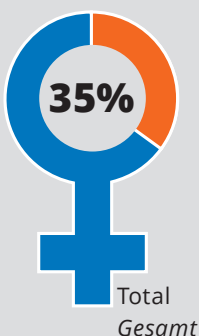
146



80 Scientific employees  
*Wissenschaftliche Mitarbeiter/innen*



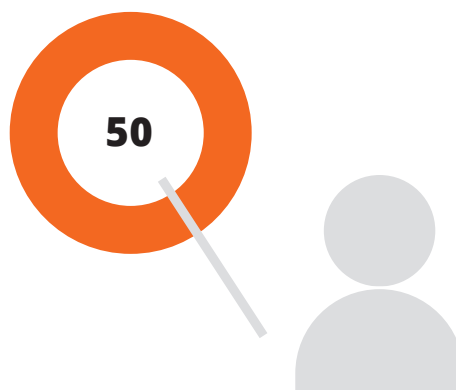
66 Infrastructure personnel  
*Infrastrukturpersonal*



## Frauenanteil Female proportion

## Eingeladene Beiträge Invited Contributions

At national and international conferences, workshops, seminars  
*Auf nationalen und internationalen Konferenzen, Workshops, Seminaren*



# The Institute

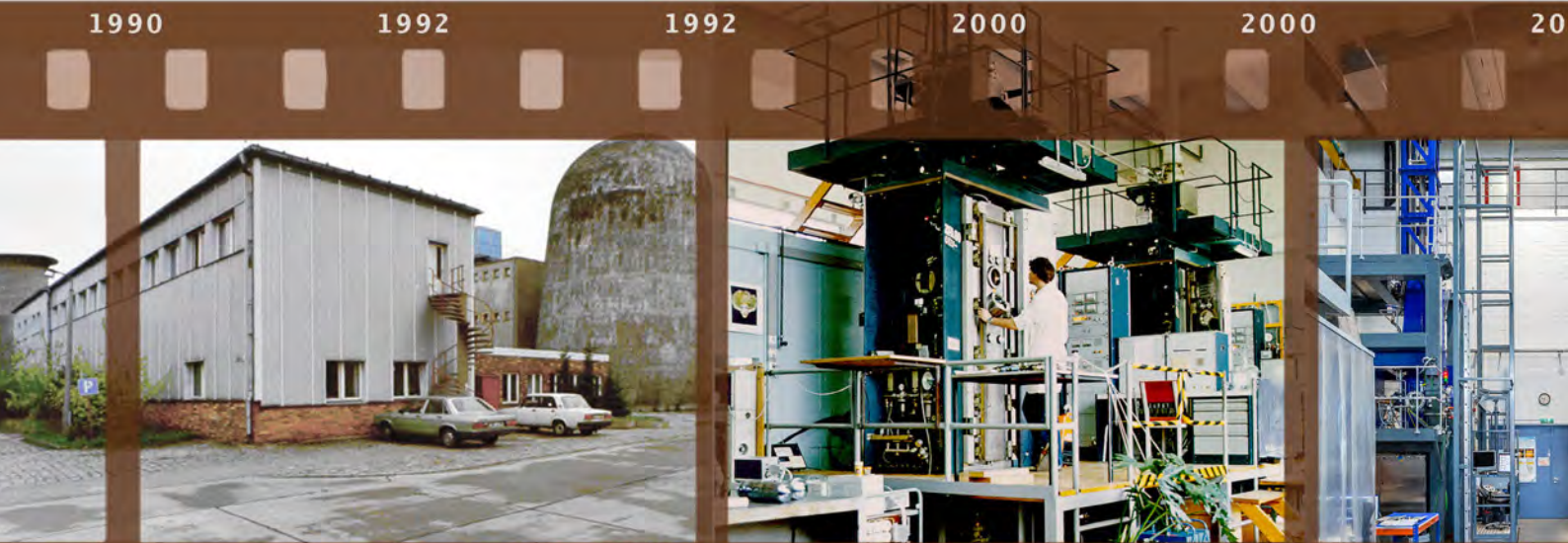


1990 Bürogebäude|Office building 1992 Eingang|Entrance 1996 Baustelle Neubau

*\*The performance of the "Technical Center for Crystal Growth", however, is considered to be extraordinarily high. This involves the development of crystal growth technologies as well as the*

Die Leistungsfähigkeit des "Technikums für Kristallzüchtung" wird dagegen als außerordentlich hoch eingeschätzt. Das betrifft sowohl die Entwicklung von Kristallwachstums-

technologien als auch die Herstellung spezieller Materialien und deren Charakterisierung. Die Arbeiten der führenden Wissenschaftler dieses Bereichs haben international Beachtung gefunden. \*



1990 Gebäude Züchtungshalle|Growth hall building 1992 Züchtungshalle|Growth hall 2000 Züchtungshalle



1993 Prof. Winfried Schröder, erster Direktor, pflanzt den „IKZ-Ginkgo“  
Prof. Winfried Schröder, first Director, planting the "IKZ Ginkgo"



2020 Bauarbeiten Foyer|Construction work lobby



1996 1996 1998 1998 2022 2022



Construction site new building-----Neubau|New building-----

*production of special materials and their characterization. The research of the leading scientists in this field has attracted international attention.*

1992		52	<b>EMPLOYEES   FUNDING</b>	ca.5,0 Mio €
2022		146		13,6 Mio €

2022 2022 2022



-----Hall|Growth hall-----Gebäude mit Aufstockung|Building with extension-----

2021 2021 2021 2022 2022 2022



-----Fertigstellung Foyer|Completion lobby-----

*Prof. Thomas Schröder, amtierender Direktor gießt den „IKZ-Ginkgo“ | Prof. Thomas Schröder, current Director watering the "IKZ Ginkgo"*

## The Institute



### 8th International Workshop on Crystal Growth Technology (IWCGT-8)

Der IWCGT-8 fand vom 29.05. – 02.06. im Pentahotel in Berlin-Köpenick statt, organisiert von Matthias Bickermann, Radhakrishnan Sumathi und Christiane Frank-Rotsch vom Leibniz-Institut für Kristallzüchtung. Ein international zusammengesetztes Steering Committee, dem weitere namhafte Kristallzüchter:innen angehören, war in die Auswahl der Vortragenden eingebunden. 79 Wissenschaftler:innen aus Forschung und Industrie trafen sich zum Austausch über Status, Entwicklungen und Perspektiven von industriell relevanten Kristallzüchtungstechnologien.

Der Workshop findet alle drei Jahre statt und wird seit 2011 vom IKZ organisiert. Vorbild für das Format sind die „Gordon Conferences“: Renommiertere Referenten werden eingeladen, einen ausführlichen Vortrag über ein spezifisches Problem oder eine Herausforderung im Bereich der anwendungsorientierten Kristallzüchtung zu halten. Lange Pausen und gemeinsame Mahlzeiten bieten Raum für Diskussionen und zum Netzwerken. Teilnehmende können ihre eigenen Arbeiten als Poster präsentieren, zudem gibt es eine Ausstellung von Industriepartnern.

Bedingt durch die Pandemie hatten wir den Workshop mehrere Male verschoben, um den persönlichen Austausch im Rahmen einer Präsenzveranstaltung zu ermöglichen. Leider war aufgrund der immer noch bestehenden Reisemöglichkeiten die Beteiligung aus Amerika und Asien geringer als üblich. Einige Vortragende konnten daher auch ihre Präsentationen nur online abhalten. Dagegen war die europäische Industrie erneut stark vertreten.

Details zum Programm finden sich hier:  
<https://iwcgt-8.ikz-berlin.de/>

Viele der Teilnehmenden besuchen die Workshopreihe regelmäßig und schätzen den persönlichen Austausch unter Fachleuten. Auch diese Veranstaltung wurde wieder sehr positiv aufgenommen. Der nächste Workshop IWCGT-9 ist für 2026 geplant. Wir freuen uns darauf!

### 8th International Workshop on Crystal Growth Technology (IWCGT-8)

IWCGT-8 was held from May 29 to June 2, 2022 at the Pentahotel Berlin-Köpenick, organized by Matthias Bickermann, Radhakrishnan Sumathi and Christiane Frank-Rotsch from the Leibniz-Institut für Kristallzüchtung. A Steering Committee with internationally renowned crystal growers is involved in the selection of the speakers. 79 scientists from companies and research institutions met to exchange information on the status, developments and perspectives of industrial crystal growth technologies.

The workshop, which takes place every three years, is hosted by IKZ since 2011. The format is inspired by the “Gordon conferences”: Renowned speakers are invited to give a detailed talk on a specific problem or challenge in application-oriented crystal growth. In addition, long breaks and shared meals provide ample space for discussion and networking opportunities. Participants can present their own work as posters during the evenings, and there is an industrial exhibition.

Due to the pandemic, we postponed the workshop several times to allow it to take place in presence and enable personal exchange. As travel was still very restrained, the participation from overseas (America and Asia) was significantly weaker than at the last workshops. This meant that also four speakers from overseas had to give their presentations remotely. On the other hand, the industry participation from Europe was again very strong.

Details on the program can be found here:  
<https://iwcgt-8.ikz-berlin.de/>

Many participants attend regularly and appreciate the personal exchange among experts. The workshop was very positively regarded by all participants. The series will be continued, and IWCGT-9 is scheduled for 2026. We are looking forward to it!

## 14. IKZ Sommerschule: Dynamics and processes in crystalline Materials

Die Entwicklungen der experimentellen Ausstattung und von entsprechenden Methoden haben den Weg für die Untersuchung von funktionellen Materialien unter operativen Bedingungen (in situ / in operando) geebnet. Ein besonders großer Fortschritt ist dabei die Möglichkeit, Übergangszustände von kristallinen Materialien unter „realistischen“ Bedingungen beobachten zu können, beispielsweise unter optischer Anregung, in elektrischen/magnetischen Feldern oder bei hohen Temperaturen. Diese Ergebnisse haben zu einem besseren Verständnis von Nichtgleichgewichtsprozessen in Materialien geführt und ermöglichen damit ihre Optimierung für hocheffiziente, stabile und nachhaltige zukünftige Technologien.

Die 14. Sommerschule des IKZ widmete sich einer Auswahl dieser methodischen Entwicklungen mit dem Schwerpunkt auf der Untersuchung der strukturellen Dynamik in kristallinen Materialien mittels Transmissionselektronenmikroskopie (TEM) und Röntgenbeugung / -Bildgebung (XRD). Diesen Methoden gemeinsam ist die Möglichkeit, Phänomene auf einer breiten Skala von Zeit- und Längeneinheiten zu erfassen, von wenigen Nanometern (nm) zu Millimetern (mm) und von Pikosekunden (ps) bis zu Millisekunden (ms). Sowohl das Potential, als auch die Limitierungen dieser Methoden wurden im Kontext von ausgewählten, aktuellen Anwendungen der Materialwissenschaften diskutiert. Ein besonderer Fokus lag dabei auf ferroischen Korrelationen, Phasenumwandlungen, sowie der Dynamik von Domänen in komplexen Systemen.

Zum ersten Mal nach den vergangenen Jahren der Pandemie wurde die Veranstaltung wieder in Präsenz abgehalten. Die Teilnehmer konnten dabei an Vorträgen von Rednern wie Prof. Xiaoqing Pan (University of California, Irvine), Dr. Miryam Arredondo (Queen's University Belfast, UK), Dr. Urs Staub (Paul Scherrer Institut, Schweiz) or Dr. Damien Alloyeau, (CNRS, France) und vielen anderen teilnehmen.

## 14<sup>th</sup> IKZ Summer School: Dynamics and processes in crystalline Materials

Advances in experimental instruments and techniques have paved the way for the investigation of functional materials in-situ and under operando conditions. A big step forward is the ability to study the transient state of crystalline materials in “realistic” conditions, such as under optical excitation, electric / magnetic fields or high temperature. These insights lead to a better understanding of non-equilibrium processes in materials and enable their optimization for highly efficient, stable and sustainable future technologies.

The 14th IKZ Summer School set the focus on a selection of the method developments with a high priority for the investigation of structural dynamics in crystalline materials in the fields of Transmission Electron Microscopy (TEM) and X-Ray Diffraction / Imaging (XRD). Common to these methods is the ability to capture phenomena on a broad range of time and length scales stretching from few nanometers (nm) to millimeters (mm) and picoseconds (ps) to milliseconds (ms). Potentials and limitations of the techniques were discussed in context of selected, recent applications in materials science. A special focus was set on ferroic correlations, phase transitions and domain dynamics in complex systems.

For the first time after the pandemic years, the event was held in presence. Participants could attend talks from speakers like Prof. Xiaoqing Pan (University of California, Irvine), Dr. Miryam Arredondo (Queen's University Belfast, UK), Dr. Urs Staub (Paul Scherrer Institut, Switzerland) or Dr. Damien Alloyeau, (CNRS, France) and many more.

<https://www.ikz-berlin.de/en/research/education>

# DYNAMICS AND PROCESSES IN CRYSTALLINE MATERIALS

Time resolved electron and X-ray studies

AUGUST 31 – SEPTEMBER 02, 2022 | BERLIN | GERMANY

## The Institute



### IKZ und FAIRmat Winterschule: Machine Learning in Materials Science and Crystal Growth

In Kooperation mit dem FAIRmat Konsortium fand vom 23.-25.1.2023 die 4. IKZ-FAIRmat Winterschule statt. Die Veranstaltung wurde als hybrides Event am Erwin-Schrödinger-Zentrum an der Humboldt Universität zu Berlin in Adlershof abgehalten. Insgesamt gab es 316 Teilnehmende aus 26 Ländern.

Machine Learning (ML) eröffnet völlig neue Möglichkeiten in der Materialwissenschaft. Fortschritte im Forschungsdatenmanagement und Softwaretools machen ML mehr und mehr zugänglich. Die gemeinsame Winter School von IKZ Berlin und FAIRmat hatte international renommierte Dozenten eingeladen, um eine Einführung des maschinellen Lernens in der Materialwissenschaft und im Kristallwachstum zu geben. Sie wandte sich damit an Wissenschaftler:innen, die sich erst seit kurzem mit diesem Gebiet beschäftigten. Die Vorlesungen behandelten die Grundlagen des maschinellen Lernens und der künstlichen Intelligenz, sowie das dazugehörige Datenmanagement. Es wurde erörtert, wie maschinelles Lernen eingesetzt werden kann, um automatisch Daten aus Experimenten zu extrahieren und wie es dazu beitragen kann, Entscheidungen zu treffen. Die Herausforderungen von ML bei kleinen Datensätzen und mögliche Lösungen wurden ebenso diskutiert wie die Frage: Was kann heute mit Hilfe von ML simuliert werden, was früher nicht möglich war? Alle Vorlesungen wurden durch ein hands-on Tutorial begleitet, in welchem die Teilnehmenden das Gelernte direkt umsetzen konnten. Die Dozenten der Winterschule waren: Dr. Luca Ghiringhelli (HU Berlin), Dr. Markus Scheidgen (HU Berlin), Prof. Bjørk Hammer (Aarhus University), Prof. Sergei Kalinin (The University of Tennessee), Dr. Daniel Schwalbe Koda (Lawrence Livermore National Laboratory), Dr. Kentaro Kutsukake (Nagoya University),

### IKZ and FAIRmat Winter School: Machine Learning in Materials Science and Crystal Growth

In cooperation with the FAIRmat consortium, the 4th IKZ-FAIRmat Winter School took place from 23-25.1.2023. The event was held as a hybrid event at the Erwin Schrödinger Center at the Humboldt University of Berlin in Adlershof. In total there were 316 participants from 26 countries.

Machine Learning (ML) opens up completely new possibilities in Materials Science. Advances in research data management and software tools make ML more and more accessible. The joint Winter School of IKZ Berlin and FAIRmat invited internationally renowned lecturers to introduce ML in materials science and crystal growth to all scientists new to this field. The lectures covered fundamentals of machine learning as well as artificial intelligence and explored the required data management. They addressed how to use ML to automatically extract data from experiments and to help making decisions. Challenges of ML with small data sets and possible solutions have been discussed, as well as the question: What can be simulated now with the help of ML which was not possible before?

All lectures were accompanied by a hands-on tutorial where participants could directly apply what they learned. The lecturers of the Winter School were: Dr. Luca Ghiringhelli (HU Berlin), Dr. Markus Scheidgen (HU Berlin), Prof. Bjørk Hammer (Aarhus University), Prof. Sergei Kalinin (The University of Tennessee), Dr. Daniel Schwalbe Koda (Lawrence Livermore National Laboratory), Dr. Kentaro Kutsukake (Nagoya University), Prof. Gian-Marco Ringanese (UC Louvain), Prof. Volker Deringer (University of Oxford).

More information, as well as slides, tutorials and video recordings at [www.ikz-berlin.de/4-ikz-winterschool](http://www.ikz-berlin.de/4-ikz-winterschool).

## The Institute

Prof. Gian-Marco Ringanese (UC Louvain), Prof. Volker Deringer (University of Oxford).

Mehr Informationen, sowie Folien, Tutorials und Videoaufzeichnungen finden sich auf [www.ikz-berlin.de/4-ikz-winterschool](http://www.ikz-berlin.de/4-ikz-winterschool).

### Workshop und Eröffnung des neuen Labors „Materialien für die Oxidelektronik“

Anlässlich der Eröffnung der Labors „Materialien für die Oxidelektronik“ fand im Februar 2022 ein Workshop mit rund 70 Teilnehmern statt, der sich mit der Herstellung, Charakterisierung und Anwendung von funktionalen Metalloxidschichten befasste. In seinem Hauptvortrag gab Prof. Dr. Josep Fontcuberta (Institut de Ciència de Materials de Barcelona ICMAB) einen Überblick über das Anwendungspotenzial von dünnen Oxidschichten für moderne Technologien. Andere Vorträge befassten sich speziell mit der Entwicklung von Leistungstransistoren auf der Grundlage von  $\text{Ga}_2\text{O}_3$ -Schichten und der Verwendung verschiedener Perowskit-Schichten für technologische Anwendungen wie akustische Oberflächenwellen (SAW), Speicher und optische Geräte.

Das Labor wurden vom Europäischen Fonds für regionale Entwicklung (EFRE) finanziert und verfügt über eine neue Anlage zur metallorganischen chemischen Gasphasenabscheidung (MOCVD) für die Epitaxie von Oxidschichten, sowie über weitere Geräte für die Charakterisierung und Materialanalytik.

Aufgrund der Pandemiesituation wurde der Workshop im Online-Format abgehalten.

### Workshop and opening of the new laboratory “Materials for Oxide Electronics”

For the opening of the laboratory “Materials for Oxide Electronics”, a workshop with about 70 participants was held in February 2022 with a focus on the fabrication, characterization and application of functional metal oxide films. In his key note lecture, Prof. Dr. Josep Fontcuberta (Institut de Ciència de Materials de Barcelona ICMAB) gave an overview on the application potential of thin oxide films for advanced technologies. Other presentations dealt specifically with the development of power transistors based on  $\text{Ga}_2\text{O}_3$  layers and the use of different perovskite layers for technological applications like surface acoustic waves (SAW), memory and optical devices.

The laboratory has been funded by the European Regional Development Fund ERDF, including a new Metal-Organic Chemical Vapor Deposition (MOCVD) system for the epitaxy of oxide layers and other equipment for characterization and material analytics.

Due to the pandemic situation, the workshop was held in online format.


**APPLICATION LABORATORY**  
**MATERIALS FOR OXIDE ELECTRONICS**  
**KICK OFF WORKSHOP**  
 FEBRUARY 10, 2022 | 10 AM BERLIN TIME (UTC+1) | ONLINE


**ikz** LEIBNIZ-INSTITUT FÜR KRISTALLZÜCHTUNG

## The Institute

### Prof. Oussama Moutanabbir mit dem IKZ International Fellowship Award 2022 ausgezeichnet

Die Zukunft wird „Quantum“. Quantentechnologien sind auf dem Vormarsch und die damit verbundene Forschung und Entwicklung an hochqualitativen Quantenmaterialien definieren diese Revolution. Das Leibniz-Institut für Kristallzüchtung (IKZ) hat seinen Fokus auf die Forschung an isopenangereicherten SiGe-basierten Quantenmaterialien gelegt und steht damit an der Spitze dieser Entwicklungen.

Der IKZ International Fellowship Award ehrt international renommierte, herausragende Wissenschaftler und Wissenschaftlerinnen auf diesem Gebiet, um in Zusammenarbeit mit dem IKZ neue Forschungsrichtungen und zukünftige drittmittelfinanzierte Projekte zu etablieren. Professor Oussama Moutanabbir von der Polytechnique Montréal, Kanada, erhielt den IKZ Award 2022 für seine herausragende Kompetenz im Bereich der isopenangereicherten SiGe-basierten Material- und Bauteilforschung, seine umfangreiche Erfolgsgeschichte an hochqualitativen wissenschaftlichen Publikationen, Drittmittelfinanzierung sowie seine Forschungsteamleitung.

Zusammen mit dem Preisgeld von 10.000 € wurde die Auszeichnung vom IKZ Direktor Prof. Thomas Schröder beim „IKZ workshop on SiGe-based materials for quantum technologies“ am 18. Mai 2022 überreicht. Der vom IKZ Nachwuchsforschungsgruppenleiter für SiGe-basierte Quantenmaterialien Dr. Kevin-Peter Gradwohl organisierte Workshop brachte führende Forschende des Feldes zusammen und wurde zu Ehren des verstorbenen langjährigen Kollegen und Freundes Dr. Petr Sennikov abgehalten. Die Veranstaltung bildete den Auftakt zu künftigen Forschungsvorhaben, Kooperationen und Industrieprojekten, wobei auch die Ausbildung von Nachwuchsforschenden im Vordergrund stand.



### Prof. Oussama Moutanabbir honored with the IKZ International Fellowship Award 2022

The future is Quantum. Quantum technologies are unfolding and the associated research and developments on high-quality quantum materials are driving this revolution. The Leibniz-Institut für Kristallzüchtung (IKZ) is at the forefront of these developments, specializing in the research on isotopically enriched SiGe-based quantum materials.

The IKZ International Fellowship Award honors internationally recognized, outstanding senior scientists in the field to establish in a collaboration with IKZ new research directions and future third-party-funded research projects. Professor Oussama Moutanabbir of the Polytechnique Montréal, Canada, received the IKZ International Fellowship Award 2022 for his outstanding expertise in isotopically enriched SiGe-based materials- and device research, extensive record of high-quality scientific publications, third-party funding, and research team supervision.

The award together with the prize money of 10.000 € was handed over by IKZ direction Professor Thomas Schröder at the “IKZ workshop on SiGe-based materials for quantum technologies” on May 18th, 2022. The workshop was organized by Dr. Kevin Gradwohl, head of the IKZ Junior Research Group on SiGe quantum materials. It brought together leading scientists of the field and was held in honor of late longtime colleague and friend Dr. Petr Sennikov. The event served as the kick-off for fruitful upcoming research proposals and rich future collaborations, including the training of next generation young researchers as well as industrial projects.

# Technologiesouveränität Technological Sovereignty

## Das Leibniz-Strategieforum „Technologische Souveränität“

## The Leibniz Strategy Forum “Technological Sovereignty”



Social crises such as the Corona pandemic or the war in Ukraine make us aware of the fragility of supply chains that we thought were secure. This makes the importance of European technological sovereignty, which is based on managing as many interlinked competences as possible along the value chain of key technologies, even more evident (see Fig. 1). Based on a highly complex, innovative system goods industry, which often requires non-linear networking of the most diverse expertise and partners, European prosperity can only be preserved in the long term through the international competitiveness of the European high-tech economy.

Abb. 1  
Technologische Souveränität erfordert einen „Deep Technology“-Ansatz entlang der gesamten Wertschöpfungskette; mittels vielfältiger Vernetzung mit Partnern mit komplementärer Expertise liefern Leibniz-Institute wesentliche Beiträge in F & E sowie der Ausbildung (blauer Bereich).



Fig. 1  
Technological sovereignty requires a “deep technology” approach along the entire value chain; by means of diverse networking with partners with complementary expertise, Leibniz institutes provide essential contributions in R & and education (blue area).

Gesellschaftliche Krisen wie die Corona-Pandemie oder der Krieg in der Ukraine vergegenwärtigen uns die Zerbrechlichkeit sicher geglaubter Lieferketten. Umso zentraler wird die Bedeutung der europäischen Technologie-Souveränität, die auf der Beherrschung möglichst vieler miteinander verknüpfter Kompetenzen entlang der Wertschöpfungskette von Schlüsseltechnologien gründet (siehe Abb. 1). Basierend auf einer hochkomplexen, innovativen Systemgüterindustrie, die oft eine nicht-lineare Vernetzung verschiedenster Expertisen und Partner erfordert, kann der europäische Wohlstand langfristig nur durch die internationale Wettbewerbsfähigkeit der europäischen Hochtechnologie-Wirtschaft gewahrt werden.

## The Institute

Mit der Gründung des Leibniz-Strategieforums „Technologische Souveränität“ (2021) möchte die Leibniz-Gemeinschaft einen effektiven Beitrag zur Stärkung der technologischen Souveränität von Deutschland und Europa leisten. Die Leibniz-Gemeinschaft konzentriert ihre Aktivitäten dabei natürlich auf Forschung und Entwicklung sowie Bildung und Vermittlung. Alleinstellungsmerkmale der Gemeinschaft sind die Fähigkeiten:

- Wertschöpfungsketten von der Grundlagen- über die Anwendungsforschung oft bis zu (kleinskaligen) prototypischen Lösungen der Gesellschaft anzubieten (siehe blaue Hinterlegung in der Abb.)
- gesellschaftliche und wirtschaftliche Herausforderungen mit hoher Inter- und Transdisziplinarität holistisch, effizient und nachhaltig anzugehen

Die Zuständigkeit des Strategieforums umfasst die interne Organisation der Leibniz-Beiträge sowie die Gewährleistung von deren Anknüpfungsfähigkeit zur Verwertung durch weitere Partner. Das IKZ übernimmt die Federführung der Organisation des Leibniz-TS-Forums mit Herrn Prof. Thomas Schröder als Sprecher. Sechs Leibniz-Cluster wurden im Forum zu den folgenden Schlüsseltechnologien entwickelt: Gesundheitstechnologien, Künstliche Intelligenz, Materialien für die Digitalisierung, Quantentechnologien, Wasserstoffwirtschaft und Kommunikation & Mikroelektronik. Um den holistischen Ansatz des Strategieforums weiter auszubauen, wurde im Herbst 2022 zudem der Cluster Wirtschafts- und Sozialwissenschaften gegründet. Clustersprecher ist hier Herr Prof. Dirk Dohse, Leiter des Forschungszentrums Innovation und Internationaler Wettbewerb am IfW Kiel.

## Veranstaltungen

### 02.12.22 Fachgespräch der UNESCO:

Open Science in Deutschland – Quo vadis?

### 06.11.22 Podiumsdiskussion bei der Berlin Science Week 2022:

Notwendigkeit von Inter- und Transdisziplinarität

### 18.10.22 Berlin University Alliance (BUA)-Paneldiskussion:

Grenzen und Chancen der Offenheit? Was Technologiesouveränität und Geopolitik für Innovation in Forschung und Technologie bedeuten (siehe Abb. 2)

### 01.10.22 Leibniz-Führungskolleg:

Lernen aus Krisen – Stärkung organisationaler Resilienz in der Leibniz-Gemeinschaft

### 09.09.22 BMBF / BMWK Workshop:

Nationale Sicherheitsstrategie – Dialogprozess; Workshop „Technologische und digitale Souveränität im Kontext der Zeitenwende“

With the establishment of the Leibniz Strategy Forum “Technological Sovereignty” (2021), the Leibniz Association aims to make an effective contribution to strengthening the technological sovereignty of Germany and Europe. The Leibniz Association certainly focuses its activities thereby on research and development along with education and outreach. Two unique selling points of the Association are its capabilities of:

- Offering value chains from basic to applied research often to (small-scale) prototypical solutions to society (see blue background in the figure).
- Addressing societal and economic challenges holistically, efficiently and sustainably with a high degree of inter- and transdisciplinarity.

The responsibility of the Strategy Forum includes the internal organisation of Leibniz contributions as well as ensuring their connectivity for utilisation by other partners. The IKZ takes the lead in organising the Leibniz TS Forum with Prof. Thomas Schröder as spokesperson. Six Leibniz clusters were developed in the forum on the following key technologies: Health Technologies, Artificial Intelligence, Materials for Digitalisation, Quantum Technologies, Hydrogen Economy and Communication & Microelectronics. To further expand the holistic approach of the Strategy Forum, the Economics and Social Sciences Cluster was also founded in autumn 2022. The cluster spokesperson here is Prof. Dirk Dohse, Head of the Research Centre Innovation and International Competition at IfW Kiel.

## Events

### 02.12.22 UNESCO expert discussion:

Open Science in Germany - Quo vadis?

### 06.11.22 Panel discussion at Berlin Science Week 2022:

Necessity of Inter- and Transdisciplinarity

### 18.10.22 Berlin University Alliance (BUA)-Panel Discussion:

Limits and Opportunities of Openness? What technology sovereignty and geopolitics mean for innovation in research and technology (see Fig. 2)

### 01.10.22 Leibniz Leadership College:

Learning from Crises - Strengthening Organisational Resilience in the Leibniz Association

### 09.09.22 BMBF / BMWK Workshop:

National Security Strategy - Dialogue Process; Workshop “Technological and digital sovereignty in the context of the changing times”.





Abb. 2

Berlin University Alliance (BUA)-Paneldiskussion zum Thema: Gibt es Grenzen der Offenheit? Und wenn ja, wer bestimmt, wie diese gezogen werden? Diesen Themenkomplex wurde am 18. Oktober 2022 im Quadriga Forum mit einem hochrangigen Panel diskutiert. Nach einem Input von Dr. Tim Rühlig (Stiftung Wissenschaft und Politik) diskutierten Laura Kraft (MdB, Bündnis90/Die Grünen, Obfrau im Ausschuss Bildung, Forschung und Technikfolgenabschätzung), Dr. Thomas Koenen (BDI e.V., Leiter der Abteilung Digitalisierung und Innovation), Dr. Henriette Litta (Geschäftsführerin der Open Knowledge Foundation DE) und Prof. Dr. Thomas Schröder (IKZ, Sprecher des Leibniz-Strategieforums Technologische Souveränität). Abbildung der Personen von links nach rechts: Clemens Blümel (DZHW), Henriette Litta (OKFN), Thomas Koenen (BDI), Thomas Schröder (IKZ).

Fig. 2

Berlin University Alliance (BUA) panel discussion on the topic: Are there limits to openness? And if so, who determines how these are drawn? This complex of topics was discussed with a high-level panel at the Quadriga Forum on 18 October 2022. After input from Dr Tim Rühlig (Stiftung Wissenschaft und Politik), Laura Kraft (Member of the German Bundestag, Bündnis90/Die Grünen, Chairwoman of the Committee on Education, Research and Technology Assessment), Dr Thomas Koenen (BDI e.V., Head of the Department of Digitalisation and Innovation), Dr Henriette Litta (Executive Director of the Open Knowledge Foundation DE) and Prof. Dr Thomas Schröder (IKZ, Spokesperson of the Leibniz Strategy Forum Technological Sovereignty) discussed the topic. Picture of the persons from left to right: Clemens Blümel (DZHW), Henriette Litta (OKFN), Thomas Koenen (BDI), Thomas Schröder (IKZ).

## Veröffentlichungen und Interviews

### 22.06.22 Pressemitteilung im

#### DGKK-Mitteilungsblatt:

Das Leibniz-Strategieforum „Technologische Souveränität“

### 09.06.22 Artikel im Forschungskosmos der ZEIT:

Das Leibniz-Strategieforum „Technologische Souveränität“

### 02.02.22 Forschungsverbund Berlin e. V.:

Interview mit Herrn Prof. Schröder:  
„Wir können Vorbild sein“

## Publications and interviews

### 22.06.22 Press release in the DGKK newsletter:

The Leibniz Strategy Forum on Technological Sovereignty

### 09.06.22 Article in the ZEIT's Forschungskosmos:

The Leibniz Strategy Forum “Technological Sovereignty”

### 02.02.22 Forschungsverbund Berlin e. V.:

Interview with Prof. Schröder: “We can be a model”

# Nachwuchs Young Talents

## Bericht der Promovierenden

Durch den Ukraine-Konflikt war das Jahr 2022 sicherlich eine Herausforderung für jeden in Deutschland und auch weltweit. Nicht nur die gestiegenen Strompreise, sondern auch das Angebot an relevanten Rohmaterialien änderte sich, was Einfluss auf die Forschenden weltweit hat. Trotzdem hat sich die IKZ-Community, einschließlich der Promovierenden, schnell und gut angepasst: Neue Stromsparpläne wurden entwickelt und wir mussten unsere Kreativität und Geduld im Umgang mit Lieferanten einsetzen. Unsere IKZ-Kollegen waren in dieser Zeit sehr hilfsbereit und halfen bei der Bewältigung von Hindernissen, mit denen wir Promovierenden konfrontiert wurden.

Was das Sozialleben betrifft, waren die Covid-19-Regelungen weniger streng, so dass Grillabende und andere Veranstaltungen wie Seminare wieder in Präsenz stattfinden konnten. Im September waren wir zu einem Ausflug zum Deutsches Elektronen-Synchrotron (DESY) in Hamburg eingeladen. Dort begrüßte uns Dr. Peter Gaal und erklärte uns, zusammen mit seinem Team, wie er sein Start-up (Txproducts UG) gegründet hat und welche Möglichkeiten DESY bietet, um verschiedene Start-ups auf ihrem Campus unterzubringen. Anschließend konnten wir ihre Labore besichtigen und auch DESY-Vertreter kennenlernen. Dies gewährte uns einen aufschlussreichen Überblick über ihre Interaktion mit der nicht-wissenschaftlichen Gemeinschaft und darüber, wie Wissenschaftler und Institute dazu beitragen können, die Gesellschaft in Richtung Nachhaltigkeit, Frieden und Wissen zu lenken. Schließlich wird eine größere Integration zwischen Promovierenden des IKZ und dem Nachbarn Max-Born-Institut (MBI) angestrebt, so dass gemeinsame Aktivitäten geplant werden.

Im Jahr 2022 traten 10 neue Doktorand:innen unserem Institut bei. Des Weiteren haben 6 von uns ihre Arbeit erfolgreich verteidigt. Wir freuen uns auf weitere Verteidigungen, neue Doktoranden, Grillabende und Ausflüge im Jahr 2023!

## Report of the PhD students

The year of 2022 was certainly a challenging one for everyone in Germany, and perhaps globally, due to the upheavals caused by the war in Ukraine. Not only electricity prices surged, but also the offer of raw materials changed, affecting researchers everywhere. Nevertheless, the IKZ community, including PhD students, adjusted quickly and well: new electricity saving plans were laid out and we had to exercise our creativity and patience when it came to dealing with suppliers. Our IKZ colleagues were very helpful during this time with providing guidance and offering new ideas for obstacles PhD students were faced with.

When it comes to socializing, the Covid-19 regulations were less strict, meaning that PhD events, such as seminars and the traditional monthly barbecue, could restart to be held in person once again. In September, we went on an excursion to the Deutsches Elektronen-Synchrotron (DESY) in Hamburg. There, Dr. Peter Gaal welcomed us and, along with his team, explained to us how he founded his Start-up (Txproducts UG) and the possibilities that DESY offers to accommodate different start-ups in their Campus. Afterwards, we got to visit their labs and to meet DESY representatives, giving us an enlightening overview of their interaction with the non-scientific community and how scientists and institutes can help in guiding society towards sustainability, peace and knowledge. Finally, more integration between PhD students from IKZ and the neighbor Max-Born-Institut (MBI) is sought, so common activities are being planned.

In 2022, 10 new PhD students joined our institute, and 6 of us successfully defended their thesis. We are looking forward to more defenses, new PhD students, barbecues and excursions in 2023!



## The Institute

### Walter Benjamin-Stipendium der DFG an IKZ Postdoc Dr. Andrew Klump

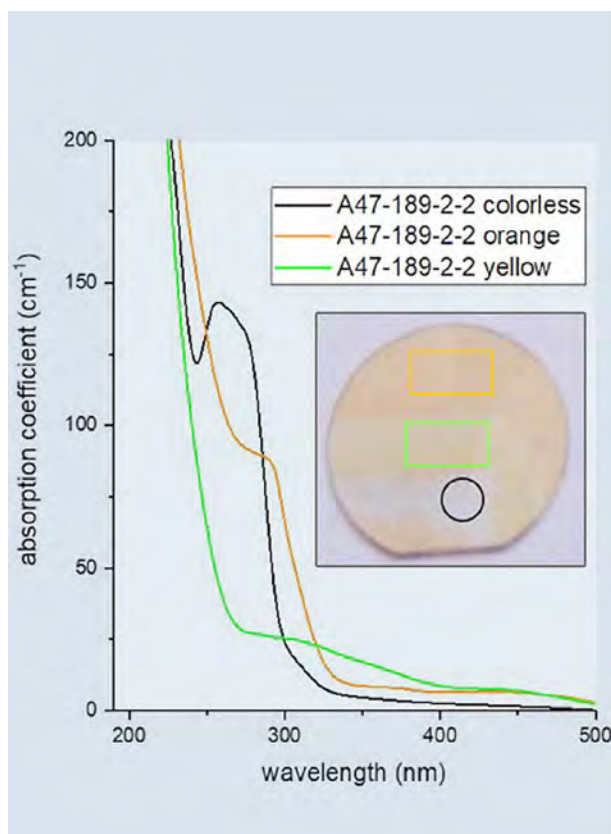
Andrew Klump von der Arbeitsgruppe Aluminiumnitrid-Kristallzüchtung wurde für sein Projekt „C, O, Si-Impurities in PVT-AIN – Incorporation and Measurement by SIMS/Absorption“ mit dem Walter Benjamin Fellowship ausgezeichnet. Das Stipendium wurde von der DFG ins Leben gerufen, um Wissenschaftlerinnen und Wissenschaftler in der Postdoc-Phase individuell zu fördern und ihnen die Möglichkeit zu geben, ihre Forschung thematisch weiterzuentwickeln.

Andrew beschäftigte sich mit dem Thema der III-Nitride bereits als Sekundärionen-Massenspektrometrie-Analyst bei EAGlabs, Inc., bevor er an der North Carolina State University bei den Professoren Zlatko Sitar und Ramón Collazo promovierte. Sein durch die DFG gefördertes Projekt befasst sich nun mit der Korrelation zwischen Verunreinigungen und UV-Absorption in PVT-gewachsenen AlN-Kristallen. Insbesondere geht es darum, die Absorption bei Wellenlängen kleiner als 270 nm zu reduzieren, ein wichtiger Punkt für die Verwendung von AlN-Substraten in UV-LEDs und LDs für die Desinfektion oder Wassersterilisation

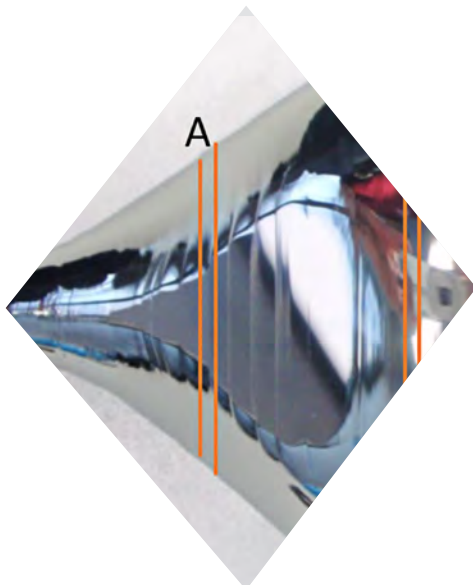
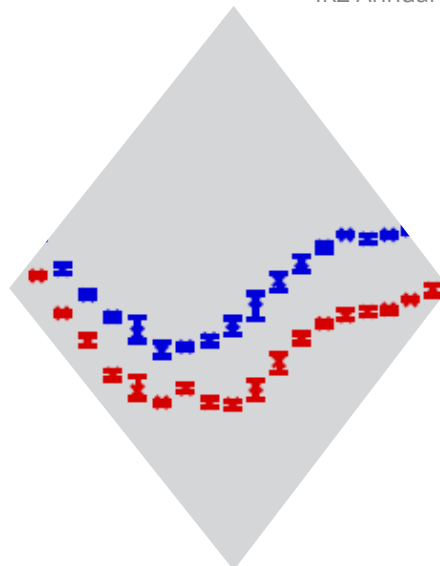
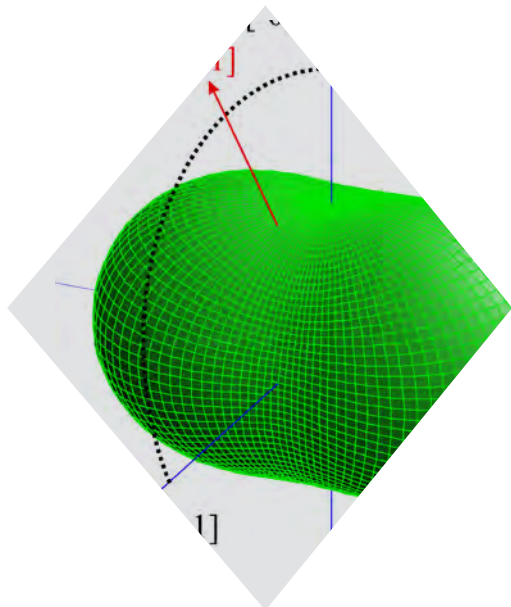
### Walter Benjamin Fellowship of the DFG for IKZ Postdoc Dr. Andrew Klump

Andrew Klump is a postdoctoral researcher in the Aluminium Nitride crystal growth group at IKZ, and has been granted the Walter Benjamin Fellowship for his project “C, O, Si-Impurities in PVT-AIN – Incorporation and Measurement by SIMS/Absorption.” The fellowship of the DFG intends to independently fund researchers in their postdoctoral phase and give them the opportunity to advance the thematic development of their research.

Andrew began his career in the III-Nitrides as a secondary ion mass spectrometry analyst at EAGlabs, inc. before earning his Ph.D. at North Carolina State University under Professors Zlatko Sitar and Ramón Collazo. With this project he addresses the correlation between impurities and UV absorption in PVT-grown AlN crystals. In particular, the aim is to reduce absorption at wavelengths shorter than 270 nm, an important issue for the use of AlN substrates in UV LEDs and LDs for disinfection or water sterilization.







# Volume Crystals

# The thermal conductivity tensor of $\beta\text{-Ga}_2\text{O}_3$ from 250 to 1275 K

D. Klimm, B. Amgalan, S. Ganschow, A. Kwasniewski, Z. Galazka, and M. Bickermann

Leibniz-Institut für Kristallzüchtung (IKZ), Berlin, Germany

For gallium oxide at least five polymorphs are reported. In the bulk and under ambient pressure, only the monoclinic  $\beta\text{-Ga}_2\text{O}_3$  structure is stable between the melting point and room temperature. The crystal structure belongs to the monoclinic point group  $C2/m$ , with lattice parameters  $a = 12.214 \text{ \AA}$ ,  $b = 3.0371 \text{ \AA}$ ,  $c = 5.7981 \text{ \AA}$ ,  $\beta = 103.83^\circ$ . This material is an emerging transparent semiconducting oxide, with possible applications in electronics and sensing. The worldwide first small Czochralski crystals were grown at IKZ more than two decades ago [1], but meanwhile diameters exceeding 2 inch are available from our institute [2].

Resulting from the low symmetry of the point group  $C2/m$ , many physical properties are expected to possess high anisotropy, and this anisotropy must be considered, e.g., for the construction of devices. Here the thermal conductivity plays a significant role, because heat resulting from thermal losses during device operation must be removed. Thermal conductivity  $\lambda$  is described by a tensor of rank two, hence, a symmetric  $3 \times 3$  matrix with 9 coefficients  $\lambda_{ij} = \lambda_{ji}$  ( $i, j = 1 \dots 3$ ). For monoclinic crystals with the 2-fold axis in  $[010]$ , the coefficients  $\lambda_{11}$ ,  $\lambda_{22}$ ,  $\lambda_{33}$ , and  $\lambda_{13} = \lambda_{31}$  are independent parameters [3]. The main axis coefficients  $\lambda_{11}$ ,  $\lambda_{22}$ , and  $\lambda_{33}$  are positive definite, because heat energy flows always from the hot to the cold.

Thermal conductivity measurements for  $\beta\text{-Ga}_2\text{O}_3$  were reported recently by several authors for temperatures between 80 K and 450 K. All these reports, however, are defective for different reasons:

Guo et al. [4] measured  $\lambda$  in the four independent directions  $[001]$ ,  $[100]$ ,  $[010]$ , and  $[-201]$ . Unfortunately, they did not analyze experimental data in terms of a proper tensor description and draw the wrong conclusion, that both the directions of highest and lowest conductivity correspond with one of the crystallographic axes. This must be wrong, because the crystal possesses only one 2-fold axis in direction  $[010]$ . The representation surface of the tensor, in contrast, has symmetry  $2/m 2/m 2/m$ , with three mutual perpendicular 2-fold axes pointing towards the directions of highest, lowest, and an intermediate conductivity – the latter typically on a saddle point.

In Fig. 1, these three directions are  $[0,1,0]$ ,  $[2.439,0,1]$ , and  $[-0.410,0,1]$ . The results by Guo et al. are for  $T \geq 300 \text{ K}$  in good agreement with our own measurements, and could even be used to extend the  $T$  range below room temperature, down to 250 K. For significantly lower  $T$ , however, their experimental data are incompatible because they would result in negative eigenvalues of the  $\lambda$  tensor, which is not allowed.

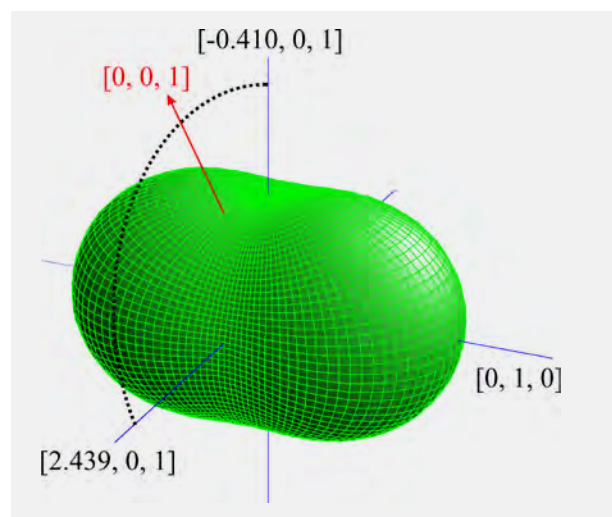


Fig. 1

The representation surface of  $\beta\text{-Ga}_2\text{O}_3$  at 300 K shows in every direction  $\mathbf{n}$  the corresponding value  $\lambda(\mathbf{n})$ . The maximum conductivity occurs in the direction of the crystallographic  $\mathbf{b}$  axis  $[0,1,0]$ .

Handwerg et al. [5] measured  $\lambda$  only in the directions of the three crystallographic axes, which is insufficient for the calculation of the four independent components of the  $\lambda$  tensor. Their maximum and minimum values at room temperature,  $29 \text{ Wm}^{-1}\text{K}^{-1}$  in  $[0,1,0]$  and  $11 \text{ Wm}^{-1}\text{K}^{-1}$  in  $[1,0,0]$ , however, are in good agreement with the results presented by Guo et al. and in this study.

## Volume Crystals

Jiang et al. [6] used the alternative setting of the monoclinic coordinate system, with the 2-fold axis parallel  $[0,0,1]$ , resulting in  $\lambda_{12} \neq 0$ . Also, their experimental data are in fairly good agreement with the results mentioned above. Unfortunately, the representation surface was fitted mistakenly by an ellipsoid. This is not justified, because the shape of this surface is significantly different from an ellipsoid – especially for strong anisotropy (cf. Fig. 1). Only the characteristic surface of this tensor, which was not used by Jiang et al., is an ellipsoid [3].

In the framework of her Bachelor thesis (TU Berlin, 2022), Bideriya Amgalan measured the thermal conductivity of  $\beta\text{-Ga}_2\text{O}_3$  between room temperature and 1200 K with the laser flash method. There a short (ca. 1 millisecond) laser pulse heats the bottom surface of a flat sample disc. By thermal conduction, the heat diffuses to the top surface which is observed by an infrared detector. From the detector signal vs. time function, the device calculates the thermal diffusivity. Thermal diffusivity, multiplied by the specific heat capacity  $c_p$  and the mass density  $\rho$ , gives the thermal conductivity.  $\lambda$  was obtained by this method perpendicular to the (001), (100), (010), and (-201) faces of the crystal, in contrast to the previous works [4-6] where  $\lambda$  was measured parallel to a crystallographic direction. This difference is significant in materials with lower than cubic symmetry.

The thesis of B. Amgalan was the basis for a recent publication in *Crystal Research & Technology* [7]; the figures shown here are slightly amended versions of figures from this article. It should be noted that for symmetry reasons only the long axis of the representation surface in Fig. 1 is pinned to the crystallographic axis  $[0,1,0]$ , but the surface is free to rotate around this axis, e.g. for different temperatures  $T$ . Fig. 2 shows that for higher  $T$  not only the representation surface shrinks, because the thermal conductivity becomes smaller. Moreover, the surface turns around the  $\mathbf{b}$  axis (which peaks out off the drawing plane) counterclockwise by ca.  $22^\circ$ , so that above ca. 500 K the minimum conductivity occurs in a direction perpendicular to the crystallographic  $\mathbf{b}$  and  $\mathbf{c}$  axes. At 300 K, the minimum value of  $\lambda$  is ca. 3.4% lower than the value in  $[1,0,0]$ .

This publication is the first self-consistent description of the  $\lambda$ -tensor for  $\beta\text{-Ga}_2\text{O}_3$  between 250 K and 1275 K, reporting for the first time the thermal conductivity for elevated  $T > 450$  K. The high-temperature conductivity data are relevant for the numerical simulation of temperature fields in the crystal growth process, as well as in electronic devices made of  $\beta\text{-Ga}_2\text{O}_3$ .

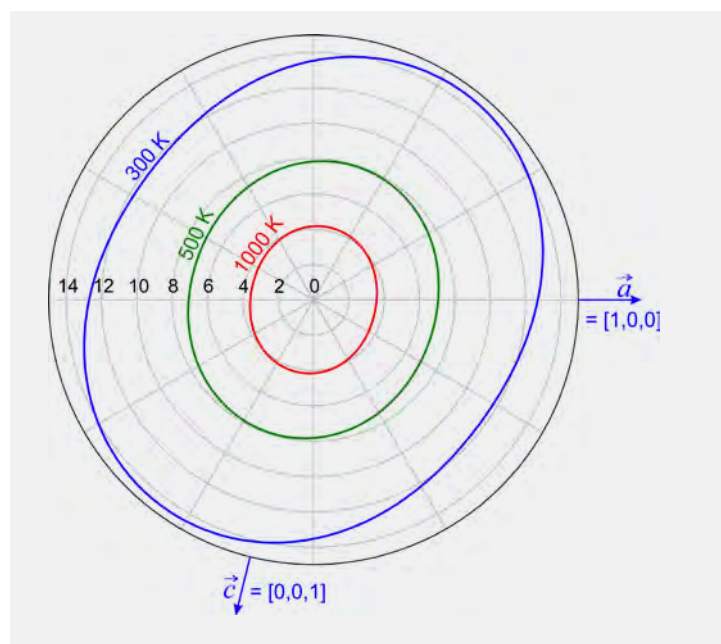


Fig. 2  
Section through the representation surface perpendicular to the 2-fold axis  $[0,1,0]$ , for three different temperatures. The  $\mathbf{b}$  axis sticks out vertically from the drawing plane. Radius scaling in  $\text{Wm}^{-1}\text{K}^{-1}$  [7]

## References

- [1] Y. Tamm, P. Reiche, D. Klimm, T. Fukuda, J. Crystal Growth (2000) Vol. 220, 510.
- [2] Z. Galazka, J. Appl. Phys. (2022) Vol. 131, 031103.
- [3] J. F. Nye, Physical Properties of Crystals, Clarendon, Oxford (1957).
- [4] Z. Guo, A. Verma, X. Wu, F. Sun, A. Hickman, T. Masui, A. Kuramata, M. Higashiwaki, D. Jena, T. Luo, Appl. Phys. Lett. (2015) Vol. 106, 111909.
- [5] M. Handweg, R. Mitdank, Z. Galazka, S. F. Fischer, Semicond. Sci. Technol. (2015) Vol. 30, 024006 & *ibid.* (2016) Vol. 31, 125006.
- [6] P. Jiang, X. Qian, X. Li, R. Yang, Appl. Phys. Lett. (2018) Vol. 113, 232105 & *ibid.* (2019) Vol. 114, 049902.
- [7] D. Klimm, B. Amgalan, S. Ganschow, A. Kwasniewski, Z. Galazka, M. Bickermann, Cryst. Res. Technol (2023) Vol. 59, 2200204.

# Quasi-monocrystalline silicon for low-noise end mirrors in cryogenic gravitational-wave detectors

F.M. Kiessling<sup>1</sup>, P. G. Murray<sup>2</sup>, M. Kinley-Hanlon<sup>2</sup>, I. Buchovska<sup>1</sup>, T. K. Ervik<sup>1,3</sup>, V. Graham<sup>2</sup>, J. Hough<sup>2</sup>, R. Johnston<sup>2</sup>, M. Pietsch<sup>1</sup>, S. Rowan<sup>2</sup>, R. Schnabel<sup>4</sup>, S. C. Tait<sup>2</sup>, J. Steinlechner<sup>2,4,5,6</sup>, and I. W. Martin<sup>2</sup>

<sup>1</sup> Leibniz-Institut für Kristallzüchtung, Berlin, Germany

<sup>2</sup> School of Physics and Astronomy, University of Glasgow, Glasgow, United Kingdom

<sup>3</sup> National Institute of Occupational Health, Oslo, Norway

<sup>4</sup> Institut für Laserphysik und Zentrum für Optische Quantentechnologien, Universität Hamburg, Hamburg, Germany

<sup>5</sup> Maastricht University, Department of Gravitational Waves and Fundamental Physics, Maastricht, Netherlands

<sup>6</sup> National Institute for Subatomic Physics, Amsterdam, Netherlands

In 1916, Albert Einstein predicted the existence of gravitational waves (GW). A century later on 14.09.2015, the Laser Interferometer Gravitational-wave Observatory (LIGO) observed GW from the merging of two black holes for the first time [2]. Gravitational-wave detectors are km-scale interferometers which measure relative strains in space induced by passing gravitational waves. Highly reflective coated mirrors form the core components of these instruments, with the detector monitoring the relative separation of the mirrors in two perpendicular arms. In order to detect more gravitational waves from a wider range of sources, the detection sensitivity has to be continuously improved. Detectors of the second generation operate at room temperature using mirror substrates made of fused silica ( $\text{SiO}_2$ ) while detectors of the 3<sup>rd</sup> generation operating at cryogenic temperatures are designed to further reduce the thermal noise of the mirrors. The mechanical loss, which determines the magnitude of the thermal noise, of fused silica increases by several orders of magnitude when cooling from room temperature to 20 K. A different material is therefore required for the mirror substrates in a cryogenic detector. The European Einstein Telescope (ET) is a vision for the next (3<sup>rd</sup>) generation of GW detectors [3]. One component of the conceptual ET design study are 200 kg test-mass mirrors from single crystalline silicon with diameters of  $\approx 50$  cm.

Although there exist various techniques to produce silicon single crystals, the diameter of the crystals is the first criterion to consider. Since the size of a mirror has to be about  $\approx 50$  cm in diameter, single crystalline silicon of highest perfection cannot be provided by the crucible-free float zone technique. Even dislocation free silicon single crystals, which have been grown by the Czochralski (Cz) method, might not fulfill the proposed

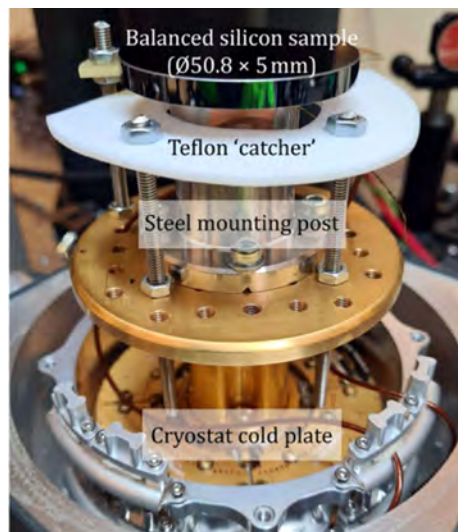


Fig. 1  
Image of the  $\langle 100 \rangle$ -oriented QM disk balanced on top of a rounded silicon lens inside the  $10 \times 10 \text{ cm}^2$  experimental chamber of the Montana Instruments s100 Cryostation [1].

size required for the Einstein Telescope [3, 4]. An interesting approach to overcome the size problem is the use of silicon grown by directional solidification (DS). DS-Si can be grown as quasi-mono ingots with far bigger sizes needed here and might be available on the market by request. Unfortunately, this quasi-mono silicon has the lowest material quality compared to the dislocation-free silicon crystals mentioned above. But, since the oxygen level in directional solidified silicon material is lower than the one in Cz-Si crystals, the use of DS-Si might nevertheless be a promising approach. Thus, the defect limits have to be investigated in order to evaluate its suitability for the use as a future gravitational-wave detector “end test mass” mirrors material.



## Volume Crystals

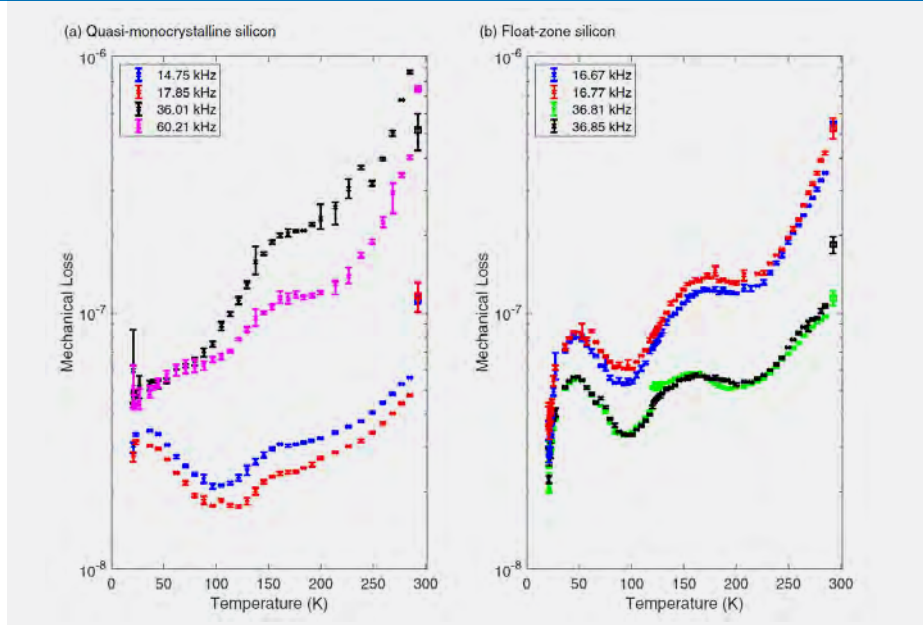


Fig. 2  
Mechanical loss as a function of temperature, from 4 to 300 K, of the 50.8-mm-diameter  $\times$  5-mm-thick QM disk (left) and FZ disk (right) samples [1].

Single-crystalline float-zone silicon used for comparison meets the requirements of low mechanical loss and low optical absorption. In this study, test samples have been prepared using a quasi-mono (QM) silicon ingot originally grown for photovoltaic applications. Microwave detected photoconductivity method, FTIR and conductivity measurements are performed in order to characterize the material regarding carrier lifetime, concentration of substitutional carbon  $C_s$ , interstitial oxygen  $O_i$  and electrical resistivity, respectively. Mechanical loss and absorption measurements have been carried out.

Figure 1 shows a photo of the setup used for cryogenic mechanical loss measurements. The polished disk with a dimension of 50.8 mm in diameter and 5 mm thickness (top of the picture) being measured was balanced on a silicon spherical lens, where it balanced freely throughout the measurements.

Mechanical loss is a measure of the magnitude of internal friction in a material. The thermal displacement noise arising from a mirror substrate in a gravitational-wave detector (in  $m/Hz^{1/2}$ ) is proportional to the square root of the mechanical loss of the mirror material. Figure 2 shows the mechanical loss as a function of temperature for four resonant modes of the  $\langle 100 \rangle$ -oriented QM disk compared with the mechanical loss of a float-zone  $\langle 111 \rangle$  silicon sample of the same dimensions (named “FZ disk”). The mechanical loss of the QM disk shows a very similar trend to the losses measured for the FZ disk. For some resonant modes, the mechanical loss is lower than that of the FZ disk. At 20 K the lowest mechanical loss measured on the QM disk was  $2.6 \times 10^{-8}$  at 17.8 kHz which is marginally higher than the lowest loss measured at 36.81 kHz on the FZ disk of  $\approx 2 \times 10^{-8}$ . At 120 K the losses of all the modes measured were below  $\approx 2 \times 10^{-7}$ . These results are very promising for the quasi-monocrystalline material, making it potentially relevant for use in cryogenic gravitational-wave detectors.

The measured optical absorption of  $\approx 5\% \text{ cm}^{-1}$  is consistent with the intentional boron-doping level of  $0.9 \text{ } \Omega \text{ cm}$ . As expected due to the doping the absorption was significantly higher than the value, of  $5\text{-}10 \times 10^{-6} \text{ cm}^{-1}$ , usually thought to be required for a gravitational-wave detector mirror. However, it is interesting to note that only the “input test masses” (ITMs) in the arm cavities of a gravitational-wave detector are required to transmit significant laser power and this absorption level of the QM material is far too high. The “end test masses” (ETMs), however, do not have significant power transmitted through them and somewhat higher absorption can therefore be tolerated in comparison to the ITMs. However, this QM material had not been optimized for low optical absorption, which would be the next obvious development step.

More detailed information can be found in the original publication [1].

## References

- [1] F. M. Kiessling, P. G. Murray, M. Kinley-Hanlon, I. Buchovska, T. K. Ervik, V. Graham, J. Hough, R. Johnston, M. Pietsch, S. Rowan, R. Schnabel, S. C. Tait, J. Steinlechner, and I. W. Martin, *Phys. Rev. Research* 4, 043043 (2022).
- [2] B. P. Abbott *et al.* (LIGO Scientific Collaboration and Virgo Collaboration), *Phys. Rev. Lett.* 116, 061102 (2016).
- [3] <https://www.et-gw.eu/index.php/relevant-et-documents>.
- [4] J. Steinlechner, *Phil. Trans. R. Soc. A* 376, 20170282 (2018).

# Development of large-diameter and very high purity Ge crystal growth technology

R. Radhakrishnan Sumathi, A. Gybin, K-P. Gradwohl, P.C. Palleti, M. Pietsch, K. Irmscher, Natasha Dropka, U. Juda

Leibniz-Institut für Kristallzüchtung, Berlin, Germany

High purity germanium (HPGe) single crystals find their application as detecting medium in radiation and spectroscopy detectors and are mostly used in experiments dealing with highest energy resolution, like astro-particle physics, dark matter research, and as best solution for precise gamma- and X-ray spectroscopy. Ge is much more pure and efficient than Silicon (Si) for radiation detection due to its high mass number ( $Z=32$ ). The optimum resolution of such semiconductor detectors can be achieved by adjustment of the dislocations and impurities in the crystal. As a rule of thumb for a detector-grade crystal, the net charge carrier (electron or hole) concentration ( $n$  or  $p$ ) must be about  $10^{10} \text{ cm}^{-3}$  and its dislocation density should be above  $100 \text{ cm}^{-2}$  but should not exceed  $10000 \text{ cm}^{-2}$ . However, it is one of the challenging tasks to grow “detector-grade” HPGe single crystals with these tailored properties uniform throughout the crystal.

At IKZ, we have established the necessary process steps to obtain HPGe single crystals with the above mentioned required properties in-house: (i) reducing  $\text{GeO}_2$  powder into Ge metal; (ii) multi-zone-refining of Ge starting source material up to ultra-high-purity (13N); (iii) Czochralski (Cz) growth of HPGe single crystals. All these processes are carried out in hydrogen atmosphere to prevent the introduction of oxygen and also other impurities. In total, 50 kg of isotopic  $^{76}\text{GeO}_2$  has been reduced into  $^{76}\text{Ge}$  at our lab. The entire process value chain for the preparation of a detector block is shown in Figure 1, where the major process steps established in our lab are highlighted in our bold.

For the realization of radiation detectors, it is necessary to have larger diameter crystals. For instance, the Large Enriched Germanium Experiment for Neutrinoless  $\beta\beta$  Decay (LEGEND) Collaboration [1] is planning a ton-scale experiment, where larger detectors are required to reduce the complicated electronics parts in the underground experimental set-up at the Gran Sasso National Laboratory (Italy). This collaboration involves more than 50 research institutes from Europe, the USA and Canada.

The motivation of using Ge to this astro-particle physics experiment is the quest for unraveling the Majorana nature of neutrinos and further more details about this expediting discovery physics program can be found elsewhere [1, 2]. The future research for the HPGe material is now also driven by other possible applications, like environmental radiation detection, isotope identification and in medical applications.



Fig. 1

Process chain of high-purity germanium (HPGe). The main process steps highlighted in bold are established at IKZ, Berlin (fig. reprinted from [3], ©copyright, under CC-BY-NC 2023)

HPGe single crystals of 3.5 kg mass and 75 – 80 mm diameter were grown using the custom-built 3-inch Cz growth system. The zone refined Ge bars of very high purity were used as starting materials for the crystal growth. Both,  $\langle 100 \rangle$ ,  $\langle 111 \rangle$  oriented, crystals were grown with a nominal growth velocity of 0.5 mm/min, using quartz crucibles. A larger hot-zone set-up is modified [3] with high purity construction materials and also optimized with various radiation shielding, to obtain high-quality crystals with pronounced structural perfection and high purity. Numerical simulations for different gas flow management were also performed. One of the biggest challenges was controlling and maintaining a constant crystal diameter during this scaled-up growth process. Because the conventional weighing

## Volume Crystals

sensors usually deployed in the Cz-growth of nominally pure (electronic-grade) Ge crystals could not be used, due to the requirement of highly pure environment.

A Dash-necking approach was used usually to control the initial dislocations, growing up to 90 mm long and down to 3 mm thin neck. The crystals possess nearly uniform dislocation densities in the order of  $\sim$  mid.  $5 \times 10^4 \text{ cm}^{-2}$  along their length. Further, HR-XRD rocking curves of the 3-inch crystals show a full-width at half-maximum (FWHM) value of 12 arcsec along the diameter of the wafers. Very high-purity and undoped p-type/n-type crystals could be obtained and one of the HPGe single crystals is shown in Figure 2.

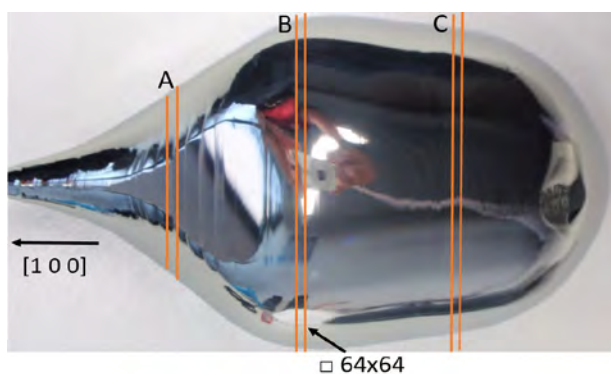


**Fig. 2**  
An ultra-high-pure Ge crystal with a net charge carrier concentration in the mid.  $10^{10} \text{ cm}^{-3}$  and a mobility of  $46,700 \text{ cm}^2/\text{V}\cdot\text{s}$  (sample A); The crystal's EPD values are of  $4,620 \text{ cm}^{-2}$  (sample A);  $8,380 \text{ cm}^{-2}$  (sample B) and  $17,000 \text{ cm}^{-2}$  (sample C).

The results of Hall-effect measurements performed for this crystal at liquid nitrogen temperature (77 K) are presented in Table 1. The vertical lines mark on the crystal picture show the respective places, where the samples were taken for the investigations: A (top), B (middle) and C (bottom). The top and middle parts of the crystal exhibit a net charge carrier concentration in the order of  $10^{10} \text{ cm}^{-3}$ , with sample A showing a high carrier mobility  $> 46000 \text{ cm}^2/\text{V}\cdot\text{s}$ . The mobility value for sample B is decreasing from the expected value, and further we could not reliably measure the sample C. The reduced mobility might be due to the compensation of charge carriers by donors or trapping of charge carriers at the defect centers. This compensation problem was taken up for further investigation and the results will be published in a forthcoming publication. Deep levels induced by the presence of impurities like Cu or Ni could also be a possibility. The p-type/top part of the crystal is good to fabricate detectors.

It is expected that the impurity concentration of single crystals should have the same representative concentration values that of the zone refined starting material. However, the type transition (n-type to p-type or vice versa) of the HPGe within the same crystal has been often observed and is a well-known problem in HPGe.

This type transition should be eliminated to get a good crystal yield with a desired conductivity type. The differences in the concentration of shallow donors or acceptors in the zone refined starting material used for the crystal growth plays a dominant role here. Further, defects such as complex donors like D (H, O) might also be responsible for the change in the conductivity type (p- to n-type or n- to p-type) along the crystal length.

Samples	Top (A)	Middle (B)
Resistivity ( $\Omega\cdot\text{cm}$ )	$2.8 \times 10^3$	$4.4 \times 10^3$
Net charge carrier concentration ( $\text{cm}^{-3}$ )	$+ 4.5 \times 10^{10}$	$- 9.6 \times 10^{10}$
Mobility ( $\text{cm}^2/(\text{V}\cdot\text{s})$ )	46,700	14,800

**Table 1**  
Hall-effect measurements (at 77K) showing ultra-high-purity of the grown crystal. Carrier concentration with negative sign means n-type, with positive sign p-type.

As a summary, important basic process steps for the very high purity, 3-inch diameter Ge crystal growth technology development were successfully established in-house at IKZ [3]. Large diameter, very high purity crystals could be grown to meet the requirements for the detector blocks. Both the conductivity type transition and compensation are real problems of industrial relevance affecting the total crystal yield. We continue to make progress with the design modification and the optimization of more growth parameters for crystals with constant diameter and also for a good overall HPGe crystal yield from run to run.

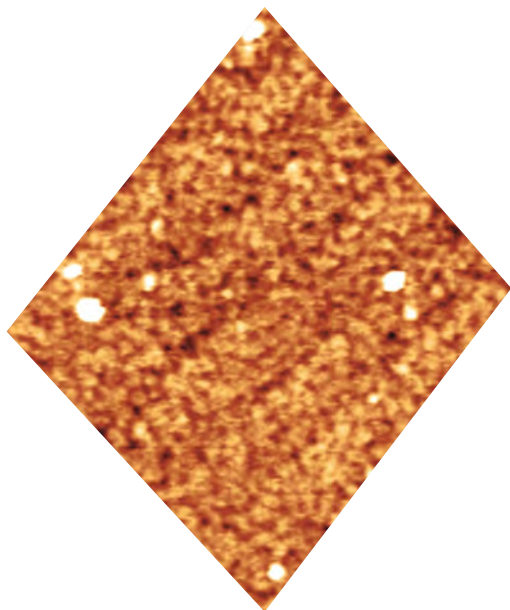
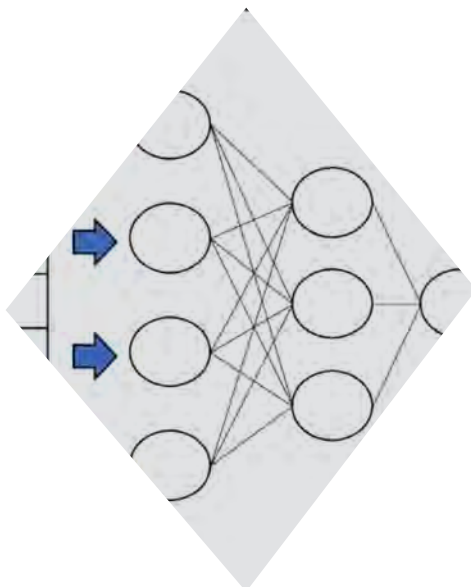
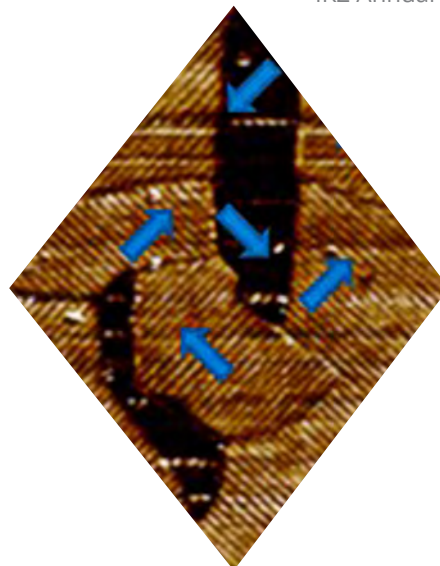
## Acknowledgement

Authors gratefully acknowledge the German Federal Ministry for Education and Research (BMBF) for the financial support through a research grant GERDA/LEGEND (project reference number 05A20BC2). The authors thank Andreas Fiedler for Hall Effect measurement discussions and Nikolay Abrosimov for the fruitful interactions.

## References

- [1] LEGEND Collaboration, <https://legend-exp.org/>
- [2] R. R. Sumathi, <https://www.fv-berlin.de/en/research/research-highlight/what-happened-to-all-the-antimatter>
- [3] R. R. Sumathi, A. Gybin, K.-P. Gradwohl, P. C. Palleti, M. Pietsch, K. Irmscher, N. Dropka, U. Juda, *Crystal Research and Technology* (2023): 2200286, <https://doi.org/10.1002/crat.202200286>





## **Nanostructures & Layers**

# Thickness effect on ferroelectric domain formation in epitaxial $K_{0.65}Na_{0.35}NbO_3$ films

Y. Wang<sup>1,2</sup>, S. Bin Anooz<sup>1</sup>, G. Niu<sup>2</sup>, M. Schmidbauer<sup>1</sup>, and J. Schwarzkopf<sup>1</sup>

<sup>1</sup> Leibniz-Institut für Kristallzüchtung Berlin, Germany

<sup>2</sup> Electronic Materials Research Laboratory, School of Electronic Science and Engineering and the International Joint Laboratory for Micro/Nano Manufacturing and Measurement Technology, Xi'an Jiaotong University, China

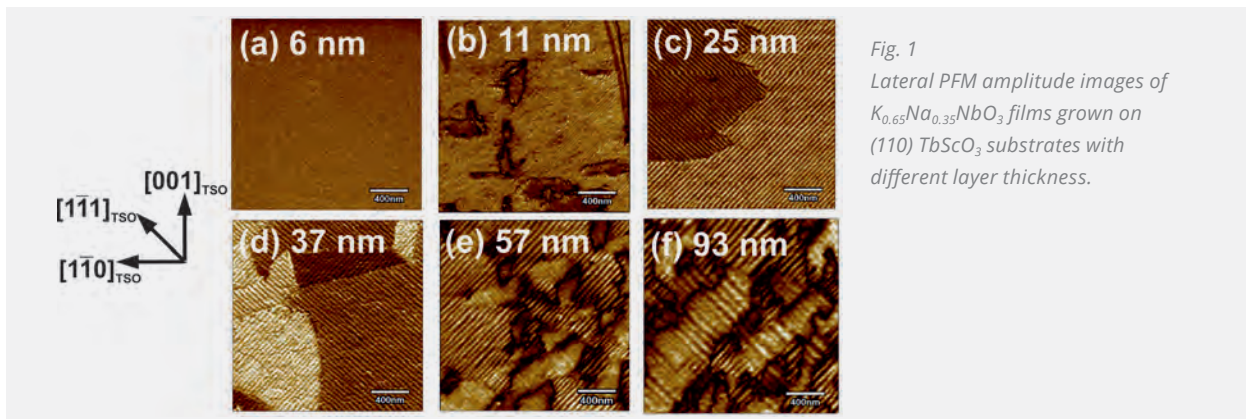


Fig. 1  
Lateral PFM amplitude images of  $K_{0.65}Na_{0.35}NbO_3$  films grown on (110)  $TbScO_3$  substrates with different layer thickness.

Recently, ferroelectrics are gaining more attention as materials for various applications, including nonvolatile memory devices, transducers, and micro-electromechanical system sensors. Ferroelectric phases exhibiting monoclinic symmetry are of special importance because in these systems the polarization vector can rotate continuously within specific mirror planes of the monoclinic unit cell. This characteristic potentially enhances the ferroelectric and piezoelectric properties of these materials.

A typical feature of ferroelectric materials is the formation of domains driven by the minimization of the total free energy, including the chemical, electrostatic, elastic, and domain wall energy of the system. In thin films, the domain sizes are typically in the range of the film thickness. As a result, the volume fraction of the domain walls is significantly more pronounced than in bulk materials. Furthermore, due to the inherent coupling between structure and ferroelectricity in perovskite oxides, lattice strain and film thickness have a strong impact on the ferroelectric properties both on local and macroscopic scales. Therefore, regarding technological applications, the precise control of domain formation is necessary and requires a fundamental understanding of how film properties can be specifically tailored through strain engineering and strain relaxation mechanisms.

In our paper [1] we studied in-depth the influence of the film thickness on the strain evolution and domain formation in strained epitaxial  $K_{0.65}Na_{0.35}NbO_3$  films on (110)  $TbScO_3$  substrates, which cause strongly anisotropic biaxial in-plane compressive strain. In order to provide well-ordered stoichiometric films, we employed the metal-organic vapor phase epitaxy (MOVPE) technique, a chemical deposition method performed under elevated oxygen partial pressure and in close proximity to the thermodynamic equilibrium.

Piezoresponse force microscopy (PFM) images in Fig. 1 show the influence of the film thickness on the formation of ferroelectric domains in the  $K_{0.65}Na_{0.35}NbO_3$  films. Pronounced stripe domains were observed for all films with the thickness  $\geq 11$  nm exhibiting both an in-plane and an out-of-plane PFM amplitude signal, while for the thinnest film (6 nm), no regular domain formation could be defined. The stripe domains are periodically arranged with domain walls running along the diagonal  $[1\bar{1}1]_{TSO}$  or  $[\bar{1}11]_{TSO}$  directions, comparable with what we have previously observed in 35 nm thick  $K_{0.70}Na_{0.3}NbO_3$  films on  $TbScO_3$  [2]. The stripe domain width was extracted directly from the lateral PFM images and plotted in Fig. 2c as a function of the film thickness (black squares). The increase of the domain width  $D$  with the film thickness  $t$  can be well described by Kittel's law with  $D \propto t^{0.5}$ , as shown in Fig. 2c with the black dashed line.

## Nanostructures & Layers

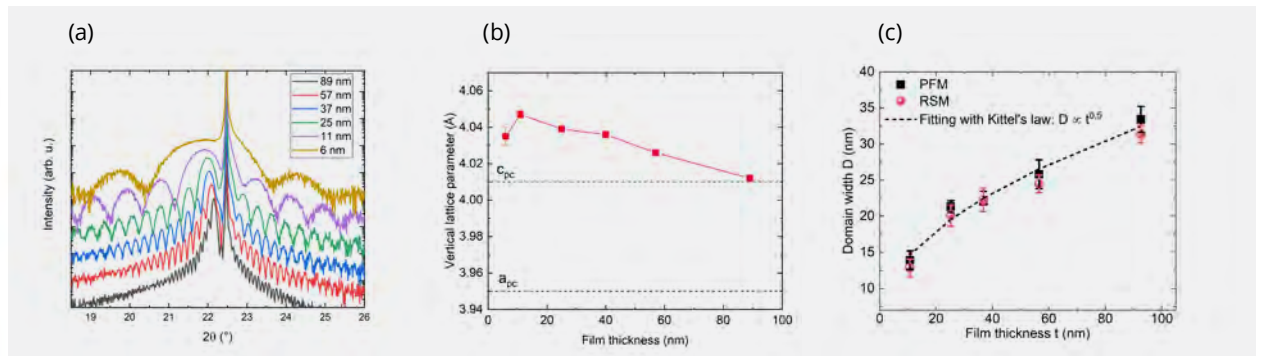


Fig. 2

(a) High-resolution X-ray diffraction  $2\theta$ - $\omega$ -scans of the same films shown in Fig. 1 in the vicinity of the (110)  $\text{TbScO}_3$  substrate Bragg reflection. (b) Vertical lattice parameter of the  $\text{K}_{0.65}\text{Na}_{0.35}\text{NbO}_3$  films as a function of the film thickness. (c) Lateral domain width  $D$  derived from lateral PFM images as a function of the film thickness  $t$ . The dashed line represents the best fit using Kittel's law.

According to Ref. [2], up to four different types of superdomains can be identified in Figs. 1(b)–(f), which are superimposed on the fine stripe domains. In contrast to the stripe domains, which are  $90^\circ$  domains, adjacent superdomains exhibit only a  $90^\circ$  domain wall in thin films up to a thickness of 25 nm (Fig. 3a). For thicker films, additional flux closure vortexlike structures are observed [see Figs. 3(b)–(d), marked by the blue arrows], the fraction of which increases with increasing film thickness. It is therefore assumed that such vortexlike structures are formed to minimize the energy generated by large local stress and charge variations.

For the structural analysis strain-sensitive  $2\theta$ - $\omega$  high-resolution X-ray diffraction (HRXRD) has been performed (see Fig. 2a). The occurrence of pronounced thickness fringes for all samples indicates smooth surfaces and sharp interfaces. All diffraction patterns exhibit film peaks at lower  $2\theta$  angles than the sharp substrate reflection. Obviously, with increasing film thickness, the angular distance between film and substrate Bragg peak decreases which reveals a slight decrease of the vertical lattice parameter with increasing film thickness except for the thinnest 6 nm film (Fig. 2b). More detailed XRD measurements verify fully strained films without remarkable plastic lattice relaxation (e.g. misfit dislocations). They also indicate the formation of an orthorhombic phase in the thinnest film, while for larger thicknesses, film structure exhibits a monoclinic  $Pm$  symmetry. Based on these results, it is concluded that pure elastic strain relaxation occurs in compressively strained  $\text{K}_{0.65}\text{Na}_{0.35}\text{NbO}_3$  for films with the thickness up to 93 nm by ferroelectric domain formation. The elastic strain relaxation proceeds in three successive phases: (i) irregularly arranged orthorhombic  $c$  domains, (ii) periodically arranged  $90^\circ$  monoclinic  $M_c$  domains, and finally, (iii) a flux closure vortexlike structure in thicker films to achieve the lowest equilibrium energy. These results show the significance of understanding the lattice relaxation mechanisms in ferroelectric thin films to intentionally adjust their properties. Strain engineering is a promising approach to achieve excellent piezoelectric properties, thereby enabling their application in nanoscale piezoelectric applications.

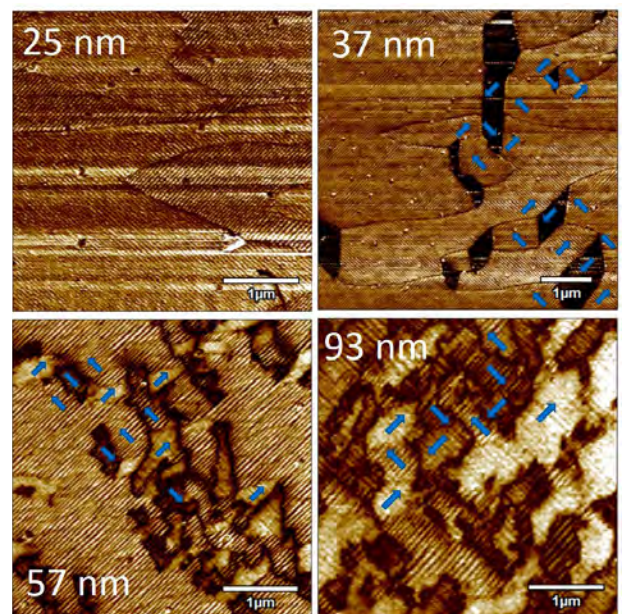


Fig. 3

Large area lateral PFM images ( $4\ \mu\text{m} \times 4\ \mu\text{m}$ ) for  $\text{K}_{0.65}\text{Na}_{0.35}\text{NbO}_3$  films grown on (110)  $\text{TbScO}_3$  substrate with film thickness ranging from (a) 25 to (d) 93 nm. The blue arrows mark the net in-plane electrical polarization direction forming flux closure vortexlike structures.

## References

- [1] Y. Wang, S. Bin Anooz, G. Niu, M. Schmidbauer, L. Wang, W. Ren, J. Schwarzkopf, *Phys. Rev. Mater.* 6 (2022) 084413
- [2] L. von Helden, M. Schmidbauer, S. Liang, M. Hanke, R. Wördenweber, J. Schwarzkopf, *Nanotechnology* 29 (2018) 415704

# Feed physics back to machine learning: An example from MOVPE-grown $\beta\text{-Ga}_2\text{O}_3$ films

T.-S. Chou, S. Bin Anooz, R. Grüneberg, N. Dropka, W. Miller, Z. Galazka, M. Albrecht, and A. Popp

Leibniz-Institut für Kristallzüchtung, Berlin, Germany

For the growth process based on the metalorganic vapor phase epitaxy (MOVPE) system, the physical properties of a grown film are usually an implicit function of many growth parameters, such as the chamber pressure, the precursor concentrations, and the growth temperature, etc., which results in a complex environment and a high-dimensional parameter space. With such a scenario, finding a proper parameter combination (so-called growth condition) is extremely time- and resource-consuming. Therefore, applying a supporting certain methodology is essential to obtain insights from the limited experimental data while saving time, labor, and material resources.

Generally, it is challenging to precisely control and have a full overview of the growth window of the MOVPE process due to its high-dimensional nonlinear nature (the parameters are not independent). This is where machine learning (ML) can play a crucial role in speeding up the exploration of MOVPE processes. ML algorithms can be trained on large datasets of MOVPE process data, including sensor readings, process parameters and film properties, to identify patterns and correlations that may be difficult to detect using traditional statistical methods. By analyzing these patterns, ML models can predict the optimal process conditions for achieving specific film properties, such as crystal quality, thickness and dopant concentration. For a research topic, the interest is not in building an accurate predictive model. Instead, revealing the relation and contribution of each input parameter (growth parameter) to the desired properties is expected to bring more scientific insights out of the target system.

Let's assuming there are growth data of 1000 experimental runs in front of you. Each experimental run has 10 growth parameters (you control daily) with only one fixed growth parameter in this case study the amount of dopant precursor. The other 9 growth parameters (i.e., chamber pressure and growth temperature) differ entirely from run to run. However, all runs show the same doping level at the end. Then the question is, what is your approach to understanding the doping mechanism and figuring out the decisive parameter (other than dopant precursors concentration)?

In the conventional approach, we used to draw a one-to-one relation, such as chamber pressure versus resulting doping level, and gave a potential explanation for the observed correlation. However, there are two disadvantages to such an approach: (1) parameters are not mutually independent, and (2) the values of parameters are different from machine to machine (lack of generality). For the machine learning approach, we apply the Random Forest algorithm (RF) and its relative Forest Deep Neural Network (fDNN) (Figure 1) [2] by feeding our experimental dataset, which contains all input (necessary) parameters of MOVPE equipment as well as the characterization results (i.e., doping level). The initial motivation is to see whether the ML models can predict the doping levels based on the provided growth parameters and determine the decisive parameter other than dopant precursor concentration (everyone expects a positive correlation between the dopant precursor concentration and the resulting doping level).

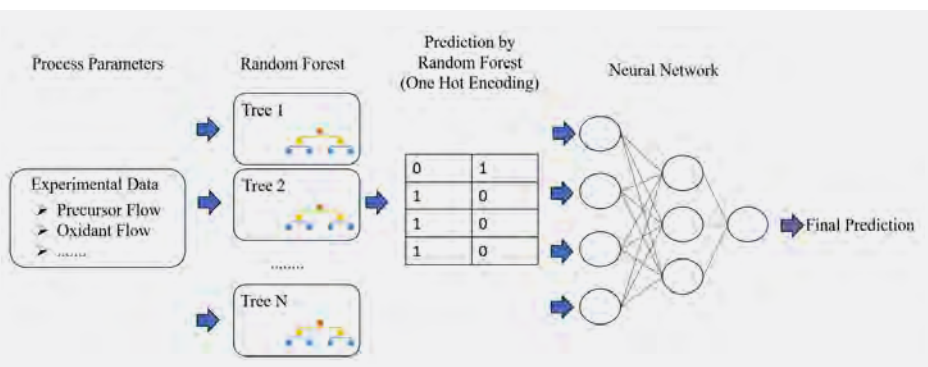
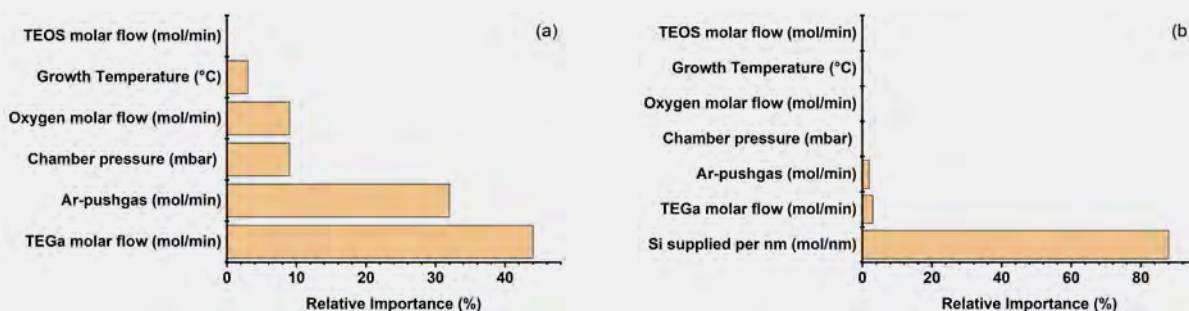


Fig. 1  
The simplified structure of the Forest Deep Neural Network (fDNN) model in this work based on Kong et al [1].



## Nanostructures & Layers



Such a machine learning approach has already been applied to IKZ's  $\text{Ga}_2\text{O}_3$  MOVPE growth development and helped to further understand the parameter impacts with respect to Si doping. Utilizing an embedded function of the RF model, the so-called variable importance mechanism, which considers the collective effect of all input growth parameters, provides a concise way to explain the results from the RF model. Simply speaking, the RF compares the prediction accuracy of the trained model before and after tuning one single process parameter and estimates how "important (or sensitive)" an individual process parameter is while predicting a certain film property (i.e., doping level in this case), as shown in Figure 2. Figure 2a thereby shows that triethylgallium (TEGa) molar flow (Ga precursor concentration) is the most impactful parameter with respect to the doping concentration, excluding tetraethylorthosilicate (TEOS) molar flow (Si precursor concentration, single donor for the n-type doping). Considering that the Ga precursor concentration is linearly correlated with the film growth rate leads to the conclusion that the doping in MOVPE-grown  $\beta\text{-Ga}_2\text{O}_3$  can be a growth-rate-controlled process which brings us to an intuitive hypothesis that the doping in  $\beta\text{-Ga}_2\text{O}_3$  might be a competition between Si and Ga on the lattice site. One can test the hypothesis by creating a growth rate-based parameter, which can be expressed by dividing the concentration of Si precursor ([TEOS], mol/min) by the film growth rate (GR, nm/min). From the practical meaning, this new parameter can be considered as the amount of Si dopant supplied while growing 1 nm of  $\beta\text{-Ga}_2\text{O}_3$  film. Furthermore, the "importance" of such a new parameter (the Si supplied per nm (mol/nm)) can be estimated by re-training the RF with it, and one can clearly see that the new parameter becomes a decisive parameter for the doping prediction (Figure 2b). Generally speaking, this new parameter allows precise control of the doping level by concisely controlling the growth rate without repetitive tests. At the same time it also simplifies the picture of doping behavior, since there are many reports regarding the influence of a single process parameter on the doping level, which in the end just influences the thin film growth rate instead of doping behavior itself [2]. Additionally, the  $\text{Ga}_2\text{O}_3$  community is struggling with the existence of background Si doping. The by-machine-learning-created parameter, which clearly shows that the silicon doping source is indirectly proportional to the growth rate leads to the strategy to lower the incorporation of the background Si by dramatically increasing the growth rate.

Fig. 2

The parameter importance based on the trained model. The importance is ranked by the features containing the most information for the model to make a prediction: (a) individual process parameters and (b) added with a created parameter: Si supplied per nm (mol/nm).

With the information above, classical physical models can be fed back to interpret the RF results further. The competitive Langmuir adsorption model (the competition between Si and Ga) is then considered to be the primary mechanism of doping behavior in MOVPE-grown  $\beta\text{-Ga}_2\text{O}_3$  film [3], and an empirical expression as a function of [TEOS]/GR can be deduced from the Langmuir model which matches the pattern found by the RF model. The obtained expression is also verified in the experimental data collected from different deposition systems and growth conditions [3], which then acts as a reference to compare the experimental data from different systems and provides a concise (and practical) approach to understand the doping mechanism from a huge parameter combination space. Now, we can simply answer the question from third paragraph that competitive Langmuir adsorption is the possible doping mechanism, and the growth rate is the decisive parameter other than the dopant precursor concentration.

In conclusion, machine learning shows promising application potential in MOVPE growth systems as a powerful tool to shorten the development cycle, which is not limited to specific tools but a general approach for any research scenario involving high-dimensional parameter space. Another practical example of ML applications can be found in Chou et al. [4].

## Reference

- [1] Y. Kong, T. Yu, *Sci. Rep.* 2018, 8, 16477.
- [2] T.-S. Chou, S. Bin Anooz, R. Grüneberg, K. Irmscher, N. Dropka, J. Rehm, T. T. V. Tran, W. Miller, P. Seyidov, M. Albrecht, A. Popp, *Crystals* 2022, 12, 8.
- [3] T.-S. Chou, S. Bin Anooz, R. Grüneberg, N. Dropka, J. Rehm, T. T. V. Tran, K. Irmscher, P. Seyidov, W. Miller, Z. Galazka, M. Albrecht, A. Popp, *Appl. Phys. Lett.* 2022, 121, 032103.
- [4] T.-S. Chou, S. Bin Anooz, R. Grüneberg, D. Natascha, W. Miller, T. T. V. Tran, J. Rehm, A. Popp, *J. Cryst. Growth* 2022, 592, 126737.

# Improving the quality of MBE-grown MoS<sub>2</sub> monolayers by annealing in sulphur atmosphere

S. Sadofev<sup>1</sup>, Rongbin Wang<sup>2</sup>, N. Koch<sup>2</sup>, and J. Martin<sup>1</sup>

<sup>1</sup> Leibniz-Institut für Kristallzüchtung, Berlin, Germany

<sup>2</sup> Institut für Physik & IRIS Adlershof, Humboldt-Universität zu Berlin, Berlin, Germany

Two-dimensional (2D) transition metal dichalcogenides (TMDCs) continue to attract considerable attention as a material platform to study the fundamental physical properties of 2D-van der Waals materials. Regarding possible applications, nanometre thin opto-electronic devices are explored based on TMDCs in the monolayer limit, or as part of multilayer heterostructures with precisely controlled layer designs. While the fundamental physical properties of individual layers and device prototypes can be studied on micrometer-sized flakes exfoliated from bulk parent materials, the exploration of the full potential of 2D-TMDCs in applications requires single crystalline wafer-scale films with tunable material composition, layer thickness, and high crystalline quality comparable to, or even exceeding that of currently available bulk crystals. The fabrication on wafer-scale layers of such quality is, however, extremely challenging.

The most widely used techniques for synthesis of large-area 2D-TMDCs are physical- (PVD) and chemical vapor deposition (CVD). PVD, especially in its sophisticated form represented by molecular beam epitaxy (MBE), offers the potential for highest material purity, areal homogeneity, layer thickness and composition tunability. However, TMDC films grown by MBE on commonly used non-van der Waals wafers, suffer from a very small size of the individual crystalline domains, often randomly oriented in-plane. In contrast, CVD can readily provide large crystalline single monolayer (ML) flakes and continuous layers [1, 2]. However, this method lacks, so far, the tunability and reproducibility compared with that of PVD due to non-sufficient understanding and control of the chemical reaction processes occurring in the gas phase and substrate interface.

A successful strategy for variable synthesis of 2D-materials could be a combination of PVD and CVD techniques. In contrast to MBE, where the maximal accessible growth temperature, which determines surface diffusion processes, is limited by desorption of sulphur species, the S vapor pressure in CVD process is several

orders of magnitude higher and can be independently adjusted to compensate for the S loss at any relevant synthesis temperature. Recently, we have demonstrated the fundamental feasibility of this approach yielding 1-2 ML thin epitaxial MoS<sub>2</sub> films on sapphire with excellent optical properties [3]. MoS<sub>2</sub> layers were deposited by MBE using pulsed thermal deposition technique [4] in a wide range of growth temperatures and S fluxes. The growth was regularly controlled by reflection high-energy electron diffraction (RHEED). After the MBE-growth the samples were annealed in a CVD furnace under S environment and optimized annealing temperature of  $T_A = 900$  °C.

Figure 1 summarizes data of the as-grown sample at representative temperature of  $T_G = 750$  °C and annealed in the CVD furnace. The as-grown layer is composed of nm-sized islands, homogeneously distributed over the entire wafer (Fig. 1a). RHEED patterns acquired along the <11-20> direction of the wafer (insert in Fig 1a), display superposition of streaky reflections of the wafer and MoS<sub>2</sub>. Two characteristic spacings between the reflections of MoS<sub>2</sub> correspond to the epitaxial registries of MoS<sub>2</sub> (10-10) || Al<sub>2</sub>O<sub>3</sub> (11-20) and MoS<sub>2</sub> (10-10) || Al<sub>2</sub>O<sub>3</sub> (10-10). The post-growth annealing leads to a recrystallisation of the layer accompanied by a dramatic change of the sample properties. Particularly, the typical size of the crystallites increases from few nm up to lateral sizes of up to 100 nm. This is clearly visible for the incomplete second layer of the annealed sample (Fig. 1b). In contrast, the first layer is fully completed and domain boundaries can be identified only by the weak contrast in the AFM-image (highlighted by arrows). Further, the RHEED data of the annealed layer clearly shows 6-fold symmetry with in-plane epitaxial relationship of (10-10) MoS<sub>2</sub> || (11-20) Al<sub>2</sub>O<sub>3</sub> (insert in Fig. 1b). The annealed samples exhibit sharp excitonic features in absorbance, labelled as A, B, and C in Fig. 1c, the characteristic Raman spectrum of 2H-phase MoS<sub>2</sub> (not shown), and a large enhancement of photoluminescence (PL) yield compared to as-grown layers (Fig. 1d) and similar to CVD-grown monolayers.

## Nanostructures & Layers

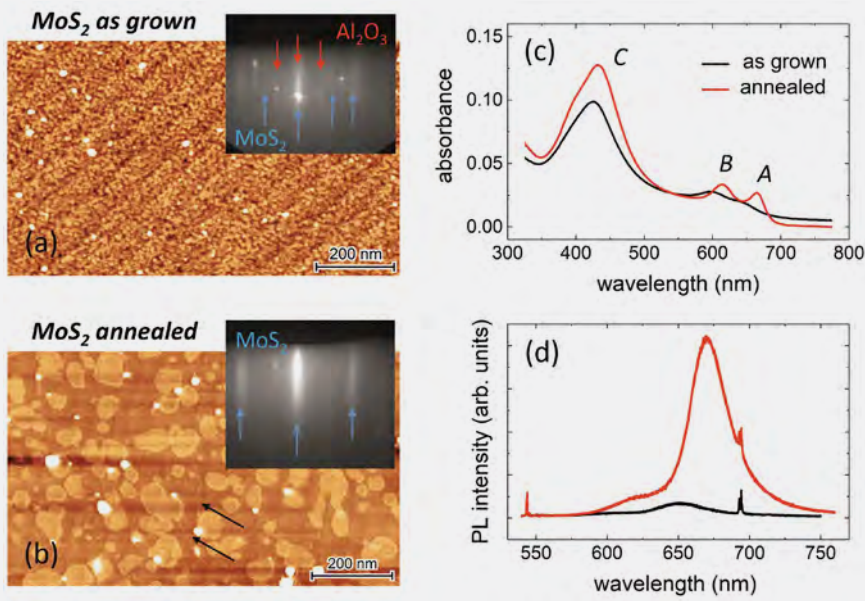


Fig. 1  
Representative properties of MBE grown and annealed nominally 1.5 ML thin  $\text{MoS}_2$  films on sapphire.

(a, b) Surface morphologies of as-grown and annealed sample. Inserts show typical RHEED patterns along  $\langle 11-20 \rangle$  direction of the wafer.

(c, d) Absorption and PL spectra of the as-grown (black curves) and annealed (red curves) sample [3].

In order to gain insight into the chemical composition and bonding character of the TMDC-samples, we conducted X-ray photoelectron spectroscopy (XPS). Figure 2 shows XPS spectra of Mo 3d and S 2p core levels of the as grown and annealed films. The Mo 3d spectra of the as grown sample (Fig. 2a) consist of one doublet at binding energy (BE) of 229.9 eV ( $\text{Mo}^{4+} 3d_{5/2}$ ) and 233.0 eV ( $\text{Mo}^{4+} 3d_{3/2}$ ), corresponding to  $\text{Mo}^{4+}$  of  $\text{MoS}_2$ . A second doublet at 233.5 eV and 236.6 eV can be assigned to the  $\text{Mo}^{6+}$  of  $\text{MoO}_3$  due to the oxidation at the near surface as the sample exposed to air before the measurement. The low BE doublet located at 162.7 eV and 163.9 eV belongs to basal  $\text{S}^{2-}$  of  $\text{MoS}_2$  (Fig. 2b). It appears, that the post-growth annealing process does not induce significant changes except for a decrease of the amount of  $\text{Mo}^{6+}$  (Fig 2 c,d) indicating a reduction in point defects. Otherwise, the non-changing of Mo 3d and S 2p spectra infers that the chemical components in the  $\text{MoS}_2$  layer maintain their original configurations. Hence, the main reasons for the improvement of the optical properties can be ascribed to the increase of the island size by the recrystallization process and the accompanied reduction of point defects.

In conclusion, the results represent a promising way towards the fabrication of wafer-scale single crystalline transition metal dichalcogenide mono- and multilayer films on non-van der Waals epi-substrates by combining the versatility of PVD with a post-growth annealing in a CVD furnace.

## References

- [1] Y. Wei, C. Hu, Y. Li, X. Hu, K. Yu, Litao Sun, M. Hohage, and Lidong Sun, *Nanotechnology* **2020**, 31, 315710.
- [2] P. Yang, X. Zou, Z. Zhang, M. Hong, J. Shi, S. Chen, J. Shu, L. Zhao, S. Jiang, X. Zhou, Y. Huan, C. Xie, P. Gao, Q. Chen, Q. Zhang, Z. Liu, and Y. Zhang, *Nat. Comm.* **2018**, 9, 979.
- [3] R. Wang, N. Koch, J. Martin, and S. Sadofev, *Phys. Stat. Solidi RRL* **2023**, 2200476.
- [4] N. Mutz, T. Meisel, H. Kirmse, S. Park, N. Severin, J. P. Rabe, E. J. W. List-Kratochvil, N. Koch, C. T. Koch, S. Blumstengel, and S. Sadofev, *Appl. Phys. Lett.* **2019**, 114, 162101.

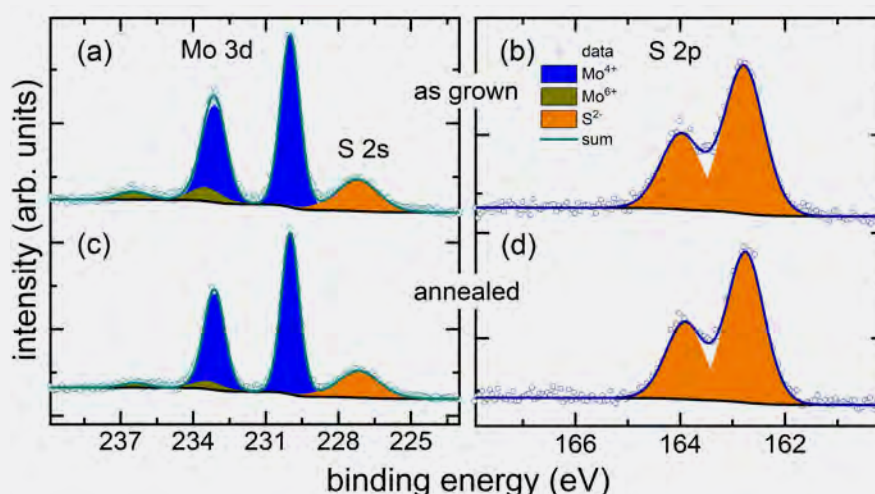
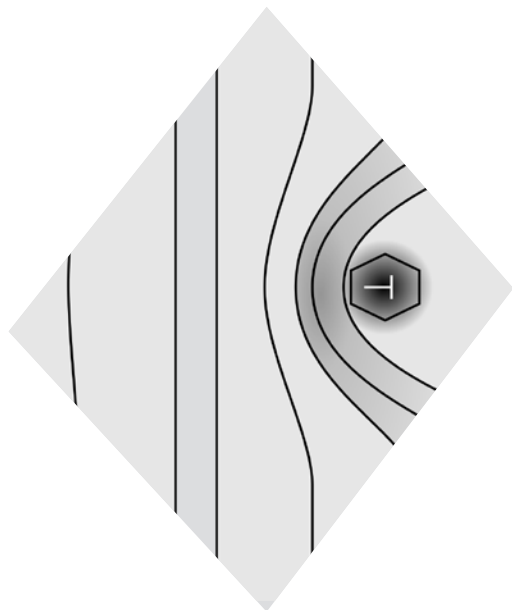
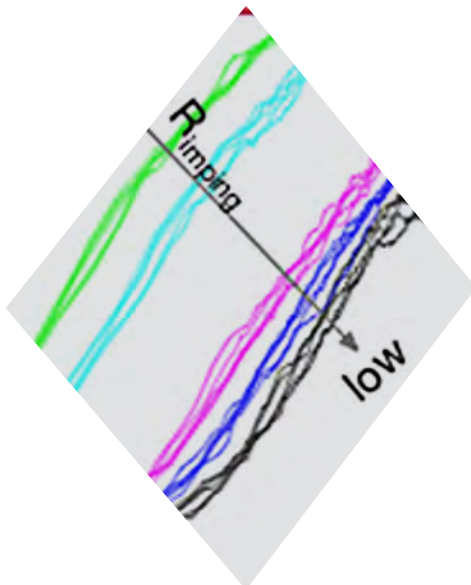
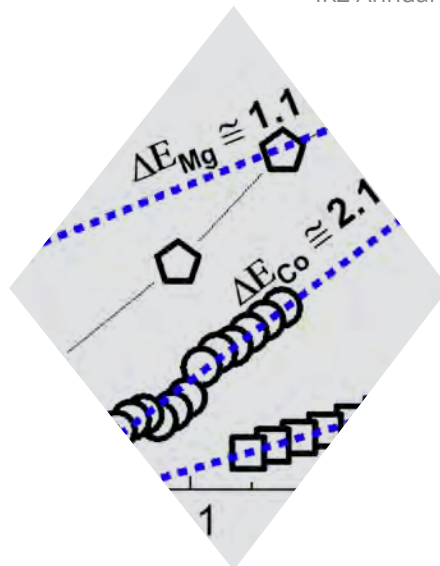


Fig. 2  
XPS spectra of Mo 3d and S 2p core levels for the as-grown MBE- $\text{MoS}_2$  film on sapphire and further annealed under S environment in a CVD furnace. (a, b) As-grown MBE- $\text{MoS}_2$  film and (c, d) after annealing in the CVD furnace [3].





# Materials Science

# Cobalt as a promising dopant for producing semi-insulating $\beta$ -Ga<sub>2</sub>O<sub>3</sub> crystals: Charge state transition levels from experiment and theory

P. Seyidov<sup>1</sup>, J. B. Varley<sup>2</sup>, Z. Galazka<sup>1</sup>, T.-S. Chou<sup>1</sup>, A. Popp<sup>1</sup>, A. Fiedler<sup>1</sup>, and K. Irmischer<sup>1</sup>

<sup>1</sup> Leibniz-Institut für Kristallzüchtung, 12489 Berlin, Germany

<sup>2</sup> Lawrence Livermore National Laboratory, Livermore, California, USA

Monoclinic gallium sesquioxide ( $\beta$ -Ga<sub>2</sub>O<sub>3</sub>) is a wide-band-gap semiconductor material that has been attracting increasing interest in the scientific community due to its unique properties and potential applications. With a bandgap of around 4.8 eV,  $\beta$ -Ga<sub>2</sub>O<sub>3</sub> has one of the highest bandgaps of any known oxide semiconductor. Additionally, it is possible to dope it n-type over a wide range  $10^{15}$  -  $10^{20}$  cm<sup>-3</sup> and the possibility to grow large scale bulk crystals from the melt promise low-cost production. The high electrical breakdown field strength, excellent thermal stability and low defect density make it an attractive material for high-temperature high-power electronics. Since p-type doping is not possible in  $\beta$ -Ga<sub>2</sub>O<sub>3</sub>, semi-insulating substrates are needed for the realization of lateral power devices. Hence, residual donor impurities need to be compensated by deep acceptor dopants. Presently, this is done by doping with magnesium or iron. While the Mg (0/-) acceptor level is reported to be positioned at about 1.1 eV above the valence band maximum (VBM), the acceptor level of Fe is located at about 0.8 eV below the conduction band minimum (CBM). Since the peak operating temperatures in power devices presumably exceed room temperature considerably, thermal ionization of both acceptor species is to be expected leading to a loss of the insulating state of the substrates. The energy level of a compensating acceptor must be as close as possible to the center of the bandgap to exhibit high ionization energy with respect to both band edges (CBM & VBM).

A comprehensive study on the charge transition levels of cobalt acceptor dopant in  $\beta$ -Ga<sub>2</sub>O<sub>3</sub> to achieve more reliable semi-insulating substrates has been performed by IKZ in collaboration with Joel Varley's group from Lawrence Livermore National Laboratory (LLNL). The charge transition levels and defect formation energies of cobalt in the band gap have been calculated using DFT calculations at LLNL. Cobalt doped semi-insulating bulk crystals were grown at IKZ using the Czochralski method. The concentration of Co in the crystals was measured by inductively coupled plasma optical emission spectrometry (ICP-OES) and was  $1.1 \times 10^{18}$  cm<sup>-3</sup> and  $2.2 \times 10^{18}$  cm<sup>-3</sup>. Photoconductivity and optical transmission measurements were performed to experimentally evaluate the charge transition levels of cobalt in  $\beta$ -Ga<sub>2</sub>O<sub>3</sub>. The obtained fitting parameters: thermal ionization (zero-phonon transition) energy, Franck-Condon shift, and effective phonon energy are compared with corresponding values predicted by first-principal calculations based on density functional theory. Fig. 1 shows a schematic band diagram showing the defect level energies derived by experiment and theory. A (+/0) donor level 0.85 eV above the VBM and a (0/-) acceptor level 2.1 eV below the CBM are consistently derived.

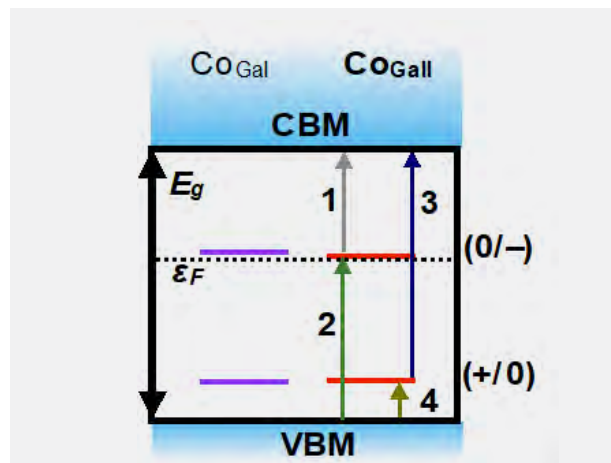


Fig. 1

Schematic band diagram showing the defect level energies and photo-excitations (1 to 4) observed for  $\text{Co}_{\text{Ga}}$  defects. The Fermi level ( $\epsilon_F$ ) is believed to be pinned below the (0/-) transition level of the  $\text{Co}_{\text{Ga}}$  defects, approximately 2.1 eV below the CBM. Reprint from [1] under the Creative Commons Attribution (CC BY) license.

## Materials Science

Fig. 2 shows temperature dependent resistivity measurements for Co, Fe, and Mg doped  $\beta$ -Ga<sub>2</sub>O<sub>3</sub>. The evaluation of the Arrhenius plots (i.e., the linear least square fitting of the data) yields thermal activation energies of  $2.1 \pm 0.1$  eV, 0.82 eV, and 1.1 eV for the resistivity of Co, Fe, and Mg-doped  $\beta$ -Ga<sub>2</sub>O<sub>3</sub>, respectively. The thermal activation energy of  $2.1 \pm 0.1$  eV of Co-doped  $\beta$ -Ga<sub>2</sub>O<sub>3</sub> is consistent with the position of the Co acceptor level derived from DFT and photoconductivity measurements. This corroborates that in our Co-doped samples the Fermi level is pinned at the Co acceptor level about 2.1 eV below the CBM. Room temperature resistivity values from least square fitting for Co, Mg and Fe-doped crystals are  $10^{27}$   $\Omega$ cm,  $10^{18}$   $\Omega$ cm and  $10^{11}$   $\Omega$ cm, respectively. Co-doped  $\beta$ -Ga<sub>2</sub>O<sub>3</sub> shows the highest resistivity for temperatures up to 640K.

We showed the possible syntheses of semi-insulating substrates utilizing cobalt doping in the Czochralski growth. Combining optical absorption spectroscopy, photoconductivity measurements, and charge state transition level calculations based on density functional theory employing hybrid functionals, we evaluated the charge transition levels of cobalt in  $\beta$ -Ga<sub>2</sub>O<sub>3</sub> showing that the (0/-) acceptor level is 2.1 eV below the CBM which is closer to the middle of the 4.85 eV band gap of  $\beta$ -Ga<sub>2</sub>O<sub>3</sub> than the acceptor level of Mg and Fe in  $\beta$ -Ga<sub>2</sub>O<sub>3</sub>. Based on the mid band gap position of the acceptor level and the resulting higher extrapolated resistivity at room temperature, as well as the theoretically calculated formation energy of Co<sub>Ga</sub>, which is similar to that of Fe<sub>Ga</sub> and Mg<sub>Ga</sub>, indicating similar solubility, we propose Co to be a suitable candidate for compensation doping of semi-insulating  $\beta$ -Ga<sub>2</sub>O<sub>3</sub> substrates. The here presented results are of very high interest for the scientific community and can be read in more detail in the featured article [1].

## References

- [1] P. Seyidov, J. B. Varley, Z. Galazka, T.-S. Chou, A. Popp, A. Fiedler, and K. Irmscher, *APL Materials* 10, 111109 (2022). <https://doi.org/10.1063/5.0112915>
- [2] A.T. Neal, S. Mou, S. Rafique, H. Zhao, E. Ahmadi, J.S. Speck, K.T. Stevens, J.D. Blevins, D.B. Thomson, N. Moser, K.D. Chabak, and G.H. Jessen, *Applied Physics Letters* 113, 1 (2018). <https://doi.org/10.1063/1.5034474>

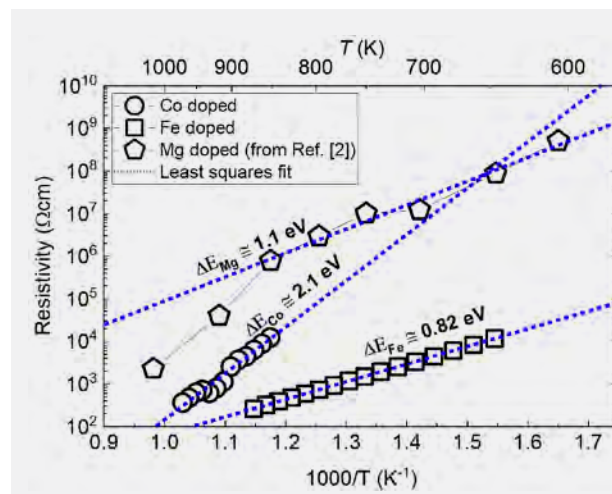


Fig. 2  
Temperature dependent resistivity measured for a Co-doped  $\beta$ -Ga<sub>2</sub>O<sub>3</sub> sample ( $[Co] \sim 2 \times 10^{18} \text{ cm}^{-3}$ ) and an Fe doped one ( $[Fe] \sim 1 \times 10^{18} \text{ cm}^{-3}$ ) plotted logarithmically versus the inverse temperature. For comparison the data for a Mg-doped sample reported by Neal et al. [2] is included. Reprint from [1] under the Creative Commons Attribution (CC BY) license.

# Epitaxial growth of AlN and AlGaN: Using kinetic Monte Carlo to understand the growth kinetics

W. Miller<sup>1</sup>, T. Schulz<sup>1</sup>, L. Lymperakis<sup>2</sup>, A. Klump<sup>1</sup>, and M. Albrecht<sup>1</sup>

<sup>1</sup> Leibniz-Institut für Kristallzüchtung (IKZ) Berlin, Germany

<sup>2</sup> Department of Physics, University of Crete, Greece

AlN and AlGaN microelectronic and optoelectronic devices are of interest for many applications. However, in particular for AlGaN layers there are still issues to achieve a high quality during the epitaxial growth process. Often hexagonal hillocks are observed in the layers, which have a severe effect on the operational performance of the device. Detailed analysis by atomic force (AFM), scanning electron (SEM), and transmission electron microscopy (TEM) reveals that step pinning at threading dislocations causes the 2D nucleation eventually manifesting in hillocks (see also report on page 48).

In order to gain a better understanding of the growth kinetics during the deposition of AlN and AlGaN layers we developed a model for kinetic Monte Carlo (KMC) simulations. For simplicity, we assume that Al, Ga, and N atoms will hit the surface to be adsorbed. We do not take into account the precursor state as trimethylaluminium and  $\text{NH}_3$ . All atoms can diffuse on the surface as well as over edges. Both Al and Ga atoms can desorb. However, the barrier for Al is high and desorption is negligible at process temperatures of 1373 K. Nitrogen can desorb as a  $\text{N}_2$  molecule, thus requiring two N atoms at adjacent positions. The details for energy and process definitions are given in [1].

Firstly, we performed runs for a flat surface at a temperature of 1373 K. We wanted to check if the 2x2 reconstruction is stable in a dynamical mode, i.e. when nitrogen atoms are attaching and leaving the surface via desorption. In the 2x2 reconstruction N surface atoms are sitting in the middle of the hexagonal structure at the so-called H3 positions. This has been proven to be the stable surface structure in the presence of  $\text{N}_2$  in the gas phase employing density functional theory (DFT) methods [2,3].

Calculations have been done for seven different impinging rates of N. We started from an Al terminated AlN(0001) surface and let attach N with different impinging rates ranging from  $5 \text{ s}^{-1}$  up to  $1000 \text{ s}^{-1}$  per unit cell. For every rate we performed 5 runs with different initialization of the random generator. In Fig. 1 the evolution of the coverage of N at the H3 position is shown. For larger impinging rates N is quickly occupying the H3 positions in the 2x2 reconstruction – please note that the time axis is logarithmic. Once the 2x2 reconstruction has been established it is stable. The dynamics in the system is reflected by additional N atoms at the T4 positions (same positions as in bulk). These atoms diffuse on the surface and eventually desorb. The amount of these atoms is less than 10% of the full coverage for all impinging rates. For low impinging rates it takes a while before the full 2x2 reconstruction is reached. The total coverage has to surmount a certain value to drive the system into the 2x2 reconstruction. It might take a long time before the fluctuations in the adatom density leads to a value larger than the critical one.

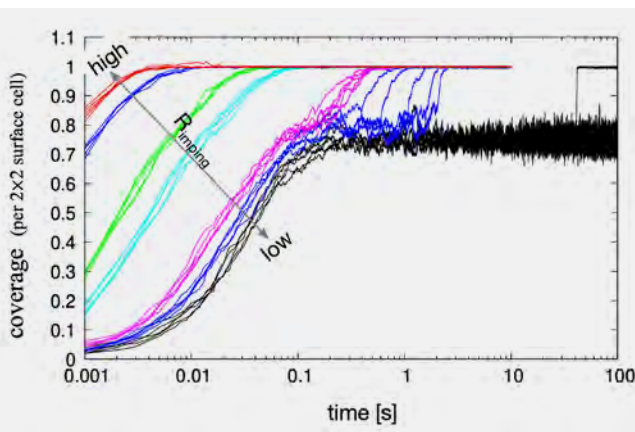
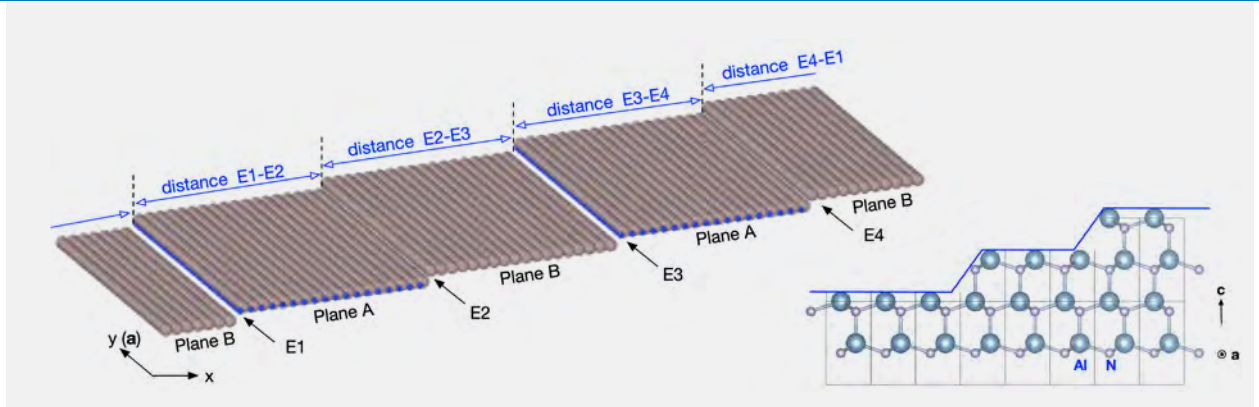


Fig. 1

Adsorption and desorption of N on a flat surface: evolution of the coverage of N at H3 positions. Complete 2x2 reconstruction is achieved at full coverage [1].  $R_{\text{imping}} = 1000 \text{ s}^{-1}$  (red),  $500 \text{ s}^{-1}$  (blue),  $100 \text{ s}^{-1}$  (green),  $50 \text{ s}^{-1}$  (cyan),  $10 \text{ s}^{-1}$  (magenta),  $7 \text{ s}^{-1}$  (blue),  $5 \text{ s}^{-1}$  (black).



# Materials Science



In the next step we considered a vicinal surface with  $3^\circ$  miscut in  $m$ -direction. The structure is shown in Fig. 2. In the case of mono atomic steps, we have two different types of edges (see Fig. 2): edges E1 and E3 end with a N atom and an additional Al atom has one bond to the N atom. Edges E2 and E4 end with an Al atom and an additional N atom has one bond to the Al atom. These differences are also reflected in the step evolution. Edges E1 and E3 becomes rough and faceted while E2 and E4 stay quite straight. The step growth behaviour depends on the impinging rate of N. For small rates edges E2 and E4 are growing slower than the others and the terrace between E1 and E2 as well as E3 and E4 become wider (see Fig. 3). For large impinging rates it is opposite and edges E2 and E4 grow faster. At  $N_{\text{imping}} = 100 \text{ s}^{-1}$  the growth rates of both types of edges are in balance. More detailed analysis revealed that the differences in step growth rate are mainly related to the diffusion of Al at the edge from the top terrace.

In the case of AlGa<sub>0.7</sub>N deposition this effect does not occur and all steps grow with almost the same velocity. With impinging rates of  $5 \text{ s}^{-1}$  and  $2 \text{ s}^{-1}$  for Al and Ga, respectively, we obtain a composition of Al<sub>0.7</sub>Ga<sub>0.3</sub>N in the layers. We also made first computations for a case with two dislocations. It is assumed that the dislocations lower all energy barriers by 5%. To be more precise, energies are scaled by  $0.05 \exp(-d/4a)$ , where  $d$  is the distance to the dislocation centre and  $a$  is the lattice constant. For  $N_{\text{imping}} = 500 \text{ s}^{-1}$  we observed a delay in the moving of a step in the vicinity of the dislocations. However, steps have only a delay in moving and will not be pinned. Further investigations are required to understand the behaviour at the dislocations in more detail.

Fig. 2

Surface structure of vicinal AlN(0001) surface with mono-atomic steps. Please note that we have periodic boundary conditions in  $x$  and  $y$  direction [1]

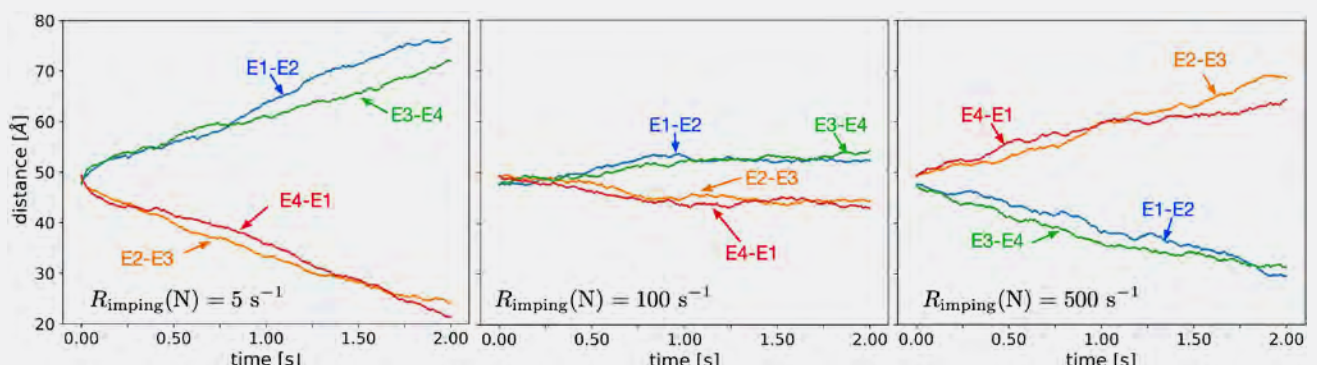
Another point concerns the use of NH<sub>3</sub> in MOVPE experiments as the precursor for N. It is most likely that NH<sub>2</sub> and/or NH<sub>3</sub> attaches to the surface instead N as considered in our calculations. There is no problem to modify the KMC program in this manner but firstly details of the surface structure should be investigated by DFT calculations.

## Publications

- [1] W. Miller, T. Schulz, L. Lymperakis, A. Klump, M. Albrecht, J. Crystal Growth 607 (2023), 127125 <https://doi.org/10.1016/j.crysgro.2023.127125>
- [2] J. E. Northrup, R. D. Felice, J. Neugebauer, Phys. Rev. B, 55 (1997), 13878;
- [3] P. Strak, K. Sakowski, P. Kempisty, S. Krukowski, J. Appl. Phys., 118 (2015), 095705.

Fig. 3

Step dynamics for different impinging rates of nitrogen. The width of the four terraces are shown as a function of the process time. Blue: distance E1-E2, orange: distance E2-E3, green: distance E3-E4, red: distance E4-E1.



# Step pinning and hillock formation in (Al,Ga)N films on native AlN substrates

T. Schulz<sup>1</sup>, S.-H. Yoo<sup>2</sup>, L. Lymparakis<sup>2</sup>, C. Richter<sup>1</sup>, E. Zatterin<sup>3</sup>, A. Lachowski<sup>1</sup>, C. Hartmann<sup>1</sup>, H. M. Foronda<sup>4</sup>, C. Brandl<sup>4</sup>, H. J. Lugauer<sup>4</sup>, M. P. Hoffmann<sup>4</sup>, and M. Albrecht<sup>1</sup>

<sup>1</sup> Leibniz Institut für Kristallzüchtung, Berlin, Germany

<sup>2</sup> Max-Planck-Institut für Eisenforschung GmbH, Düsseldorf, Germany

<sup>3</sup> The European Synchrotron Radiation Facility (ESRF), Grenoble, France

<sup>4</sup> ams-OSRAM International GmbH, Regensburg, Germany

Light emitting or laser diodes operating in the UVC (ultraviolet C) range between 200-280 nm offer potential applications in sterilization, water purification, and medical products. Such devices have several advantages over traditional UV lamps, such as a higher energy efficiency, longer lifespan, more compact and lightweight design, as well as instant on/off capabilities. Moreover, they do not contain hazardous substances such as mercury, which makes them more environmentally friendly. However, to date, UVC emitters are much more expensive than traditional UV lamps, and their total output power is generally lower. One reason for the reduced efficiency of such devices are problems related to the growth of the material system, which is based on  $\text{Al}_x\text{Ga}_{1-x}\text{N}$ . While layer deposition of  $\text{Al}_x\text{Ga}_{1-x}\text{N}$  in an atomically flat surface morphology is highly desirable, the layers often exhibit rough surfaces with 3D structures, denoted as “hillocks”. Such a surface morphology impedes any further processing towards fabrication of a working device. Together with our partners ams-OSRAM and the Max-Planck Institute für Eisenforschung, we have investigated the reason for this surface roughening by combining atomic force microscopy (AFM), cathodoluminescence (CL), transmission electron microscopy (TEM) with theory ([1], see also report on page 46). Figure 1(a) and (b) shows AFM images of the surface of a 1  $\mu\text{m}$  thick  $\text{Al}_{0.7}\text{Ga}_{0.3}\text{N}$  film grown on native AlN. In close agreement with other groups, the surface exhibits large hexagonal hillocks with a height of around 40 nm and a lateral dimension of about 10  $\mu\text{m}$ , as can be seen in Figure 1(a). The density of these hillocks varies locally but is on the order of  $10^4 \text{ cm}^{-2}$ -  $10^5 \text{ cm}^{-2}$ . A close up of one of the hillocks is displayed in Figure 1(b) revealing concentric and closed growth terraces circumventing a depression near the geometric center. Such a morphology indicates that the hillocks are formed in an entirely different growth mode than the desired step-flow growth regime.

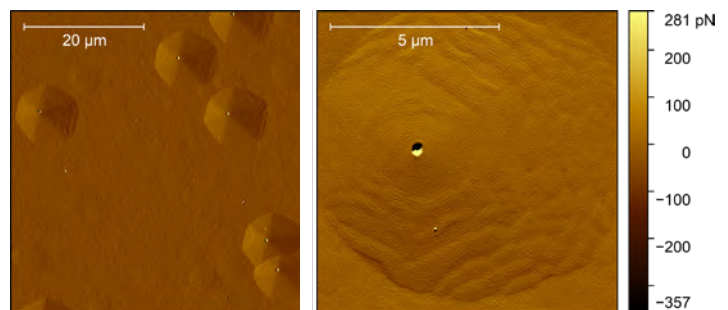


Fig. 1

AFM of the surface of a 1  $\mu\text{m}$  thick  $\text{Al}_{0.7}\text{Ga}_{0.3}\text{N}$  film.

Cathodoluminescence studies of the emission from the  $\text{Al}_{0.7}\text{Ga}_{0.3}\text{N}$  film reveals another structural property of the hillock: Next to its 3D morphology, its formation is accompanied by a substantial deviation of the intended  $\text{Al}_x\text{Ga}_{1-x}\text{N}$  composition. As can be seen in Fig 2 (a) and (b), respectively, while the flat  $\text{Al}_x\text{Ga}_{1-x}\text{N}$  film is mainly emitting around 245 nm, which is consistent with the intentional composition of  $\text{Al}_{0.7}\text{Ga}_{0.3}\text{N}$ , the CL in the hillock region occurs at much longer wavelengths. This clearly evidences a Ga enrichment in the hillock region, which poses another problem regarding devices fabrication, since these regions may act as electrical short circuit paths.

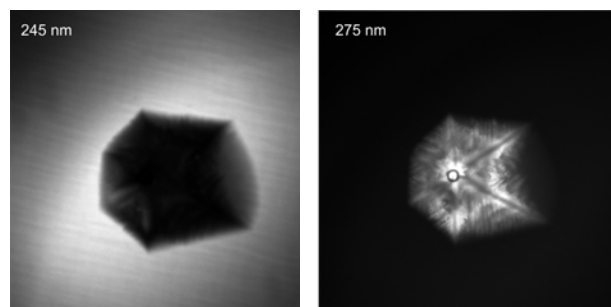


Fig. 2

Monochromatic CL of a hillock at (a) 245 nm and (b) 275 nm.

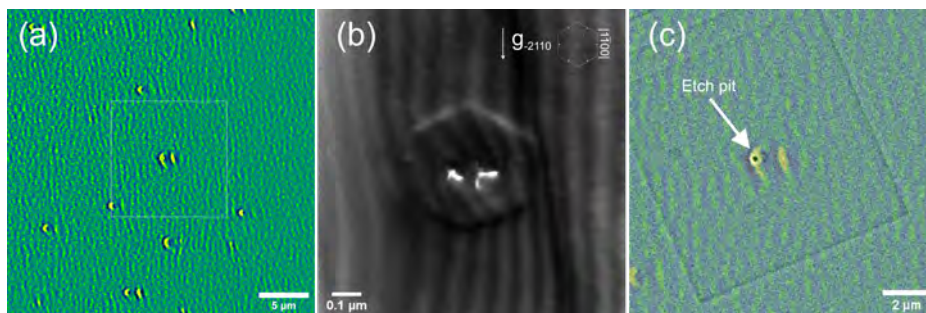


Fig. 3  
(a) Color coded Cathodoluminescence image of a 20 nm  $\text{Al}_{0.7}\text{Ga}_{0.3}\text{N}$  layer  
(b) zoomed in image additionally superimposed with the corresponding SEM image.

To track down the origin of the hillock formation we performed investigations on very thin samples, i.e. in a stage where the perturbations on the growth due to the hillock formation are less severe. A panchromatic CL image of a 20 nm thin  $\text{Al}_{0.7}\text{Ga}_{0.3}\text{N}$  film is displayed in Figure 3(a) showing larger intensity fluctuations which indicate growth perturbations. Spectrally resolved CL evidences that the brighter appearing, slightly curved regions are Ga enriched. By means of plan-view TEM image of the very same sample see Figure 3(b), we find small, hexagonally shaped structures. Assuming a constant lateral growth, such hexagonal structure with diameters of about 500 nm in the 20 nm thick film would expand to a diameter of 22  $\mu\text{m}$  for a film thickness of 1  $\mu\text{m}$ . These macroscopic sizes perfectly agree with the lateral dimensions of the hillocks observed in our 1  $\mu\text{m}$  thick film, which allows to conclude that these structures represent the hillocks in a very early stage of growth. Starting from the assumption that all these growth perturbations, i.e. compositional changes and hillock formation are related to threading dislocations, we have conducted defect selective etching experiments. By counting, we quantify an etch pit density on the order of  $10^6 \text{ cm}^{-2}$ . Since this number is much higher than the initial TD density in the substrate, this implies that the majority of these TDs have formed during the  $\text{Al}_{0.7}\text{Ga}_{0.3}\text{N}$  epitaxy. Superimposing the CL with a SEM image of an etched sample, as shown in Figure 3(c), reveals the impact of TDs on the epitaxial growth of the  $\text{Al}_{0.7}\text{Ga}_{0.3}\text{N}$  film. We find that each etch pit, i.e. TD causes the characteristic, slightly curved and Ga enriched region in their vicinity.

In light of the results discussed above, we conclude that the formation of hillocks is triggered by the presence of TDs. We have been working with our partners at the Max Planck Institute to understand this mechanism in more detail. According to theoretical considerations of the adatom kinetics and surface energies, we find that the hillock formation is caused by an initial pinning of surface steps at a TD as a consequence of their strain field. The situation is depicted in a sketch in Figure 4(a). This causes the initially straight surface steps to be curved and bunched in the vicinity of the TD due to collision with following steps. Since Ga adatoms have a smaller surface diffusion length, regions where steps

are bunched exhibit a higher Ga content. This results in curved, Ga enriched segments as depicted in Figure 4(a) in darker colors, or as found experimentally in CL in Fig 3(b). If the blocking is very severe, step pinning will also create areas where the terrace width is greatly increased as the retained steps are prevented from flowing in. These regions serve as precursors for hexagonal hillock growth via 2D island nucleation, as depicted in Figure 4(b). This represents a transition of the growth mode which resembles spontaneous island nucleation on an atomically flat surface. Continuous nucleation of layers enlarges these islands along the [0001] direction while lateral expansion occurs due to adatom incorporation at the m-facets. In  $\mu\text{m}$  thick films, this results in hexagonally shaped hillocks with lateral diameters of tens of  $\mu\text{m}$ .

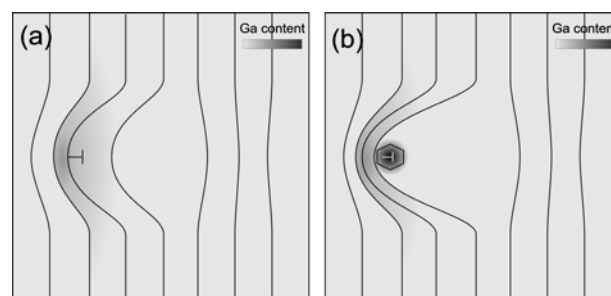


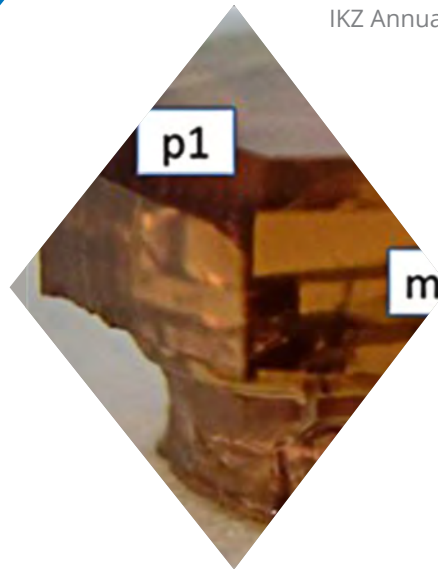
Fig. 4  
Sketch of the blocking of surface steps at TDs causing (a) altered Ga/Al composition and (b) serve as precursor for hillock formation.

These results reveal, that hillock formation can be prevented by, in the first place, reducing the number of TDs created during  $\text{Al}_{0.7}\text{Ga}_{0.3}\text{N}$  epitaxy. Also, a higher supersaturation may be desirable to prevent the surface steps from being blocked.

## References

- [1] T. Schulz, S.-H. Yoo, L. Lympirakis, C. Richter, E. Zatterin, A. Lachowski, C. Hartmann, H. M. Foronda, C. Brandl, H. J. Lugauer, M. P. Hoffmann, M. Albrecht; Journal of Applied Physics 132, 223102 (2022) <https://doi.org/10.1063/5.0125480>





# Application Science

# Dislocation climb in AlN crystals grown at low temperature gradients revealed by 3D X-ray diffraction imaging

T. Straubinger, C. Hartmann, C. Richter, M. Albrecht, A. Klump, T. Schröder, M. Bickermann, and C. Richter

Leibniz-Institut für Kristallzüchtung, Berlin, Germany

Due to its outstanding material properties aluminum nitride (AlN) has a high potential for the use as substrate material for various electronic devices in particular deep ultraviolet (UVC) light-emitting-diodes (LED) or laser-diodes (LD) and lateral 2DEG-power devices.

AlN-substrates are already commercially available with diameters up to 2-inch, but dislocation formation mechanisms are still not fully understood, and therefore dislocation densities in the substrates can still exceed  $10^4 \text{ cm}^{-2}$ . One of the main reasons for dislocation formation in AlN-crystals is a too high temperature gradient ( $> 0.5 \text{ K/mm}$ ) leading to glide of threading edge dislocations in m-planes and subsequent dislocation multiplication [1]. For basic investigations [2] we grew crystals with only a few millimeters diameter (Fig. 1 – A/B) at temperature gradients of approx.  $0.1 \text{ K/mm}$  on seeds with low dislocation density ( $10^3 \text{ cm}^{-2}$ ) prepared from spontaneous nucleated crystals. The crystals were grown without guiding crystal channel and therefore show a hexagonal shape with one main c-plane growth surface and six m-plane growth surfaces at the crystal rim. For structural characterization a cross section cut (Fig. 1 – C) parallel to the a-plane was prepared which shows areas of different color in transmission due to different doping incorporation depending on the local growth conditions.

White-Beam-X-Ray-Topography (WB-XRT) images corresponding to different reflections (Fig. 2 – A/B) show that there are only pure a-type dislocations (burgers vector perpendicular to c-direction) present in the main crystal volume, but single dislocations cannot be distinguished and the area with high background contrast above the seed surface is not accessible at all. A Monochromatic-Weak-Beam-X-Ray-Topography image corresponding to the 1-100 reflection (Fig. 2 – C/D) with significantly improved spatial resolution confirmed that there are no dislocations in the lateral grown bulk volume outside the seed diameter and similar dislocation densities (approx.  $10^3 \text{ cm}^{-2}$ ) in both the seed and bulk grown volume could be counted indicating that dislocations from the seed were inherited in vertical direction. As the area above the seed surface still was not accessible in the MB-XRT 2D-a-plane projection a X-Ray-Diffraction-Laminography (XDL) series was taken to access this area in a tilted view (Fig. 2 – E) and to generate a 3D image of the dislocations in the bulk volume.

From the 3D-XDL-data we could extract the course of the dislocations in an a-plane projection (Fig. 2 – A) with strong bending in the seed near volume and straight dislocation lines with slight tilt to the c-direction in the main bulk volume. The c-plane projection of the same

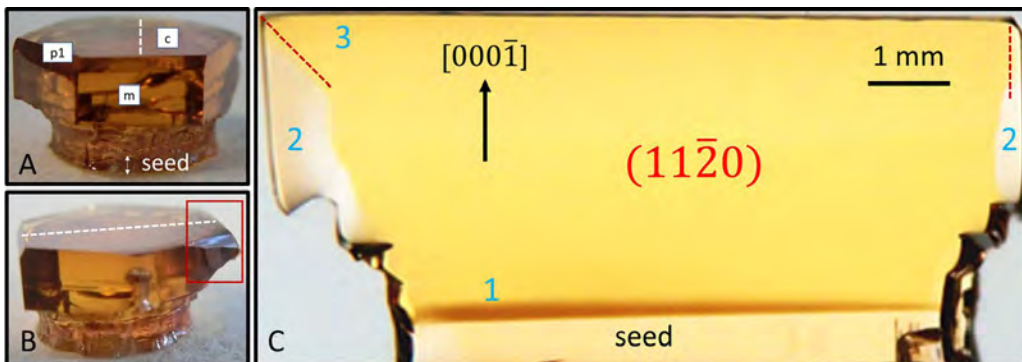


Fig. 1

AlN crystal with hexagonal shape grown on a seed with 5 mm diameter – A: Main c-facet and side facets (m, p1). B: Local multi facet structure (red square). C: Cross section cut parallel to the a-plane (see dashed white line in A/B) in transmission showing a strip with dark color directly above the seed surface (1), a main growth volume with yellow color (3) and areas with bright color at the crystal rim (2) correlated with lateral growth on facets with tilt to the c-plane.

## Application Science

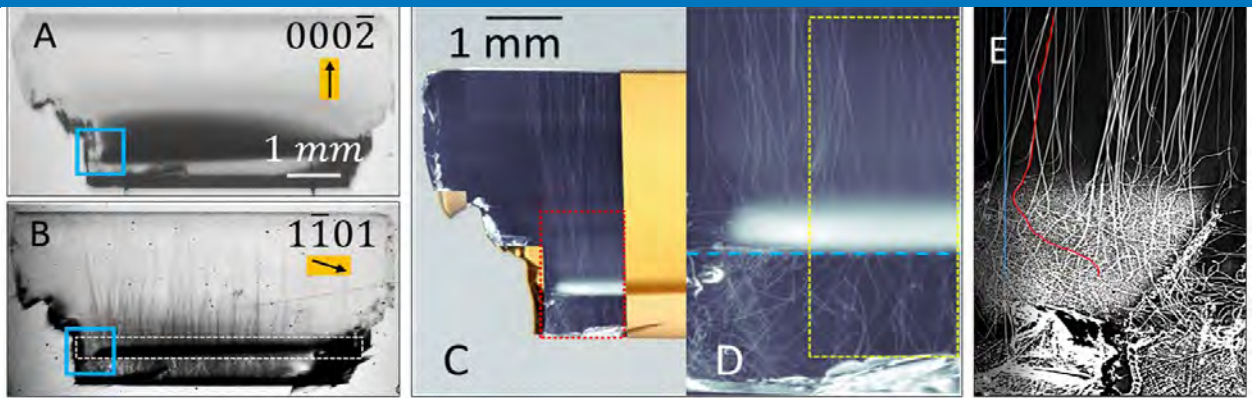
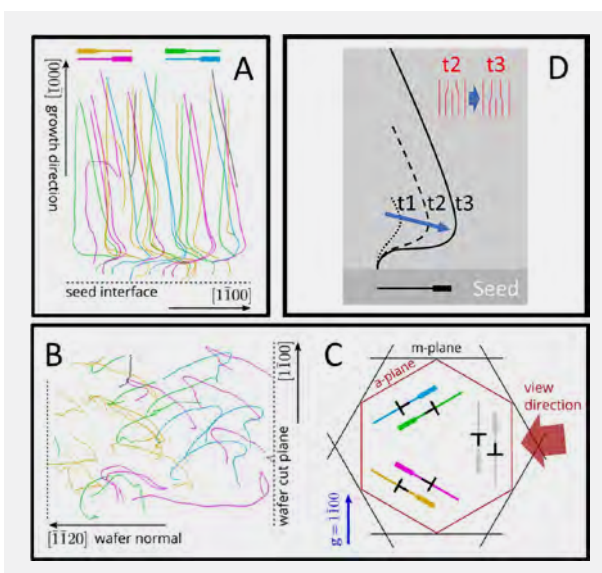


Fig. 2

Cross section cut through crystal from Fig. 1 – A: WB-XRT images corresponding to the 000-2 reflection (c- and mixed type visible). B: WB-XRT images corresponding to the 1-101 reflection (c-, mixed- and a-type visible). C: MB-XRT image corresponding to the 1-100 reflection (a-type visible). D: Magnified area from C (red square) with area of strong background contrast between seed surface and bulk. E: MB-XRT image with tilted view into area with high background contrast.

crystal volume (Fig. 2 – B) reveals that the dislocations are bended inside a-planes and not in m-planes like one would expect for dislocation glide. As the bending direction is correlated with the burgers vector direction (Fig. 2 – C) we propose a strain driven climb mechanism in the main bulk volume (Fig. 3 – D) during growth at temperatures  $> 2000^{\circ}\text{C}$  while the dislocation is pinned in the seed near crystal volume (distance to seed  $< 300\ \mu\text{m}$ ) and on the growth surface. The pinning of the dislocation lines in the seed near volume with high background contrast is explained by different point defect densities. At a medium point defect density (distance to seed  $> 300\ \mu\text{m}$ ), the climb of dislocations is facilitated and driven by the comparatively low thermomechanical stresses. At a high point defect density (distance to seed  $< 300\ \mu\text{m}$ ) climb is inhibited by increased local stress fluctuations that exceed the thermomechanical stress and become the dominating force.

Monochromatic weak beam X-ray diffraction imaging provides a high-resolution insight in the arrangement and evolution of dislocations in AlN-crystals at medium dislocation densities ( $< 10^5\ \text{cm}^{-2}$ ). In particular the 3D view extracted from the XDL data was helpful to access areas with strong diffraction background.



The laterally grown dislocation-free crystal volume could be used to prepare seeds with a diameter of a few millimeters which then could be the starting point for the development of dislocation free 2-inch seeds by gradually increasing the seed diameter utilizing growth processes with low temperature gradients.

## Acknowledgements

The work was funded by the Bundesministerium für Bildung und Forschung (BMBF) under grant numbers 03ZZ0112A and 03ZZ0138A. The authors would like to thank Merve Pinar Kabukcuoglu, Simon Bode, Elias Hamann, Simon Haaga, Mathias Hurst and Daniel Hänschke from the Laboratory for Applications of Synchrotron Radiation (LAS) at KIT for the MB-XRT images.

## References

- [1] S. Hu, H. Fang, Y. Liu, H. Peng, Q. Cheng, Z. Chen, R. Dalmau, J. Britt, R. Schlessler, B. Raghothamachar and M. Dudley, *Journal of Crystal Growth*, 2022, 584, 126548.
- [2] T. Straubinger, C. Hartmann, M. P. Kabukcuoglu, M. Albrecht, M. Bickermann, A. Klump, S. Bode, E. Hamann, S. Haaga, M. Hurst, T. Schröder, D. Hänschke and C. Richter, *Crystal Growth and Design*, 2023, 23, 3, 1538-1546.

Fig. 3

Dislocations in AlN bulk crystal from Fig. 1 – A: Vertical course between seed and cap surface in a-plane projection. B: Horizontal course with bending in c-plane projection. C: Schematic drawing of six different dislocation groups corresponding to three independent a-planes and two burgers vector directions (upward bending direction indicated by thick tail). The dislocations shown in grey color are lost during the automatic data extraction from the XDL data due to their low MB-XRT contrast. D: Schematic drawing of the temporal evolution of a dislocation line in a-plane projection.

# Visible Tb<sup>3+</sup>- and Pr<sup>3+</sup>-based solid-state lasers

H.Tanaka, M. Badtke, S. Kalusniak, and C. Kränkel

Leibniz-Institut für Kristallzüchtung (IKZ), Berlin, Germany

Visible lasers are sought in many applications. They are required in fields as diverse as medicine, materials processing, display and entertainment technology, and many others. In contrast to infrared lasers, which require multiple conversion processes to reach the ultra-violet (UV) spectral range, visible lasers enable very simple and efficient access to the UV by a single frequency doubling step.

The choice of directly visible emitting lasers is limited: The 'green gap' prohibits the development of semiconductor lasers with emission in the green and yellow spectral range and only few laser active ions allow for efficient direct visible lasing. In particular the trivalent rare-earth ions praseodymium (Pr<sup>3+</sup>) and terbium (Tb<sup>3+</sup>) are suitable for efficient high-power diode-pumped visible solid-state lasers.

Compared to semiconductor lasers, solid-state lasers provide various advantages, e.g., higher energy storage in Q-switched operation and a better beam quality at high output power. Since the recent development of GaN-based blue-emitting pump diodes, researchers at IKZ's Center for Laser Materials (ZLM) have been pioneering this young field of research. Recently, we reviewed the amazing progress and state of the art in this field in a detailed invited review paper [1].

## Yellow and green Tb<sup>3+</sup>-lasers

Diode-pumped solid-state lasers are a key technology in our modern society. Many of their applications are in strong demand of radiation at a specific wavelength. In particular in the yellow range there are currently no direct emitting sources available. Tb<sup>3+</sup> has unique properties for the direct generation of yellow laser light and enables efficient laser operation under pumping at wavelengths around 488 nm in the blue spectral range. In the past years, ZLM researchers realized proof-of-concept diode-pumped Tb<sup>3+</sup>-based solid-state lasers [2], but the low absorption cross-sections in the blue require the use of quite long gain crystals, in which it is difficult to achieve a good mode overlap under pumping with low-brightness high-power laser diodes.

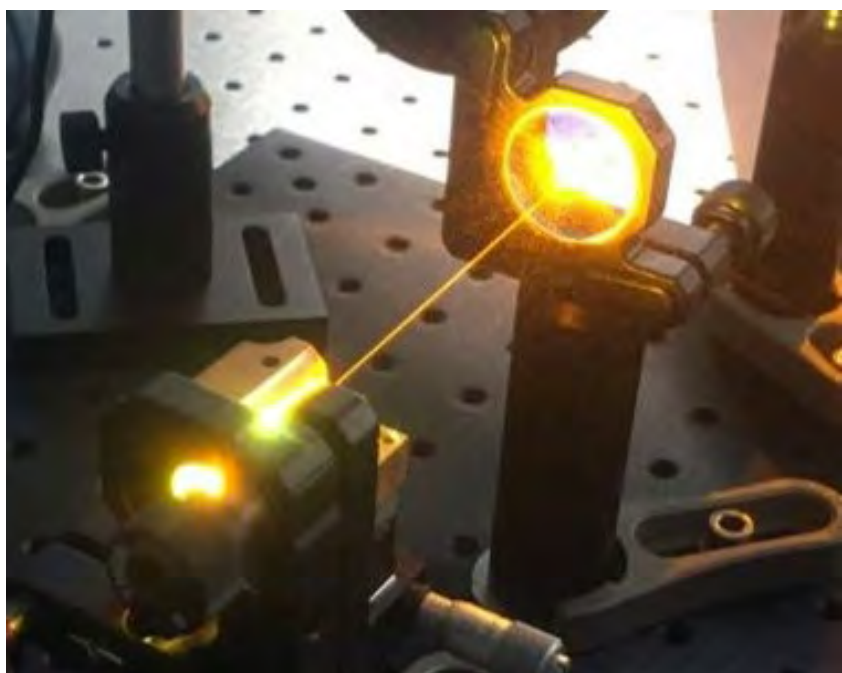


Fig. 1

Photograph of an UV-pumped, yellow-emitting Tb<sup>3+</sup>-laser. Due to the invisible UV pump beam, the yellow beam appears to come out of nothing.

To overcome this disadvantage, the ZLM introduced green and yellow Tb<sup>3+</sup> lasers pumped at wavelengths in the UV spectral range (see Fig. 1). The large absorption cross-sections found at UV wavelengths enabled to shorten the length of the gain media by nearly an order of magnitude to only a few millimeters [3]. Our spectroscopic investigations revealed that at sufficiently high doping concentrations the fluorescence from the excited <sup>5</sup>D<sub>3</sub> level is strongly quenched by a cross-relaxation process, which efficiently populates the upper laser level <sup>5</sup>D<sub>4</sub> (see Fig. 2). This process enables very high quantum efficiencies of green and yellow Tb<sup>3+</sup>-lasers under UV-pumping at wavelengths between 350 nm and 380 nm [4].

We recently demonstrated the first UV-diode-pumped solid-state laser utilizing a 3 mm short Tb<sup>3+</sup>(28 at.):LiLuF<sub>4</sub> crystal yielding slope efficiencies of 36 % at 544 nm and 17 % at 587 nm with a minimum laser threshold as low as 4 mW.



## Application Science

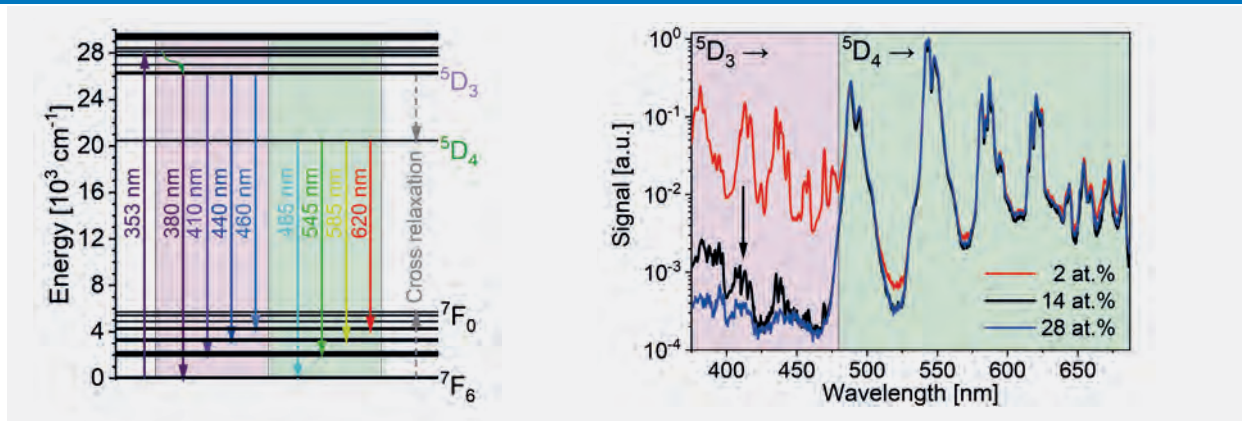


Fig. 2

The left side shows the energy level diagram of Tb<sup>3+</sup> with the relevant transitions (upward arrows: pump, downward arrows: fluorescence). The right side shows that the fluorescence intensity from the <sup>5</sup>D<sub>3</sub> multiplet (pink background) is quenched by more than two orders of magnitude for Tb<sup>3+</sup>-doping concentrations of 14 at.% or higher compared to the fluorescence from <sup>5</sup>D<sub>4</sub> (green background) indicating efficient cross relaxation (dashed grey lines in the left figure).

The efficiencies of Tb<sup>3+</sup>-lasers are significantly below the theoretical limit given by the ratio of the pump and the laser photon energy, the so-called Stokes efficiency. In recent spectroscopic investigations we found an accidental, but almost perfect spectral match of the main emission peaks with the excited state absorption wavelengths in Tb:LiLuF<sub>4</sub> and also Tb:LiYF<sub>4</sub> to be responsible [4]. This finding motivates the investigation of alternative host materials with stronger crystal field strengths. In this respect, the IKZ internal collaboration with the junior research group on fluoride crystal growth at IKZ is a great advantage for our efforts.

### Continuous wave and pulsed Pr<sup>3+</sup>-lasers

ZLM researchers are involved in the highest efficiencies and highest output power levels achieved with Pr<sup>3+</sup>-lasers to date. This doping ion allows for slope efficiencies as high as 70% in the red and green at 640 nm and 523 nm, respectively when pumped at 479 nm. Under pumping with blue-emitting high-power laser diodes, output power levels in the 10-W-range were obtained with slightly lower efficiencies [1]. A photograph of a Pr<sup>3+</sup>-laser is shown in Fig. 3.

The IKZ is also active in the investigation of novel saturable absorber materials for passive Q-switching of visible lasers and established transition-metal doped spinel-structure crystals such as Co:MgAl<sub>2</sub>O<sub>4</sub> as efficient materials for this purpose. This allowed us to demonstrate the shortest pulses from any passively Q-switched Pr<sup>3+</sup>-laser. In the red, the pulses were as short as 2.3 ns, while the pulse duration for the orange transition amounted to 5.3 ns. In both cases, the peak powers of these pulses reached values of more than 1 kW [5].

## References

- [1] H. Tanaka, S. Kalusniak, M. Badtke, M. Demesh, N. V. Kuleshov, F. Kannari, and C. Kränkel; Prog. Quantum Electron. **84**, 100411 (2022) (37 pp) (**invited paper**), <https://doi.org/10.1016/j.pquantelec.2022.100411>
- [2] E. Castellano-Hernández, S. Kalusniak, P. W. Metz, and C. Kränkel; Laser Photon. Rev. **14** (2), 1900229 (2020), <https://doi.org/10.1002/lpor.201900229>
- [3] S. Kalusniak, H. Tanaka, E. Castellano-Hernández, and C. Kränkel; Opt. Lett. **45** (22), 6170-6173 (2020), <https://doi.org/10.1364/OL.411072>
- [4] S. Kalusniak, E. Castellano-Hernández, H. Yalçinoğlu, H. Tanaka, and C. Kränkel; Appl. Phys. B **128**, 33 (16 pp) (2022) (**invited paper**), <https://doi.org/10.1007/s00340-022-07759-1>
- [5] M. Badtke, H. Tanaka, S. Kalusniak, M. Demesh, N. Kuleshov, and C. Kränkel; Appl. Phys. Express **15** (8), 082006 (4p) (2022), <https://doi.org/10.35848/1882-0786/ac8414>



Fig. 3

Detail of a blue-pumped, red-emitting Pr<sup>3+</sup>-laser in the ZLM laboratory.



**58 Publications**

**65 Talks**

**68 Patents**

**70 Teaching and Education**

**71 Membership in Committees**

# **Appendix**

## Publications

### Articles in peer-reviewed journals

- Abbasi, P.; Barone, M. R.; Cruz-Jauregui, M. D.; Valdespino-Padilla, D.; Paik, H.; Kim, T.; Kornblum, L.; Schlom, D. G.; Pascal, T. A.; Fenning, D. P., *Ferroelectric Modulation of Surface Electronic States in BaTiO<sub>3</sub> for Enhanced Hydrogen Evolution Activity*. Nano Letters; 22 (2022), 4276-4284 DOI: <https://doi.org/10.1021/acs.nanolett.2c00047>.
- Aggoune, W.; Eljarrat, A.; Nabok, D.; Irmscher, K.; Zupancic, M.; Galazka, Z.; Albrecht, M.; Koch, C.; Draxl, C., *A consistent picture of excitations in cubic BaSnO<sub>3</sub> revealed by combining theory and experiment*. Communication Materials 3 (2022) 12, DOI: <https://doi.org/10.1038/s43246-022-00234-6>
- Agostini, M.; Alexander, A.; Araujo, G.; Bakalyarov, A. M.; Balata, M.; Barabanov, I.; Baudis, L.; Bauer, C.; Belogurov, S.; Bettini, A.; Bezrukov, L.; Biancacci, V.; Bossio, E.; Bothe, V.; Brugnera, R.; Caldwell, A.; Calgaro, S.; Cattadori, C.; Chernogorov, A.; Comellato, T.; D'Andrea, V.; Demidova, E. V.; Di Giacinto, A.; Di Marco, N.; Doroshkevich, E.; Fischer, F.; Fomina, M.; Gangapshev, A.; Garfagnini, A.; Gooch, C.; Grabmayr, P.; Gurentsov, V.; Gusev, K.; Hakenmuller, J.; Hemmer, S.; Hofmann, W.; Huang, J.; Hult, M.; Inzhechik, L. V.; Csathy, J. J.; Jochum, J.; Junker, M.; Kazalov, V.; Kermaidic, Y.; Khushbakht, H.; Kihm, T.; Kilgus, K.; Kirpichnikov, I. V.; Klimenko, A.; Knopfle, K. T.; Kochetov, O.; Kornoukhov, V. N.; Krause, P.; Kuzminov, V. V.; Laubenstein, M.; Lindner, M.; Lippi, I.; Lubashevskiy, A.; Lubsandorzhiev, B.; Lutter, G.; Macolino, C.; Majorovits, B.; Maneschg, W.; Manzanillas, L.; Marshall, G.; Miloradovic, M.; Mingazheva, R.; Misiaszek, M.; Morella, M.; Muller, Y.; Nemchenok, I.; Pandola, L.; Pelczar, K.; Pertoldi, L.; Piseri, P.; Pullia, A.; Ransom, C.; Rauscher, L.; Redchuk, M.; Riboldi, S.; Romyantseva, N.; Sada, C.; Sailer, S.; Salamida, F.; Schonert, S.; Schreiner, J.; Schutt, M.; Schuetz, A. K.; Schulz, O.; Schwarz, M.; Schwingenheuer, B.; Selivanenko, O.; Shevchik, E.; Shirchenko, M.; Shtembari, L.; Simgen, H.; Smolnikov, A.; Stukov, D.; Vasenko, A. A.; Veresnikova, A.; Vignoli, C.; von Sturm, K.; Wester, T.; Wiesinger, C.; Wojcik, M.; Yanovich, E.; Zatschler, B.; Zhitnikov, I.; Zhukov, S. V.; Zinatulina, D.; Zschocke, A.; Zsigmond, A. J.; Zuber, K.; Zuzel, G.; Collaboration, G., *Search for exotic physics in double- $Q$  decays with GERDA Phase II*. Journal of Cosmology and Astroparticle Physics; 012 (2022), 012 DOI: <https://doi.org/10.1088/1475-7516/2022/12/012>.
- Astrov, Y. A.; Portsel, L. M.; Shuman, V. B.; Lodygin, A. N.; Abrosimov, N. V., *Magnesium-Related Donors in Silicon: State of the Art*. Physica Status Solidi a-Applications and Materials Science; 219 (2022), DOI: <https://doi.org/10.1002/pssa.202200463>.
- Badtke, M.; Tanaka, H.; Kalusniak, S.; Demesh, M.; Kuleshov, N.; Kränkel, C., *Few-fs, kW peak power Q-switched pulses from orange and red Pr:YLF lasers*. Applied Physics Express; 15 (2022), 082006 DOI: <https://doi.org/10.35848/1882-0786/ac8414>.
- Bae, J. E.; Calmano, T.; Kränkel, C.; Rotermond, F., *Controllable Dynamic Single- and Dual-Channel Graphene Q-Switching in a Beam-Splitter-Type Channel Waveguide Laser*. Laser & Photonics Reviews; 16 (2022), 2100501 DOI: <https://doi.org/10.1002/lpor.202100501>.
- Barone, M.; Du, C. J.; Radosavljevic, L.; Werder, D.; Pan, X. Q.; Schlom, D. G., *Epitaxial Synthesis of a Vertically Aligned Two-Dimensional van der Waals Crystal: (110)-Oriented SnO*. Crystal Growth & Design; 22 (2022), 7248-7254 DOI: <https://doi.org/10.1021/acs.cgd.2c00905>.
- Barone, M.; Foody, M.; Hu, Y. Q.; Sun, J. X.; Frye, B.; Perera, S. S.; Subedi, B.; Paik, H.; Hollin, J.; Jeong, M.; Lee, K.; Winter, C. H.; Podraza, N. J.; Cho, K.; Hock, A.; Schlom, D. G., *Growth of Ta<sub>2</sub>SnO<sub>6</sub> Films, a Candidate Wide-Band-Gap p-Type Oxide*. Journal of Physical Chemistry C; 126 (2022), 3764-3775 DOI: <https://doi.org/10.1021/acs.jpcc.1c10382>.
- Barone, M. R.; Jeong, M.; Parker, N.; Sun, J. X.; Tenne, D. A.; Lee, K.; Schlom, D. G., *Synthesis of meta-stable Ruddlesden-Popper titanates, (ATiO<sub>3</sub>)<sub>n</sub>AO, with n >= 20 by molecular-beam epitaxy*. Apl Materials; 10 (2022), 091106 DOI: <https://doi.org/10.1063/5.0101202>.
- Bein, N.; Kmet, B.; Rojac, T.; Golob, A. B.; Malic, B.; Moxter, J.; Schneider, T.; Fulanovic, L.; Azadeh, M.; Fromling, T.; Egert, S.; Wang, H. G.; van Aken, P.; Schwarzkopf, J.; Klein, A., *Fermi energy, electrical conductivity, and the energy gap of NaNbO<sub>3</sub>*. Physical Review Materials; 6 (2022), 084404 DOI: <https://doi.org/10.1103/PhysRevMaterials.6.084404>.
- Bin Anooz, S.; Wang, Y.; Petrik, P.; Guimaraes, M. D.; Schmidbauer, M.; Schwarzkopf, J., *High temperature phase transitions in NaNbO<sub>3</sub> epitaxial films grown under tensile lattice strain*. Applied Physics Letters; 120 (2022), 202901 DOI: <https://doi.org/10.1063/5.0087959>.
- Boschker, J. E.; Spengler, U.; Ressel, P.; Schmidbauer, M.; Mogilatenko, A.; Knigge, A., *Stability of ZnSe-Passivated Laser Facets Cleaved in Air and in Ultra-High Vacuum*. IEEE Photonics Journal; 14 (2022), 1531606 DOI: <https://doi.org/10.1109/jphot.2022.3176675>.

## Publications

- Bose, A.; Schreiber, N. J.; Jain, R.; Shao, D. F.; Nair, H. P.; Sun, J. X.; Zhang, X. S.; Muller, D. A.; Tsybal, E. Y.; Schlom, D. G.; Ralph, D. C., *Tilted spin current generated by the collinear antiferromagnet ruthenium dioxide*. *Nature Electronics*; 5 (2022), 267-274 DOI: <https://doi.org/10.1038/s41928-022-00744-8>.
- Boy, J.; Mitdank, R.; Galazka, Z.; Fischer, S. F., *Thermal conductivity, diffusivity and specific heat capacity of as-grown, degenerate single-crystalline ZnGa<sub>2</sub>O<sub>4</sub>*. *Materials Research Express* 9 (2022) 65902 DOI: <https://doi.org/10.1088/2053-1591/ac5f8a>.
- Buchovska, I.; Dadzis, K.; Dropka, N.; Kiessling, F. M., *Adjustment of resistivity for phosphorus-doped n-type multicrystalline silicon*. *Solar Energy Materials and Solar Cells*; 248 (2022), 111989 DOI: <https://doi.org/10.1016/j.solmat.2022.111989>.
- Burkle, F.; Forste, M.; Dadzis, K.; Tsiapkinis, I.; Patzold, O.; Charitos, A.; Dues, M.; Czarske, J.; Buttner, L., *Application of optical velocity measurements including a novel calibration technique for micron-resolution to investigate the gas flow in a model experiment for crystal growth*. *Flow Measurement and Instrumentation*; 88 (2022), 102258 DOI: <https://doi.org/10.1016/j.flowmeasinst.2022.102258>.
- Cancellara, L.; Hagedorn, S.; Walde, S.; Jaeger, D.; Albrecht, M., *Formation of voids and their role in the recovery of sputtered AlN during high-temperature annealing*. *Journal of Applied Physics*; 131 (2022), 215304 DOI: <https://doi.org/10.1063/5.0088948>.
- Celi, E.; Galazka, Z.; Laubenstein, M.; Nagorny, S.; Pagnanini, L.; Pirro S.; Puiu, A., *Development of a cryogenic In<sub>2</sub>O<sub>3</sub> calorimeter to measure the spectral shape of <sup>115</sup>In β-decay*. *Nuclear Instruments and Methods in Physics Research Section A* 1033 (2022) 166682 DOI: <https://doi.org/10.1016/j.nima.2022.166682>.
- Chou, T. S.; Bin Anooz, S.; Grüneberg, R.; Dropka, N.; Miller, W.; Tran, T. T. V.; Rehm, J.; Albrecht, M.; Popp, A., *Machine learning supported analysis of MOVPE grown beta-Ga<sub>2</sub>O<sub>3</sub> thin films on sapphire*. *Journal of Crystal Growth*; 592 (2022), 126737 DOI: <https://doi.org/10.1016/j.jcrysgro.2022.126737>.
- Chou, T. S.; Bin Anooz, S.; Grüneberg, R.; Dropka, N.; Rehm, J.; Tran, T. T. V.; Irmscher, K.; Seyidov, P.; Miller, W.; Galazka, Z.; Albrecht, M.; Popp, A., *Si doping mechanism in MOVPE-grown (100) beta-Ga<sub>2</sub>O<sub>3</sub> films*. *Applied Physics Letters*; 121 (2022), 032103 DOI: <https://doi.org/10.1063/5.0096846>.
- Chou, T. S.; Bin Anooz, S.; Grüneberg, R.; Irmscher, K.; Dropka, N.; Rehm, J.; Tran, T. T. V.; Miller, W.; Seyidov, P.; Popp, A., *Toward Precise n-Type Doping Control in MOVPE-Grown beta-Ga<sub>2</sub>O<sub>3</sub> Thin Films by Deep-Learning Approach*. *Crystals*; 12 (2022), 8 DOI: <https://doi.org/10.3390/cryst12010008>.
- Dai, L. Y.; Zhao, J. Y.; Li, J. R.; Chen, B. H.; Zhai, S. J.; Xue, Z. Y.; Di, Z. F.; Feng, B. Y.; Sun, Y. X.; Luo, Y. Y.; Ma, M.; Zhang, J.; Ding, S. N.; Zhao, L. B.; Jiang, Z. D.; Luo, W. B.; Quan, Y.; Schwarzkopf, J.; Schroeder, T.; Ye, Z. G.; Xie, Y. H.; Ren, W.; Niu, G., *Highly heterogeneous epitaxy of flexoelectric BaTiO<sub>3</sub>-delta membrane on Ge*. *Nature Communications*; 13 (2022), 2990 DOI: <https://doi.org/10.1038/s41467-022-30724-7>.
- De Guzman, J. A. T.; Markevich, V. P.; Coutinho, J.; Abrosimov, N. V.; Halsall, M. P.; Peaker, A. R., *Electronic Properties and Structure of Boron-Hydrogen Complexes in Crystalline Silicon*. *Solar Rrl*; 6 (2022), 2100459 DOI: <https://doi.org/10.1002/solr.202100459>.
- Dessmann, N.; Pavlov, S. G.; Pohl, A.; Shuman, V. B.; Portsel, L. M.; Lodygin, A. N.; Astrov, Y. A.; Abrosimov, N. V.; Redlich, B.; Hubers, H. W., *Combination of ultrafast time-resolved spectroscopy techniques for the analysis of electron dynamics of heliumlike impurity centers in silicon*. *Physical Review B*; 106 (2022), 195205 DOI: <https://doi.org/10.1103/PhysRevB.106.195205>.
- Dropka, N.; Tang, X.; Chappa, G. K.; Holena, M., *Smart Design of Cz-Ge Crystal Growth Furnace and Process*. *Crystals*; 12 (2022), 1764 DOI: <https://doi.org/10.3390/cryst12121764>.
- Drozdowski, W.; Makowski, M.; Bachiri, A.; Witkowski, M. E.; Wojtowicz, A. J.; Swiderski, L.; Irmscher, K.; Schewski, R.; Galazka, Z., *Heading for brighter and faster β-Ga<sub>2</sub>O<sub>3</sub> scintillator crystals*. *Optical Materials: X* 15 (2022) 100157 DOI: <https://doi.org/10.1016/j.omx.2022.100157>.
- Echavarri-Bravo, V.; Amari, H.; Hartley, J.; Maddalena, G.; Kirk, C.; Tuijtel, M. W.; Browning, N. D.; Horsfall, L. E., *Selective bacterial separation of critical metals: towards a sustainable method for recycling lithium ion batteries*. *Green Chemistry*; 24 (2022), 8512-8522 DOI: <https://doi.org/10.1039/d2gc02450k>.
- Ecklebe, S.; Woittennek, F.; Frank-Rotsch, C.; Dropka, N.; Winkler, J., *Toward Model-Based Control of the Vertical Gradient Freeze Crystal Growth Process*. *IEEE Transactions on Control Systems Technology*; 30 (2022), 384-391 DOI: <https://doi.org/10.1109/tcst.2021.3058006>.

## Publications

- Emtsev, V.; Abrosimov, N.; Kozlovski, V.; Lastovskii, S.; Oganessian, G.; Poloskin, D., *Electron- and proton irradiation of strongly doped silicon of p-type: Formation and annealing of boron-related defects*. Journal of Applied Physics; 131 (2022), 125705 DOI: <https://doi.org/10.1063/5.0078043>.
- Emtsev, V. V.; Abrosimov, N. V.; Kozlovski, V. V.; Lastovskii, S. B.; Oganessian, G. A.; Poloskin, D. S.; Aref'ev, A. A., *Boron-doped silicon: a possible way of testing and refining models of non-ionizing energy loss under electron- and proton irradiation*. Physics of the Solid State 64, No. 12 (2022) 1878 DOI: <https://doi.org/10.21883/PSS.2022.12.54380.469>.
- Enders-Seidlitz, A.; Pal, J.; Dadzis, K., *Development and validation of a thermal simulation for the Czochralski crystal growth process using model experiments*. Journal of Crystal Growth; 593 (2022), 126750 DOI: <https://doi.org/10.1016/j.jcrysgro.2022.126750>.
- Enders-Seidlitz, A.; Pal, J.; Dadzis, K., *Model experiments for Czochralski crystal growth processes using inductive and resistive heating*. IOP Conf. Ser.: Mater. Sci. Eng., 1223 (2022) 012003 DOI: <https://doi.org/10.1088/1757-899X/1223/1/012003>.
- Eom, K.; Paik, H.; Seo, J.; Campbell, N.; Tsymbal, E. Y.; Oh, S. H.; Rzechowski, M. S.; Schlom, D. G.; Eom, C. B., *Oxide Two-Dimensional Electron Gas with High Mobility at Room-Temperature*. Advanced Science; 9 (2022), 2105652 DOI: <https://doi.org/10.1002/advs.202105652>.
- Ernst, O. C.; Bottcher, K.; Fischer, D.; Uebel, D.; Teubner, T.; Boeck, T., *Morphogenesis of Liquid Indium Microdroplets on Solid Molybdenum Surfaces during Solidification at Normal Pressure and under Vacuum Conditions*. Langmuir; 38 (2022), 762-768 DOI: <https://doi.org/10.1021/acs.langmuir.1c02744>.
- Ernst, O. C.; Liu, Y. J.; Boeck, T., *Leveraging dewetting models rather than nucleation models: current crystallographic challenges in interfacial and nanomaterials research Contemporary and prospective opportunities to exploit dewetting theory for energy conversion devices and quantum computing*. Zeitschrift Für Kristallographie-Crystalline Materials; 237 (2022), 191-200 DOI: <https://doi.org/10.1515/zkri-2021-2078>.
- Galazka, Z., *Growth of bulk beta-Ga<sub>2</sub>O<sub>3</sub> single crystals by the Czochralski method*. Journal of Applied Physics; 131 (2022), 031103 DOI: <https://doi.org/10.1063/5.0076962>.
- Galazka, Z.; Ganschow, S.; Seyidov, P.; Irmscher, K.; Pietsch, M.; Chou, T. S.; Bin Anooz, S.; Grueneberg, R.; Popp, A.; Dittmar, A.; Kwasniewski, A.; Suendermann, M.; Klimm, D.; Straubinger, T.; Schroeder, T.; Bickermann, M., *Two inch diameter, highly conducting bulk beta-Ga<sub>2</sub>O<sub>3</sub> single crystals grown by the Czochralski method*. Applied Physics Letters; 120 (2022), 152101 DOI: <https://doi.org/10.1063/5.0086996>.
- Gamov, I.; Lyons, J. L.; Gartner, G.; Irmscher, K.; Richter, E.; Weyers, M.; Wagner, M. R.; Bickermann, M., *Fingerprints of carbon defects in vibrational spectra of GaN considering the isotope effect*. Physical Review B; 106 (2022), 184110 DOI: <https://doi.org/10.1103/PhysRevB.106.184110>.
- Gavva, V. A.; Troshin, O. Y.; Adamchik, S. A.; Lashkov, A. Y.; Abrosimov, N. V.; Gibin, A. M.; Otopkova, P. A.; Sozin, A. Y.; Bulanov, A. D., *Preparation of Single-Crystal Isotopically Enriched Ge-70 by a Hydride Method*. Inorganic Materials; 58 (2022), 246-251 DOI: <https://doi.org/10.1134/s0020168522030050>.
- Goodge, B. H.; Nair, H. P.; Baek, D. J.; Schreiber, N. J.; Miao, L. D.; Ruf, J. P.; Waite, E. N.; Carubia, P. M.; Shen, K. M.; Schlom, D. G.; Kourkoutis, L. F., *Disentangling types of lattice disorder impacting superconductivity in Sr<sub>2</sub>RuO<sub>4</sub> by quantitative local probes*. APL Materials; 10 (2022), 041114 DOI: <https://doi.org/10.1063/5.0085279>.
- Gradwohl, K. P.; Benedek, P.; Popov, M.; Matkovic, A.; Spitaler, J.; Yarema, M.; Wood, V.; Teichert, C., *Crystal habit analysis of LiFePO<sub>4</sub> microparticles by AFM and first-principles calculations*. Crystengcomm; 24 (2022), 6891-6901 DOI: <https://doi.org/10.1039/d2ce00788f>.
- Gradwohl, K. P.; Miller, W.; Dropka, N.; Sumathi, R. R., *Quantitative dislocation multiplication law for Ge single crystals based on discrete dislocation dynamics simulations*. Computational Materials Science; 211 (2022), 111537 DOI: <https://doi.org/10.1016/j.commatsci.2022.111537>.
- Gregory, B. Z.; Stremper, J.; Weinstock, D.; Ruf, J. P.; Sun, Y. F.; Nair, H.; Schreiber, N. J.; Schlom, D. G.; Shen, K. M.; Singer, A., *Strain-induced orbital-energy shift in antiferromagnetic RuO<sub>2</sub> revealed by resonant elastic x-ray scattering*. Physical Review B; 106 (2022), 195135 DOI: <https://doi.org/10.1103/PhysRevB.106.195135>.

## Publications

- Guguschev, C.; Richter, C.; Brutzam, M.; Dadzis, K.; Hirschle, C.; Gesing, T. M.; Schulze, M.; Kwasniewski, A.; Schreuer, J.; Schlom, D. G., *Revisiting the Growth of Large (Mg,Zr):SrGa<sub>12</sub>O<sub>19</sub> Single Crystals: Core Formation and Its Impact on Structural Homogeneity Revealed by Correlative X-ray Imaging*. *Crystal Growth & Design*; 22 (2022), 2557-2568 DOI: <https://doi.org/10.1021/acs.cgd.2c00030>.
- Guimaraes, M. D.; Richter, C.; Hanke, M.; Anooz, S. B.; Wang, Y. K.; Schwarzkopf, J.; Schmidbauer, M., *Ferroelectric phase transitions in tensile-strained NaNbO<sub>3</sub> epitaxial films probed by in situ x-ray diffraction*. *Journal of Applied Physics*; 132 (2022), 154102 DOI: <https://doi.org/10.1063/5.0113949>.
- Haak, J.; Kruger, J.; Abrosimov, N. V.; Helling, C.; Schulz, S.; Cutsail III, G. E., *X-Band Parallel-Mode and Multifrequency Electron Paramagnetic Resonance Spectroscopy of S=1/2 Bismuth Centers*. *Inorganic Chemistry*; 61 (2022), 11173-11181 DOI: <https://doi.org/10.1021/acs.inorgchem.2c01141>.
- Hamada, M.; Ganschow, S.; Klimm, D.; Serghiou, G.; Reichmann, H. J.; Bickermann, M., *Wüstite (Fe<sub>1-x</sub>O) - Thermodynamics and crystal growth*. *Zeitschrift Für Naturforschung Section B-a Journal of Chemical Sciences*; 77 (2022), 463-468 DOI: <https://doi.org/10.1515/znb-2022-0071>.
- Hanke, M.; Richter, C.; Lange, F.; Reis, A.; Parker, J.; Boeck, T., *Scanning x-ray microscopy: A sub-100 nm probe toward strain and composition in seeded horizontal Ge(110) nanowires*. *Applied Physics Letters*; 120 (2022), 101902 DOI: <https://doi.org/10.1063/5.0085788>.
- Hennecke, M.; Schick, D.; Sidiropoulos, T.; Willems, F.; Heilmann, A.; Bock, M.; Ehrentraut, L.; Engel, D.; Hessing, P.; Pfau, B.; Schmidbauer, M.; Furchner, A.; Schnuerer, M.; von Korff Schmising, C.; Eisebitt, S., *Ultrafast element- and depth-resolved magnetization dynamics probed by transverse magneto-optical Kerr effect spectroscopy in the soft x-ray range*. *Physical Review Research* 4 (2022) L022062
- Hensling, F. V. E.; Smeaton, M. A.; Show, V.; Azizie, K.; Barone, M. R.; Kourkoutis, L. F.; Schlom, D. G., *Epitaxial growth of the first two members of the Ba<sub>n+1</sub>In<sub>n</sub>O<sub>2.5n+1</sub> Ruddlesden-Popper homologous series*. *Journal of Vacuum Science & Technology A*; 40 (2022), 062707 DOI: <https://doi.org/10.1116/6.0002205>.
- Hepting, M.; Bejas, M.; Nag, A.; Yamase, H.; Coppola, N.; Betto, D.; Falter, C.; Garcia-Fernandez, M.; Agrestini, S.; Zhou, K. J.; Minola, M.; Sacco, C.; Maritato, L.; Orgiani, P.; Wei, H. I.; Shen, K. M.; Schlom, D. G.; Galdi, A.; Greco, A.; Keimer, B., *Gapped Collective Charge Excitations and Interlayer Hopping in Cuprate Superconductors*. *Physical Review Letters*; 129 (2022), 047001 DOI: <https://doi.org/10.1103/PhysRevLett.129.047001>.
- Hilfiker, M.; Williams, E.; Kilic, U.; Traouli, Y.; Koeppe, N.; Rivera, J.; Abakar, A.; Stokey, M.; Korlacki, R.; Galazka, Z.; Irmscher, K.; Schubert, M., *Elevated temperature spectroscopic ellipsometry analysis of the dielectric function, exciton, band-to-band transition, and high-frequency dielectric constant properties for single-crystal ZnGa<sub>2</sub>O<sub>4</sub>*. *Applied Physics Letters*; 120 (2022), 132105 DOI: <https://doi.org/10.1063/5.0087623>.
- Hollenbach, M.; Jagtap, N. S.; Fowley, C.; Baratech, J.; Guardia-Arce, V.; Kentsch, U.; Eichler-Volf, A.; Abrosimov, N. V.; Erbe, A.; Shin, C.; Kim, H.; Helm, M.; Lee, W.; Astakhov, G. V.; Berencen, Y., *Metal-assisted chemically etched silicon nanopillars hosting telecom photon emitters*. *Journal of Applied Physics*; 132 (2022), 033101 DOI: <https://doi.org/10.1063/5.0094715>.
- Hollenbach, M.; Klingner, N.; Jagtap, N. S.; Bischoff, L.; Fowley, C.; Kentsch, U.; Hlawacek, G.; Erbe, A.; Abrosimov, N. V.; Helm, M.; Berencen, Y.; Astakhov, G. V., *Wafer-scale nanofabrication of telecom single-photon emitters in silicon*. *Nature Communications*; 13 (2022), 7683 DOI: <https://doi.org/10.1038/s41467-022-35051-5>.
- Islam, A. E.; Sepelak, N. P.; Liddy, K. J.; Kahler, R.; Dryden, D. M.; Williams, J.; Lee, H. W.; Gann, K.; Popp, A.; Leedy, K. D.; Hendricks, N. S.; Brown, J. L.; Heller, E. R.; Wang, W. S.; Zhu, W. J.; Thompson, M. O.; Chabak, K. D.; Green, A. J., *500 degrees C operation of β-Ga<sub>2</sub>O<sub>3</sub> field-effect transistors*. *Applied Physics Letters*; 121 (2022), 243501 DOI: <https://doi.org/10.1063/5.0113744>.
- Jahelka P.R.; Ptak, A. Kiessling, F.M.; Frank-Rotsch, Ch.; Kelzenberg, M.; Atwater, H.A., *23.5% Efficiency GaAs Solar Cells Fabricated with Low-cost, Non-vacuum Processing*, 2022 IEEE 49th Photovoltaics Specialists Conference (PVSC), Philadelphia, PA, USA, 2022, pp. 0247-0247, DOI: <https://doi.org/10.1109/PVSC48317.2022.9938538>.
- Janzen, B. M.; Gillen, R.; Galazka, Z.; Maultzsch, J.; Wagner, M. R., *First- and second-order Raman spectroscopy of monoclinic beta-Ga<sub>2</sub>O<sub>3</sub>*. *Physical Review Materials*; 6 (2022), 054601 DOI: <https://doi.org/10.1103/PhysRevMaterials.6.054601>.

## Publications

- Kalusniak, S.; Castellano-Hernandez, E.; Yalcinoglu, H.; Tanaka, H.; Kränkel, C., *Spectroscopic properties of Tb<sup>3+</sup> as an ion for visible lasers*. Applied Physics B-Lasers and Optics; 128 (2022), 33 DOI: <https://doi.org/10.1007/s00340-022-07759-1>.
- Karuppanan, S. K.; Martin, J.; Xu, W. T.; Pasula, R. R.; Lim, S.; Nijhuis, C. A., *Biomolecular control over local gating in bilayer graphene induced by ferritin*. Iscience; 25 (2022), 104128 DOI: <https://doi.org/10.1016/j.isci.2022.104128>.
- Khurunenko, L. I.; Sosnin, M. G.; Duvanskii, A. V.; Abrosimov, N. V.; Riemann, H., *New properties of boron-oxygen dimer defect in boron-doped Czochralski silicon*. Journal of Applied Physics; 132 (2022), 135703 DOI: <https://doi.org/10.1063/5.0114809>.
- Kiessling, F. M.; Murray, P. G.; Kinley-Hanlon, M.; Buchovska, I.; Ervik, T. K.; Graham, V.; Hough, J.; Johnston, R.; Pietsch, M.; Rowan, S.; Schnabel, R.; Tait, S. C.; Steinlechner, J.; Martin, I. W., *Quasi-monocrystalline silicon for low-noise end mirrors in cryogenic gravitational-wave detectors*. Physical Review Research 4 (2022), 043043 <https://doi.org/10.1103/PhysRevResearch.4.043043>.
- Klimm, D.; Szczefanowicz, B.; Wolff, N.; Bickermann, M., *Phase diagram studies for the growth of (Mg,Zr):SrGa<sub>12</sub>O<sub>19</sub> crystals*. Journal of Thermal Analysis and Calorimetry; 147 (2022), 7133-7139 DOI: <https://doi.org/10.1007/s10973-021-11050-4>.
- Klimm, D.; Wolff, N., *On Thermodynamic Aspects of Oxide Crystal Growth*. Applied Sciences-Basel; 12 (2022), 2774 DOI: <https://doi.org/10.3390/app12062774>.
- Kränkel, C.; Uvarova, A.; Gugushev, C.; Kalusniak, S.; Hülshoff, L.; Tanaka, H.; Klimm, D., *Rare-earth doped mixed sesquioxides for ultrafast lasers Invited*. Optical Materials Express; 12 (2022), 1074-1091 DOI: <https://doi.org/10.1364/ome.450203>.
- Lee, H. J.; Ahn, Y.; Marks, S. D.; Gyan, D. S.; Landahl, E. C.; Lee, J. Y.; Kim, T. Y.; Unithrattil, S.; Chun, S. H.; Kim, S.; Park, S. Y.; Eom, I.; Adamo, C.; Schlom, D. G.; Wen, H. D.; Lee, S.; Jo, J. Y.; Evans, P. G., *Subpicosecond Optical Stress Generation in Multiferroic BiFeO<sub>3</sub>*. Nano Letters; 22 (2022), 4294-4300 DOI: <https://doi.org/10.1021/acs.nanolett.1c04831>.
- Lee, M. H.; Chou, T. S.; Bin Anooz, S.; Galazka, Z.; Popp, A.; Peterson, R. L., *Effect of post-metallization anneal on (100) Ga<sub>2</sub>O<sub>3</sub>/Ti-Au ohmic contact performance and interfacial degradation*. Apl Materials; 10 (2022), 091105 DOI: <https://doi.org/10.1063/5.0096245>.
- Lee, M. H.; Chou, T. S.; Bin Anooz, S.; Galazka, Z.; Popp, A.; Peterson, R. L., *Exploiting the Nanostructural Anisotropy of beta-Ga<sub>2</sub>O<sub>3</sub> to Demonstrate Giant Improvement in Titanium/Gold Ohmic Contacts*. ACS Nano; 16 (2022), 11988-11997 DOI: <https://doi.org/10.1021/acsnano.2c01957>.
- Liu, T.; Xiang, D.; Ng, H. K.; Han, Z. C.; Hippalgaonkar, K.; Suwardi, A.; Martin, J.; Garaj, S.; Wu, J., *Modulation of Spin Dynamics in 2D Transition-Metal Dichalcogenide via Strain-Driven Symmetry Breaking*. Advanced Science; 9 (2022), 2200816 DOI: <https://doi.org/10.1002/advs.202200816>.
- Liu, Y. J.; Gradwohl, K. P.; Lu, C. H.; Remmele, T.; Yamamoto, Y.; Zoellner, M. H.; Schroeder, T.; Boeck, T.; Amari, H.; Richter, C.; Albrecht, M., *Role of critical thickness in SiGe/Si/SiGe heterostructure design for qubits*. Journal of Applied Physics; 132 (2022), 085302 DOI: <https://doi.org/10.1063/5.0101753>.
- Liu, Y. J.; Rinner, S.; Remmele, T.; Ernst, O.; Reiserer, A.; Boeck, T., *(28)Silicon-on-insulator for optically interfaced quantum emitters*. Journal of Crystal Growth; 593 (2022), 126733 DOI: <https://doi.org/10.1016/j.jcrysgro.2022.126733>.
- Luo, A.; Gorobtsov, O. Y.; Nelson, J. N.; Kuo, D. Y.; Zhou, T.; Shao, Z. M.; Bouck, R.; Cherukara, M. J.; Holt, M. V.; Shen, K. M.; Schlom, D. G.; Suntivich, J.; Singer, A., *X-ray nano-imaging of defects in thin film catalysts via cluster analysis*. Applied Physics Letters; 121 (2022), 153904 DOI: <https://doi.org/10.1063/5.0125268>.
- Manganelli, C. L.; Kayser, S.; Virgilio, M., *A proof of concept of the bulk photovoltaic effect in non-uniformly strained silicon*. Journal of Applied Physics; 131 (2022), 125706 DOI: <https://doi.org/10.1063/5.0074426>.
- Matiwe, L.; Hartmann, C.; Cancellara, L.; Bickermann, M.; Klump, A.; Wollweber, J.; Hagedorn, S.; Weyers, M.; Straubinger, T., *Molten Barium Hydroxide as Defect Selective Drop Etchant for Dislocation Analysis on Aluminum Nitride Layers*. Physica Status Solidi a-Applications and Materials Science; 219 (2022), 2100707 DOI: <https://doi.org/10.1002/pssa.202100707>.
- Moncorge, R.; Guyot, Y.; Kränkel, C.; Lebbou, K.; Yoshikawa, A., *Mid-infrared emission properties of the Tm<sup>3+</sup>-doped sesquioxide crystals Y<sub>2</sub>O<sub>3</sub>, Lu<sub>2</sub>O<sub>3</sub>, Sc<sub>2</sub>O<sub>3</sub> and mixed compounds (Y,Lu,Sc)<sub>2</sub>O<sub>3</sub> around 1.5-, 2- and 2.3- $\mu$ m*. Journal of Luminescence; 241 (2022), 118537 DOI: <https://doi.org/10.1016/j.jlumin.2021.118537>.



## Publications

- Muhin, A.; Guttmann, M.; Montag, V.; Susilo, N.; Ziffer, E.; Sulmoni, L.; Hagedorn, S.; Lobo-Ploch, N.; Rass, J.; Cancellara, L.; Wu, S. J.; Wernicke, T.; Kneissl, M., *Radiative Recombination and Carrier Injection Efficiencies in 265 nm Deep Ultraviolet Light-Emitting Diodes Grown on AlN/Sapphire Templates with Different Defect Densities*. *Physica Status Solidi a-Applications and Materials Science*; (2022), 2200458 DOI: <https://doi.org/10.1002/pssa.202200458>.
- Mundy, J. A.; Grosso, B. F.; Heikes, C. A.; Segedin, D. F.; Wang, Z.; Shao, Y. T.; Dai, C.; Goodge, B. H.; Meier, Q. N.; Nelson, C. T.; Prasad, B.; Xue, F.; Ganschow, S.; Muller, D. A.; Kourkoutis, L. F.; Chen, L. Q.; Ratcliff, W. D.; Spaldin, N. A.; Ramesh, R.; Schlom, D. G., *Liberating a hidden antiferroelectric phase with interfacial electrostatic engineering*. *Science Advances*; 8 (2022), eabg5860 DOI: <https://doi.org/10.1126/sciadv.abg5860>.
- Nelson, J. N.; Schreiber, N. J.; Georgescu, A. B.; Goodge, B. H.; Faeth, B. D.; Parzyck, C. T.; Zeledon, C.; Kourkoutis, L. F.; Millis, A. J.; Georges, A.; Schlom, D. G.; Shen, K. M., *Interfacial charge transfer and persistent metallicity of ultrathin SrIrO<sub>3</sub>/SrRuO<sub>3</sub> heterostructures*. *Science Advances*; 8 (2022), eabj0481 DOI: <https://doi.org/10.1126/sciadv.abj0481>.
- Papadogianni, A.; Wouters, C.; Schewski, R.; Feldl, J.; Lahnemann, J.; Nagata, T.; Kluth, E.; Feneberg, M.; Goldhahn, R.; Ramsteiner, M.; Albrecht, M.; Bierwagen, O., *Molecular beam epitaxy of single-crystalline bixbyite (In<sub>1-x</sub>Ga<sub>x</sub>)<sub>2</sub>O<sub>3</sub> films (x ≤ 0.18): Structural properties and consequences of compositional inhomogeneity*. *Physical Review Materials*; 6 (2022), 033604 DOI: <https://doi.org/10.1103/PhysRevMaterials.6.033604>.
- Parzyck, C. T.; Galdi, A.; Nangoi, J. K.; DeBenedetti, W. J. I.; Balajka, J.; Faeth, B. D.; Paik, H.; Hu, C.; Arias, T. A.; Hines, M. A.; Schlom, D. G.; Shen, K. M.; Maxson, J. M., *Single-Crystal Alkali Antimonide Photocathodes: High Efficiency in the Ultrathin Limit*. *Physical Review Letters*; 128 (2022), 114801 DOI: <https://doi.org/10.1103/PhysRevLett.128.114801>.
- Pätzold, O.; Dadzis, K.; Kirmse, C.; Weik, D.; Büttner, L.; Czarske, J.; Charitos, A., *Model experiments for melt flow in Czochralski growth of silicon*. *Journal of Crystal Growth*; 588 (2022), 126656 DOI: <https://doi.org/10.1016/j.jcrysgro.2022.126656>.
- Pfützenreuter, D.; Kim, S.; Cho, H.; Bierwagen, O.; Zupancic, M.; Albrecht, M.; Char, K.; Schwarzkopf, J., *Confinement of Electrons at the LaInO<sub>3</sub>/BaSnO<sub>3</sub> Heterointerface*. *Advanced Materials Interfaces*; 9 (2022), DOI: <https://doi.org/10.1002/admi.202201279>.
- Püschel, S.; Mauerhoff, F.; Kränkel, C.; Tanaka, H., *Laser cooling in Yb:KY<sub>3</sub>F<sub>10</sub>: a comparison with Yb:YLF*. *Optics Express*; 30 (2022), 47235-47248 DOI: <https://doi.org/10.1364/oe.472633>.
- Püschel, S.; Mauerhoff, F.; Kränkel, C.; Tanaka, H., *Solid-state laser cooling in Yb:CaF<sub>2</sub> and Yb:SrF<sub>2</sub> by anti-Stokes fluorescence*. *Optics Letters*; 47 (2022), 333-336 DOI: <https://doi.org/10.1364/ol.449115>.
- Ratcliff, L. E.; Oshima, T.; Nippert, F.; Janzen, B. M.; Kluth, E.; Goldhahn, R.; Feneberg, M.; Mazzolini, P.; Bierwagen, O.; Wouters, C.; Nofal, M.; Albrecht, M.; Swallow, J. E. N.; Jones, L. A. H.; Thakur, P. K.; Lee, T. L.; Kalha, C.; Schlueter, C.; Veal, T. D.; Varley, J. B.; Wagner, M. R.; Regoutz, A., *Tackling Disorder in gamma-Ga<sub>2</sub>O<sub>3</sub>*. *Advanced Materials*; 34 (2022), 2204217 DOI: <https://doi.org/10.1002/adma.202204217>.
- Rehm, J.; Chou, T. S.; Anooz, S. B.; Seyidov, P.; Fiedler, A.; Galazka, Z.; Popp, A., *Perspectives on MOVPE-grown (100) beta-Ga<sub>2</sub>O<sub>3</sub> thin films and its Al-alloy for power electronics application*. *Applied Physics Letters*; 121 (2022), 240503 DOI: <https://doi.org/10.1063/5.0122886>.
- Reichmann, F.; Dabrowski, J.; Becker, A. P.; Klesse, W. M.; Irmscher, K.; Schewski, R.; Galazka, Z.; Mulazzi, M., *Experimental and Theoretical Investigation of the Surface Electronic Structure of ZnGa<sub>2</sub>O<sub>4</sub>(100) Single-Crystals*. *Physica Status Solidi B-Basic Solid State Physics*; 259 (2022), 2100452 DOI: <https://doi.org/10.1002/pssb.202100452>.
- Richter, C.; Kaganer, V. M.; Even, A.; Dussaigne, A.; Ferret, P.; Barbier, F.; Le Vaillant, Y. M.; Schulli, T. U., *Nanoscale Mapping of the Full Strain Tensor, Rotation, and Composition in Partially Relaxed In<sub>x</sub>Ga<sub>1-x</sub>N Layers by Scanning X-ray Diffraction Microscopy*. *Physical Review Applied*; 18 (2022), 064015 DOI: <https://doi.org/10.1103/PhysRevApplied.18.064015>.
- Sabanskis, A.; Dadzis, K.; Menzel, R.; Virbulis, J., *Application of the Alexander-Haasen Model for Thermally Stimulated Dislocation Generation in FZ Silicon Crystals*. *Crystals*; 12 (2022), 174 DOI: <https://doi.org/10.3390/cryst12020174>.
- Saring, P.; Abrosimov, N. V.; Seibt, M., *Nucleation of Nickel Disilicide Precipitates in Float-Zone Silicon: The Role of Vacancies*. *Physica Status Solidi a-Applications and Materials Science*; 219 (2022), 2200220 DOI: <https://doi.org/10.1002/pssa.202200220>.

## Publications

- Scheffler, M.; Aeschlimann, M.; Albrecht, M.; Bereau, T.; Bungartz, H. J.; Felser, C.; Greiner, M.; Gross, A.; Koch, C. T.; Kremer, K.; Nagel, W. E.; Scheidgen, M.; Woll, C.; Draxl, C., *FAIR data enabling new horizons for materials research*. Nature; 604 (2022), 635-642 DOI: <https://doi.org/10.1038/s41586-022-04501-x>.
- Schimmel, S.; Sun, W. H.; Dropka, N., *Artificial Intelligence for Crystal Growth and Characterization*. Crystals; 12 (2022), 1232 DOI: <https://doi.org/10.3390/cryst12091232>.
- Schubert, M.; Knight, S.; Richter, S.; Kuhne, P.; Stanishev, V.; Ruder, A.; Stokey, M.; Korlacki, R.; Irmscher, K.; Neugebauer, P.; Darakchieva, V., *Terahertz electron paramagnetic resonance generalized spectroscopic ellipsometry: The magnetic response of the nitrogen defect in 4H-SiC*. Applied Physics Letters; 120 (2022), 102101 DOI: <https://doi.org/10.1063/5.0082353>.
- Schulz, T.; Yoo, S. H.; Lymperakis, L.; Richter, C.; Zatterin, E.; Lachowski, A.; Hartmann, C.; Foronda, H. M.; Brandl, C.; Lugauer, H. J.; Hoffmann, M. P.; Albrecht, M., *Step pinning and hillock formation in (Al,Ga)N films on native AlN substrates*. Journal of Applied Physics; 132 (2022), 223102 DOI: <https://doi.org/10.1063/5.0125480>.
- Schwabe, S.; Lunser, K.; Schmidt, D.; Nielsch, K.; Gaal, P.; Fahler, S., *What is the speed limit of martensitic transformations?* Science and Technology of Advanced Materials; 23 (2022), 633-641 DOI: <https://doi.org/10.1080/14686996.2022.2128870>.
- Seyidov, P.; Ramsteiner, M.; Galazka, Z.; Irmscher, K., *Resonant electronic Raman scattering from Ir<sup>4+</sup> ions in beta-Ga<sub>2</sub>O<sub>3</sub>*. Journal of Applied Physics; 131 (2022), 035707 DOI: <https://doi.org/10.1063/5.0080248>.
- Seyidov, P.; Varley, J. B.; Galazka, Z.; Chou, T. S.; Popp, A.; Fiedler, A.; Irmscher, K., *Cobalt as a promising dopant for producing semi-insulating beta-Ga<sub>2</sub>O<sub>3</sub> crystals: Charge state transition levels from experiment and theory*. Apl Materials; 10 (2022), 111109 DOI: <https://doi.org/10.1063/5.0112915>.
- Song, Q.; Sun, J. X.; Parzyck, C. T.; Miao, L. D.; Xu, Q.; Hensling, F. V. E.; Barone, M. R.; Hu, C.; Kim, J.; Faeth, B. D.; Paik, H.; King, P. D. C.; Shen, K. M.; Schlom, D. G., *Growth of PdCoO<sub>2</sub> films with controlled termination by molecular-beam epitaxy and determination of their electronic structure by angle-resolved photo-emission spectroscopy*. Apl Materials; 10 (2022), 091113 DOI: <https://doi.org/10.1063/5.0101837>.
- Sun, J. X.; Parzyck, C. T.; Lee, J. H.; Brooks, C. M.; Kourkoutis, L. F.; Ke, X. L.; Misra, R.; Schubert, J.; Hensling, F. V.; Barone, M. R.; Wang, Z.; Holtz, M. E.; Schreiber, N. J.; Song, Q.; Paik, H.; Heeg, T.; Muller, D. A.; Shen, K. M.; Schlom, D. G., *Canonical approach to cation flux calibration in oxide molecular-beam epitaxy*. Physical Review Materials; 6 (2022), 033802 DOI: <https://doi.org/10.1103/PhysRevMaterials.6.033802>.
- Surovovs, K.; Surovovs, M.; Sabanskis, A.; Virbulis, J.; Dadzis, K.; Menzel, R.; Abrosimov, N., *Numerical Simulation of Species Segregation and 2D Distribution in the Floating Zone Silicon Crystals*. Crystals; 12 (2022), 1718 DOI: <https://doi.org/10.3390/cryst12121718>.
- Suzuki, A.; Kalusniak, S.; Tanaka, H.; Brützmam, M.; Ganschow, S.; Tokurakawa, M.; Kränkel, C., *Spectroscopy and 2.1 μm laser operation of Czochralski-grown Tm<sup>3+</sup>:Y-ScO<sub>3</sub> crystals*. Optics Express; 30 (2022), 42762-42771 DOI: <https://doi.org/10.1364/oe.475711>.
- Tanaka, H.; Kalusniak, S.; Badtke, M.; Demesh, M.; Kuleshov, N. V.; Kannari, F.; Kränkel, C., *Visible solid-state lasers based on Pr<sup>3+</sup> and Tb<sup>3+</sup>*. Progress in Quantum Electronics; 84 (2022), 100411 DOI: <https://doi.org/10.1016/j.pquantelec.2022.100411>.
- Tetzner, K.; Egbo, K.; Klupsch, M.; Unger, R. S.; Popp, A.; Chou, T. S.; Bin Anooz, S.; Galazka, Z.; Trampert, A.; Bierwagen, O.; Wurfl, J., *SnO/beta-Ga<sub>2</sub>O<sub>3</sub> heterojunction field-effect transistors and vertical p-n diodes*. Applied Physics Letters; 120 (2022), 112110 DOI: <https://doi.org/10.1063/5.0083032>.
- Tetzner, K.; Schewski, R.; Popp, A.; Bin Anooz, S.; Chou, T.-S.; Ostermay, I.; Kirmse, H.; Würfl, J., *Refractory metal-based ohmic contacts on β-Ga<sub>2</sub>O<sub>3</sub> using TiW*. APL Materials 10 (2022) 71108 DOI: <https://doi.org/10.1063/5.009466>.
- Vahapoglu, E.; Slack-Smith, J. P.; Leon, R. C. C.; Lim, W. H.; Hudson, F. E.; Day, T.; Cifuentes, J. D.; Tantt, T.; Yang, C. H.; Saraiva, A.; Abrosimov, N. V.; Pohl, H.-J.; Thewalt, M. L. W.; Laucht, A.; Dzurak, A. S.; Pla, J. J., *Coherent control of electron spin qubits in silicon using a global field*; npj Quantum Information 8 (2022) 126 DOI: <https://doi.org/10.1038/s41534-022-00645-w>
- Vogt, P.; Hensling, F. V. E.; Azizie, K.; McCandless, J. P.; Park, J.; DeLello, K.; Muller, D. A.; Xing, H. G.; Jena, D.; Schlom, D. G., *Extending the Kinetic and Thermodynamic Limits of Molecular-Beam Epitaxy Utilizing Suboxide Sources or Metal-Oxide-Catalyzed Epitaxy*. Physical Review Applied; 17 (2022), 034021 DOI: <https://doi.org/10.1103/PhysRevApplied.17.034021>.

## Talks

Wang, Y. K.; Bin Anooz, S.; Niu, G.; Schmidbauer, M.; Wang, L. Y.; Ren, W.; Schwarzkopf, J., *Thickness effect on ferroelectric domain formation in compressively strained  $K_{0.65}Na_{0.35}NbO_3$  epitaxial films*. Physical Review Materials; 6 (2022), 084413 DOI: <https://doi.org/10.1103/PhysRevMaterials.6.084413>.

Wang, Y. K.; Wang, Q.; Zhao, J. Y.; Niermann, T.; Liu, Y. Y.; Dai, L. Y.; Zheng, K.; Sun, Y. X.; Zhang, Y. J.; Schwarzkopf, J.; Schroeder, T.; Jiang, Z. D.; Ren, W.; Niu, G., *A robust high-performance electronic synapse based on epitaxial ferroelectric  $Hf_{0.5}Zr_{0.5}O_2$  films with uniform polarization and high Curie temperature*. Applied Materials Today; 29 (2022), 101587 DOI: <https://doi.org/10.1016/j.apmt.2022.101587>.

Witkowski, M. E.; Drozdowski, K. J.; Makowski, M.; Drozdowski, W.; Wojtowicz, A. J.; Irmscher, K.; Schewski, R.; Galazka, Z., *Low temperature thermoluminescence of  $\beta$ - $Ga_2O_3$  scintillator*. Optical Materials: X 16 (2022) 100210 DOI: <https://doi.org/10.1016/j.omx.2022.100210>

Wolff, N.; Klimm, D., *Determination of the phase diagram  $Tb_2O_3$ - $SiO_2$  and crystal growth of the rare earth pyrosilicate  $Tb_2Si_2O_7$  by the optical floating-zone (OFZ) technique*. Journal of Solid State Chemistry; 312 (2022), 123269 DOI: <https://doi.org/10.1016/j.jssc.2022.123269>.

Zakhar'in, A. O.; Andrianov, A. V.; Petrov, A. G.; Abrosimov, N. V.; Zhukavin, R. K.; Shastin, V. N., *Excitation of intracenter terahertz radiation by plasma oscillations in electron-hole liquid*. Materials Science and Engineering B-Advanced Functional Solid-State Materials; 286 (2022), 115979 DOI: <https://doi.org/10.1016/j.mseb.2022.115979>.

Zhukavin, R. K.; Bushuikin, P. A.; Kukotenko, V. V.; Choporova, Y. Y.; Dessmann, N.; Kovalevsky, K. A.; Tsyplenkov, V. V.; Gerasimov, V. V.; Knyazev, B. A.; Abrosimov, N. V.; Shastin, V. N., *Detection of Ramsey Oscillations in Germanium Doped with Shallow Donors upon the Excitation of the  $1s \rightarrow 2p(0)$  Transition*. Jap Letters; 116 (2022), 137-143 DOI: <https://doi.org/10.1134/s0021364022601191>.

## Books and chapters

Dropka, Natascha; Gradwohl, Kevin-Peter: *Crystal Growth, Bulk: Theory and Models*. In: *Encyclopedia of Condensed Matter Physics*, 2nd Edition, Elsevier, 2023. Reference Module in Materials Science and Materials Engineering, Elsevier, 2022, ISBN 9780128035818, <https://doi.org/10.1016/B978-0-323-90800-9.00108-6>.

Klimm, Detlef: *Thermal Analysis and Thermodynamics*. In: *Materials Science*, Berlin, Boston: De Gruyter, 2022. ISBN: 9783110743777. <https://doi.org/10.1515/9783110743784>.

Kräinkel, Christian: *8.5 Crystals for solid-state lasers*. In: *Volume 2 From Energy Storage to Photofunctional Materials*, edited by Rainer Pöttgen, Thomas Jüstel and Cristian A. Strassert, Berlin, Boston: De Gruyter, 2023, pp. 371-406. ISBN 978-3-11-073814-8. <https://doi.org/10.1515/9783110798890-024>.

## Talks

### Invited talks at national and international conferences and workshops

M. Bickermann; *Favorable growth conditions and diameter enlargement of bulk AlN single crystals grown by physical vapor transport*; 7th European Conference on Crystal Growth; 25-27 July, Paris, France

M. Bickermann; *Preparation of perovskite, pyrochlore and magnetoplumbite crystals for advanced functional oxides*; 7th European Conference on Crystal Growth; 25-27 July, Paris, France

M. Bickermann; *Bulk  $\beta$ -Ga<sub>2</sub>O<sub>3</sub> Single Crystals Grown by the Czochralski Method*, DGKK workshop on Bulk Semiconductor Crystals, 5-6 October, Freiberg, Germany

I. Buchovska; *Directional solidification of Si in travelling magnetic fields: control of material properties*; 7th European Conference on Crystal Growth; 25-27 July, Paris, France

K. Dadzis, A. Wintzer, I. Tsiapkinis; *Open source models for multiphysical simulation of crystal growth*; The 10th International Workshop on Modeling in Crystal Growth; 16-19 October, Xi'an, China

K. Dadzis, A. Wintzer, I. Tsiapkinis, and S. Foroushani; *Multiphysical model experiments for crystal growth*, DGKK Arbeitskreistreffen Herstellung und Charakterisierung von massiven Halbleiterkristallen, 5-6 October, Freiberg, Germany

N. Dropka, M. Holena; *Can Machine Learning Help Us Grow Advanced Crystals?*; International Workshop on Crystal Growth Technology IWCGT-8; 29 May - 2 June, Berlin, Germany

O.C. Ernst; *From thin crystalline layers to bulk crystals: leveraging de-wetting models rather than nucleation theory to overcome size scales*; 7th European Conference on Crystal Growth; 25-27 July, Paris, France

A. Fiedler, P. Seyidov, M. Ramsteiner, Z. Galazka, K. Irmscher; *Electronic Raman scattering in  $\beta$ -Ga<sub>2</sub>O<sub>3</sub>*; The 4<sup>th</sup> International Workshop on Gallium Oxide and Related Materials; 23-27 October, Nagano, Japan

Z. Galazka; *Overview of the growth and physical properties of Czochralski-grown bulk  $\beta$ -Ga<sub>2</sub>O<sub>3</sub> single crystals and related compounds*; The 4th International Workshop on Gallium Oxide and Related Compounds (IWGO 2022); 3-27 October, Nagano, Japan

Z. Galazka; *Transparent Semiconducting Oxides (TSOs): bulk single crystals and basic physical properties*; MRS Webinar, 31 March, online

S. Ganschow, Z.H. Amber, M. Brützam, K. Böttcher, H. Fritze, U.B. Ganie, D. Klimm, M. Rüsing, Y. Suhak; *Li(Nb,Ta)O<sub>3</sub> - phase diagram and growth of solid solution single crystals*; Materials Science and Engineering MSE Congress; 27 -29 September, Darmstadt, Germany

K.-P. Gradwohl, Y. Liu, T. Schroeder, T. Boeck; *SiGe/Ge/SiGe Heterostructures for Quantum Dot Hole Spin Qubits: Surface Treatment and Epitaxial Growth*; 9th International Symposium on Control of Semiconductor Interfaces; 4-8 September, Nagoya, Japan

K.-P. Gradwohl, M. Roder, A.N. Danilewsky, A. Gybin, U. Juda, R. Sumathi; *Structural defects in Czochralski-grown Ge crystals for neutrinoless double beta decay experiments*; 7th European Conference on Crystal Growth; 25-27 July, Paris, France

C. Hartmann, C. Richter, D. Schulz, A. Klump, M. Kabukcuoglu, E Hamann, M. Schilling, T. Wernicke, M. Bickermann, D. Hänschke, M. Kneissl and T. Straubinger; *Efficient diameter enlargement of bulk AlN single crystals with high structural quality*; International Workshop on Nitride Semiconductors, 9-14 October, Berlin, Germany

C. Kränkel; *Short course: Crystalline gain materials for solid-state lasers*; Advanced Solid-State Lasers Conference 2022, 11 - 15 December, Barcelona, Spain

Y. Liu, K.P. Gradwohl, C. Lu, Y. Yamamoto, M. H. Zöllner, T. Remmele, T. Boeck, C. Richter, M. Albrecht; *Viewing SiGe Heterostructure for Qubits with Dislocation Theory*; 242nd ECS Meeting; 9-13 October, Atlanta, USA

R. Menzel, K. Dadzis, F. M. Kießling, N. Lorenz-Meyer, B. Faraji-Tajrishi, A. Nikiforova, N. Abrosimov, H. Riemann; *Growth of Silicon Crystals Using a Self-Crucible Concept*; International Workshop on Crystal Growth Technology IWCGT-8; 29 May - 2 June, Berlin, Germany

W. Miller, M. Albrecht, T. Schulz, A. Klump, A. Popp, S. Bin Anooz; *Kinetic Monte Carlo Simulation for understanding epitaxial growth*; Leibniz MMS Days 2022; 25-27 April, Potsdam, Germany

W. Miller, T. Schulz, L. Lymperakis, A. Klump, M. Albrecht; *Kinetic Monte Carlo simulations of AlN and AlGaN epitaxy on AlN(0001)*; 7th European Conference on Crystal Growth; 25-27 July, Paris, France

W. Miller, M. Albrecht, T. Schulz, A. Klump, A. Popp, S. Bin Anooz; *Kinetic Monte Carlo Simulation simulations of AlN and AlGaN epitaxy on AlN(0001)*; 10<sup>th</sup> International Workshop on Modeling in Crystal Growth; 16-19 October, Xi'an, China

## Talks

A. Popp S. Bin Anooz, T.-S. Chou, J. Rehm, V. Tran, R. Grüneberg, A. Fiedler, Palvan Seyidov, Z. Galazka, R. Schewski, M. Pietsch, A. Kwasniewski, M. Schmidbauer, W. Miller, K. Irmscher, M. Albrecht and J. Schwarzkopf; *Epitaxial Growth development of (100)  $\beta$ -Ga<sub>2</sub>O<sub>3</sub> by MOVPE*; Polish Conference on Crystal Growth, 19-22 June, Gdansk, Poland

T. Schröder; *The Importance of Crystals for Science & Technology: Modern Examples from Electronics & Photonics*; Materials Science and Engineering Seminar Series; January 14, 2022 zoom-Seminar

J. Schwarzkopf, S. Bin Anooz, Yankun Wang, M. Guimaraes, S. Liang, R. Wördenweber, M. Schmidbauer; *Strain engineering in ferroelectric (K,Na)NbO<sub>3</sub> thin films*; International Workshop On Polar Oxides: Lithium Niobate and Related Compounds, 11-13 May, Goslar, Germany

K. Stolze, Ch. Frank-Rotsch; *Semiconductor Single Crystals – Defect Engineering in Volume Crystal Growth*; 9th Carnival Conference of the Department of Chemistry, University of Cologne, 8 June, Cologne, Germany

R.R. Sumathi, *Classical Semiconductor Crystals: A new journey for a new world*, International Conference on Crystal Growth and Technological applications of crystals (CGTA) (virtual) - 'SSN Institute of Technology, 10-12 Jan.2022, Chennai (online)

A. Suzuki, C. Kränkel, and M. Tokurakawa; *Mode-locked lasers using Tm-doped sesquioxide gain media*; 69<sup>th</sup> JSAP Spring Meeting 2022, 22 - 26 March, online

H. Tanaka, S. Püschel, F. Mauerhoff, S. Kalusniak, and C. Kränkel; *Growth of highly pure fluoride crystals for laser cooling*; SPIE Photonics West 2022, 31 January - 2 February, San Francisco, USA

H. Tanaka, S. Püschel, F. Mauerhoff, S. Kalusniak, and C. Kränkel; *Latest developments in self-cooled laser crystals*; Photonics Days Berlin Brandenburg 2022, 9 - 12 October, Berlin, Germany

## Invited seminars and lectures at national and international institutions

M. Bickermann: *Melt Growth of  $\beta$ -Ga<sub>2</sub>O<sub>3</sub> Bulk Crystals*, Semiconductor Colloquium of the Cluster Power Electronics at the Fraunhofer IISB, online, November 2022.

C. Guguschev: *IKZ-Cornell Joint Lab activities: Overview about selected crystal growth techniques and crystal growth developments of the last years*, Cornell University, USA, 7 October 2022

C. Kränkel: *Tailored gain materials for lasers from the visible to the mid-infrared spectral range* Universität Stuttgart, Group Seminar H. Giessen (2022)

C. Kränkel, M. Badtke, E. Castellano-Hernandez, S. Kalusniak, H. Tanaka and H. Yalcinoglu: *Diode-pumped solid-state lasers with direct emission in the visible spectral range*; OSRAM Opto Semiconductors, Internal Seminar, Online (2022)

C. Kränkel: *Tailored gain materials for visible and infrared lasers*; Optica Webinar, Laser Systems Technical group, Online (2022)

T. Schröder: *The Importance of Crystals for Science & Technology: Modern Examples from Electronics & Photonics*, UCLA Samueli School of Engineering, Materials Science & Engineering Seminar Series 2022: Online Seminar, Germany/Los Angeles, CA, USA, 14 January 2022

T. Schröder: *Crystals and Components: IKZ's EU flagship role in Technology Sovereignty*, IMEC, Leuven, Belgium, 23 March 2022

T. Schröder: Panel discussion: *Neuromorphic Computing Day Jülich-Aachen*, Forschungszentrum Jülich, Germany, 25 May 2022

T. Schröder: *IKZ's EU Flagship Role on Crystals for Science & Technology: Key Components for Electronics & Photonics*, Research Center Jülich Summer School by Peter Grünberg Center Number 9, Scheerenberg (Germany), 30 June 2022

T. Schröder: *Novel Synthesis Methods for Artificial Crystals by Layer-Transfer*, CHyN, DESY - Deutsches Elektronen-Synchrotron, Hamburg, Germany, 18 November 2022

T. Schröder: *New directions in electronics, optoelectronics, and devices*, Beamline Review Committee Member at the ESRF, Grenoble, France, November 2022

## Patents

T. Schröder: *Modern X-Ray Microscopy for Academia & Industry*, Beamline Review Committee Member at the ESRF, Grenoble, France, November 2022

T. Schröder: *Leibniz Mentoring for Postdocs*, Leibniz Association, Berlin, Germany, March 2022

T. Schröder: *Führung Leibniz – im Institut und im Forum*, Leibniz Leadership Academy, Leibniz Association, Berlin, Germany, March 2022

T. Schröder: *Geteilte Führung (Joint Leadership)*, Leibniz Annual Meeting Gender Equality, Leibniz Association, Berlin, Germany, March 2022

T. Schröder: Participant in the expert dialog: Federal Ministry for Economic Affairs and Climate (BMWK) "Technological and Digital Sovereignty", 'Advanced Materials and Materials Technologies' within the framework of the National Security Strategy of the Federal Foreign Office", July 2022

T. Schröder: Panel discussion: Leibniz Quadriga Format, Leibniz Association Berlin, Germany, October 2022

T. Schröder and M. Bickermann: Crystals & Components for Science & Technology: The European perspective, Lecture at the GDCh Berlin Chapter, TU Berlin, April 2022

J. Schwarzkopf: *Epitaxial growth of lead-free ferroelectric (K,Na)NbO<sub>3</sub> thin films and the impact of strain*, FerroSchool 2022, Lyon, France, June 2022

R. R. Sumathi, *Current research works at the semiconductors section of IKZ-Berlin*, Helsinki University, Finland, December 2022

### Crystal growth in magnet fields (semiconductors group III-V, IV)

Ch. Frank-Rotsch, P. Rudolph, O. Klein, B. Nacke, R.-P. Lange

**Vorrichtung und Verfahren zur Herstellung von Kristallen aus elektrisch leitenden Schmelzen (Device and method for producing crystals from electrically conductive melts)**

DE102007028548B4; KRISTMAG®

R.-P. Lange, D. Jockel, B. Nacke, H. Kasjanow, M. Ziem, P. Rudolph, F. Kießling, Ch. Frank-Rotsch, M. Czupalla

**Vorrichtung zur Herstellung von Kristallen aus elektrisch leitenden Schmelzen (Device for producing crystals from electro-conductive melts)**

DE102007028547B4; KRISTMAG®

M. Ziem, P. Rudolph, R.-P. Lange

**Vorrichtung zum Züchten von Einkristallen aus elektrisch leitfähigen Schmelzen (Device for the manufacture of crystals from electrically conductive melts)**

DE102007020239B4; KRISTMAG®

R.-P. Lange, P. Rudolph, M. Ziem

**Vorrichtung zur Herstellung von Kristallen aus elektrisch leitenden Schmelzen (Device for producing crystals from electro-conductive melts)**

DE102008035439B4

F. Büllesfeld, N. Dropka, W. Miller, U. Rehse, U. Sahr, P. Rudolph

**Verfahren zum Erstarren einer Nichtmetall-Schmelze (Method for freezing a nonmetal melt)**

EP 2370617B1 (09749132.8) (DE, NO), TW 201035391

N. Dropka, Ch. Frank-Rotsch, P. Rudolph, R.-P. Lange, U. Rehse

**Kristallisationsanlage und Kristallisationsverfahren zur Herstellung eines Blocks aus einem Material, dessen Schmelze elektrisch leitend ist (Crystallization system and crystallization process for producing a block from a material with an electrically conductive molten mass)**

DE102010041061B4

## Patents

M. Czupalla, B. Lux, F. Kießling, O. Klein, P. Rudolph, W. Miller, M. Ziem, F. Kirscht, R.-P. Lange  
**Verfahren zur Züchtung von Kristallen aus elektrisch leitenden Schmelzen, die in der Diamant- oder Zinkblendestruktur kristallisieren (Method for growing crystals that crystallize in diamond or zinc blende structure from electrically conductive melts)**  
 DE102009027436B4

J. Boschker, Ch. Frank-Rotsch, M. Zorn, T. Schröder  
**Substrat für ein Halbleiterbauelement Halbleitervorrichtung und Verfahren zum Herstellen eines Substrats für ein Halbleiterbauelement**  
 DE102020131850, PCT/EP2021/082758

K. Stolze, P. Steglich, K. Berger, U. Juda, J. Martin  
**Verfahren und Vorrichtung zum Herstellen einer Halbleiterstruktur (Transfer Printable Single-Crystalline Coupons)**  
 DE 102022100661.1, EP23151074.4

### Registered Trademark

KRISTMAG®

### Semiconductors group IV

M. Wünscher, H. Riemann  
**Vorrichtung für das tiegelfreie Zonenziehen von Kristallstäben (Apparatus for continuous zone-melting a crystalline rod)**  
 DE102012022965B4, EP 2920342B1 (DE, DK, LV)

N. Abrosimov, J. Fischer, H. Riemann, M. Renner  
**Verfahren und Vorrichtung zur Herstellung von Einkristallen aus Halbleitermaterial (Process and apparatus for producing semiconductor single crystals)**  
 EP2504470B1 (NO, ES, NL, FR, DK, GB, BE, IT), DE102010005520B4, JP 5484589B2, US 9422636

### Oxides and laser materials

Z. Galazka, R. Uecker, D. Klimm, M. Bickermann  
**Method for growing beta phase of gallium oxide ( $\beta$ -Ga<sub>2</sub>O<sub>3</sub>) single crystals from the melt contained within a metal crucible**  
 EP3242965B1 (AT, BE, CH, DE, CZ, ES, FR, GB, IT, NL, PL), KR101979130B1, US20170362738A1

Z. Galazka, R. Uecker, R. Fornari  
**Method and apparatus for growing indium oxide (In<sub>2</sub>O<sub>3</sub>) single crystals and indium oxide (In<sub>2</sub>O<sub>3</sub>) single crystal**  
 EP2841630B1 (DE, BE, FR, GB, IT), JP 6134379B2, US10208399

C. Guguschev, M. Brützam, D. Schlom, H. Paik  
**Method and setup for growing bulk single crystals**  
 DE102020114524A1, US20200378030A1, KR1020200138082A

C. Guguschev, E. Haurat, D. Klimm, C. Kränkel, A. Uvarova  
**Verfahren und Vorrichtung zum Züchten eines Seltenerd-Sesquioxid-Kristalls (Method and device for growing a rare earth sesquioxide crystal)**  
 DE102020120715, WO/EP21748512.7

S. Ganschow, Ch. Kränkel  
**Oxidkristall mit Perowskit-Struktur (Oxide crystal with perovskite structure)**  
 DE 102021134215.5

Z. Galazka, S. Ganschow, M. Bickermann, T. Schröder, W. Häckl  
**Method and apparatus for producing electrically conducting bulk  $\beta$ -Ga<sub>2</sub>O<sub>3</sub> single crystals and electrically conducting bulk  $\beta$ -Ga<sub>2</sub>O<sub>3</sub> single crystal**  
 EP22154305.1, PCT/EP/2023051212

Z. Galazka, S. Ganschow, M. Bickermann, T. Schröder  
**Melt-grown bulk  $\beta$ -(Al<sub>x</sub>Ga<sub>1-x</sub>)<sub>2</sub>O<sub>3</sub> single crystals and method for producing bulk  $\beta$ -(Al<sub>x</sub>Ga<sub>1-x</sub>)<sub>2</sub>O<sub>3</sub> single crystals**  
 PCT/EP2022/078252

### Aluminium nitride

A. Dittmar, C. Hartmann, J. Wollweber, M. Bickermann  
**(Sc, Y):AlN Einkristalle für Gitter-angepasste AlGaN Systeme ((Sc,Y):AlN single crystals for lattice-adapted AlGaN systems)**  
 DE102015116068A1, KR1020180048926A

C. Hartmann, T. Straubinger  
**Kristallzüchtungsvorrichtung und Verfahren zum Züchten eines Halbleiters (Crystal growth design and method for growing a semiconductor)**  
 DE 102022119343.8

### Semiconducting layers and nanostructures

O. Ernst, T. Boeck, F. Lange, H.-P. Schramm, T. Teubner, D. Uebel  
**Verfahren zur Mikrostrukturierung (Method for Microstructuring)**  
 DE102020126553

## Patents

D. Uebel, R. Bansen, T. Boeck, O. Ernst, H.-P. Schramm, T. Teubner

**Silizium-basierte Wafer und Verfahren zur Herstellung von Silizium-basierten Wafern (Silicon-based wafers and method of fabricating silicon-based wafers)**

DE102020132900

O. Ernst, D. Uebel, T. Boeck

**Verfahren zur Herstellung von isopenangereicherten Germanium-Wasserstoffverbindungen (Process for the preparation of isotope-enriched germanium-hydrogen compounds)**

DE 102022105177.3, PCT/EP2023/054384

S. Zahedi-Azad, T. Boeck, O. Ernst, H.-P. Schramm, D. Uebel

**Verfahren und Züchtungsaufbau zum Herstellen lokalisierter Strukturen (Method and growth setup for the fabrication of localized structures)**

DE 102022116962.6

### Oxide layers

M. Albrecht, A. Baki, K. Irmscher, T. Schulz, J. Schwarzkopf, J. Stöver

**Verfahren zum Herstellen eines Kristalls mit Perowskitstruktur (Formingless Resistive Switching by Off-Stoichiometry Control of ABO<sub>3</sub> Perovskites)**

DE1020132049, PCT/EP2021/082505

T. Chou, A. Popp, W. Häckl

**Method for producing a gallium oxide layer on a substrate**

EP 21187231.2

S. Bin-Anooz, T.-S. Chou, W. Häckl, A. Popp

**Method for producing a gallium oxide layer on a substrate**

EP 22194558.7

### Characterization

P. Gaal

**Bereitstellen eines transienten Gitters (Providing a transient grid)**

DE102019132393B4, PCT/EP2020/082942

## Teaching and Education

**Matthias Bickermann**

*Kristallzüchtung I: Grundlagen und Methoden*

Technische Universität Berlin,  
Institute of Chemistry

*Kristallzüchtung II: Methoden und Anwendungen*

Technische Universität Berlin,  
Institute of Chemistry

**Peter Gaal, Christian Heyn (Universität Hamburg UHH), Guido Meier (UHH), Lars Tiemann (UHH)**

*Proseminar: Grundlagen nanostrukturierter Festkörper*  
Universität Hamburg

**Peter Gaal, Andreas Stierle (DESY)**

*Physik für Studierende der Nanowissenschaften*  
Universität Hamburg

**Frank Kießling**

*Versuche und Messungen zu Kristallzüchtung und Kristallstrukturen*

Schüler-Kristallographielabor an der  
Lise-Meitner-Schule Berlin

**Detlef Klimm**

*Phase Diagrams*

Humboldt-Universität zu Berlin,  
Department of Chemistry

**Christian Kränkel, Tim Schröder (HU Berlin)**

*Applied Photonics*

Humboldt-Universität zu Berlin,  
Department of Physics

**Martin Schmidbauer**

*X-Ray Scattering: Basics and Applications in Materials Science*

Humboldt-Universität zu Berlin,  
Department of Physics

**Thomas Schröder, Ted Masselink (HU Berlin), Roman Engel-Herbert (PDI)**

*New directions in electronics, optoelectronics and devices*

Humboldt-Universität zu Berlin,  
Department of Physics

**Thomas Schröder, Radhakrishnan Sumathi, Jens Martin**

*Grundlagen und Methoden der modernen Kristallzüchtung*

Humboldt-Universität zu Berlin,  
Department of Physics



## Membership in Committees

### Committees

#### M. Bickermann

- IGFA e.V. - the scientific network of the non-university research institutions located in Berlin-Adlershof e.V.; member of the board and treasurer
- DFG Review Board 406-03: Thermodynamics and Kinetics as well as Properties of Phases and Microstructure of Materials; elected member

#### C. Frank-Rotsch

- Deutsche Gesellschaft für Kristallwachstum und Kristallzüchtung (DGKK) (German Association for Crystal Growth); secretary
- European Network of Crystal Growth ENCG; member of the council
- International Organization for Crystal Growth IOCG; member of the executive committee

#### C. Guguschev

- Commission on Crystal Growth and Characterization of Materials der International Union of Crystallography (IUCr), consultant

#### D. Klimm

- Deutsche Gesellschaft für Kristallographie (DGK), member of the scientific college (German Society for Crystallography (DGK); member of the Wissenschaftskolleg

#### T. Schröder

- Forschungsverbund Berlin e.V.; executive committee spokesman, chairman of the Board
- Deutsche Gesellschaft für Kristallzüchtung DGKK; deputy chairman
- European Network on Crystal Growth (ENCG); coordinator
- DESY Photon Science Committee; member
- Humboldt Universität zu Berlin: Strategic committee of the Department of Physics; member
- Leibniz Association: Leibniz Mentoring Program; mentor and member of the committee
- Leibniz Association: Strategy Forum on Technological Sovereignty; speaker
- BMBF & BMWK Expert Dialogue on "Technological and Digital Sovereignty" as part of the Federal Foreign Office's National Security Strategy
- Beamline Review Committee at the ESRF; member
- W3-S-Professorship for "Experimental Ultra Short Time Physics", together with the position of the director of Max-Born-Institute; member of the appointment board

### Conference Committees

#### M. Albrecht

- 4th International Workshop on Gallium Oxide and Related Materials, Nagano, Japan; member of the program committee
- International Workshop on Nitride Semiconductors, Berlin, Germany; member of the program committee

#### M. Bickermann

- 7th European Conference on Crystal Growth (ECCG7), Paris, France; member of the program committee
- International Workshop on Crystal Growth and Technology (IWCGT-8), Berlin, Germany; chair
- 14th International Conference on Nitride Semiconductors (ICNS-14), Fukuoka, Japan; member of the program committee
- 19th International Conference on Defects-Recognition, Imaging and Physics in Semiconductors (DRIP19), online; member of the steering committee
- 5th International Workshop on UV Materials and Devices (IWUMD), Jeju Island, Korea; member of the program committee
- International Workshop on Nitride Semiconductors, Berlin, Germany; member of the program committee
- Advanced Solid State Laser Conference ASSL 2022, Barcelona, Spain; member of the program committee
- 12th German-French Workshop on Oxide, Dielectric and Laser single crystals (WODIL 2023), Berlin, Germany; co-chair

#### N. Dropka

- 7th European Conference on Crystal Growth (ECCG7), Paris, France; session chair
- The 10th International Workshop on Modeling in Crystal Growth; session chair
- IKZ-WIAS virtual workshop; co-organizer and chair
- IKZ-BTU-LZKI virtual workshop on artificial intelligence; co-organizer

#### C. Frank-Rotsch

- International Conference on Crystal Growth and Epitaxy ICCGE-20, Naples, Italy; member of the international advisory board
- 7th European Conference on Crystal Growth (ECCG7), Paris, France; member of the program committee
- International Workshop on Crystal Growth and Technology (IWCGT-8), Berlin, Germany; co-chair

#### F. M. Kießling

- International Workshop on Crystal Growth and Technology (IWCGT-8), Berlin, Germany; member of the steering committee

## Membership in Committees

### C. Kränkel

- SPIE Photonics West, Solid State Lasers XXXI: Technology and Devices, San Francisco, USA; member of the program committee
- 12th German-French Workshop on Oxide, Dielectric and Laser single crystals (WODIL 2023), Berlin, Germany; member of the steering committee
- Optica Laser Congress, Advanced Solid State Laser Conference 2023, Tacoma, Washington, USA; program committee member

### W. Miller

- International Conference on Crystal Growth and Epitaxy-ICCGE-20, Naples, Italy; member of the international advisory board
- 7th European Conference on Crystal Growth (ECCG7), Paris, France; member of the international scientific committee
- International Workshop on Modeling in Crystal Growth (IWMCG-10), Xi'an, China; member of the Advisory Committee
- MMS Days, Potsdam; member of scientific board

### T. Schröder

- 12th German-French Workshop on Oxide, Dielectric and Laser single crystals (WODIL 2023), Berlin, Germany; chair

### R. Radhakrishnan Sumathi

- International Workshop on Crystal Growth and Technology (IWCGT-8), Berlin, Germany; co-chair
- Symposium: Recycling of technology materials from WEEE, in the Materials Science and Engineering Congress (MSE-2022) - I: Circular Materials, A German Materials Society (DGM) flagship event; co-chair

### Jutta Schwarzkopf

- EFRE Kick-off-Workshop „Materials for Oxide Electronics“, Berlin, Germany, organizer
- 8th European Crystallography School 2023 at HZB, Berlin, Germany, local organizing committee

## Editorial committees

### M. Bickermann

- Progress in Crystal Growth and Characterization of Materials, Elsevier, associate editor
- Journal of Crystal Growth; editor

### N. Dropka

- Journal of Crystal Growth; editor
- Special issue in Crystals “Artificial Intelligence for Crystal Growth and Characterization”, guest editor

### W. Miller

- Crystals, member of editorial board



### **Leibniz-Institut für Kristallzüchtung (IKZ)**

Max-Born-Straße 2  
12489 Berlin  
Germany

Phone +49 (0)30 6392 3001  
Fax +49 (0)30 6392 3003  
Email [cryst@ikz-berlin.de](mailto:cryst@ikz-berlin.de)

**[www.ikz-berlin.de](http://www.ikz-berlin.de)**